Exoskeletonwindow

Thin-Glass window embedded with soft pnuematic actuators

M.sc. Thesis in Building Technology
Faculty of Architecture and Building Environment

Congrui Zha
02-07-2018

MSc. in Architecture, Urbanism and Building Sciences Building Technology	MASTER THESIS
Faculty of architecture and the built environment Delft University of Technology	
Congrui Zha Student number: 4601335	STUDENT NAME
Christian Louter Structural Design	MAIN MENTOR
Tillmann Klein Facade Design	SECOND MENTOR
Serdar Asut Design informatics	EXTERNAL CONSULTANT
Frank Huijben ABT.B.V	EXTERNAL MENTOR
Chris van der Ploeg ABT.B.V	
Dirk Dubbeling	EXTERNAL EXAMINER
02/07/2016	DATE

1. ACKNOWLEDGMENT

First, I would like to thank my mentors Christian Louter and Tillmann Klein helping me from the beginning. Christian Louter helped me to pick the topic which is related to computational design and thin glass. He is very patient with me on developing this project and helps me to solve the difficulties. Without his help, I can not narrow down the topic so fast that I have time to develop it further. Tillmann Klein is my second mentor, he helps me also from the beginning. Even my question is not related to facade design, he is very patient to solve the problem and he has a board view in my project, always helping me to plan steps further and to arrange timeline. Especially, I would like to thank James O´Callaghan, our guest professor. Every time we meet, he always inspires me with his knowledge and experience in glass technology. Also, I will thank my external consultant Serdar Asut, he helps me in the beginning to develop my robotic concept and gives me very important suggestions in P2 presentation.

Especially, I would like to say thank you to my mentors in ABT Engineering, Frank Huijben and Chris van der ploeg. Frank helps me from the beginning until P2 presentation because of his left from ABT. He helps me to arrange my graduation plan and keeps asking me questions until I clear up my logic. I learned scientific thinking and computational mindset from him. Chris van der ploeg is my mentor after Frank left. In this mentorship, he helps me with structure calculation and simulation. In this project, structure calculation plays the most important role, without his help, I might lose my direction. Also, I would like to thank Dino van Deijzen, Ad van der Aa, Rudi Roijakkers and DIANA group in ABT.

Also, without the help from Rob Scharff, I can not get knowledge on soft robotics fast and comprehensive. As an expert on soft robotics, he explained his master thesis to me in detail and taught me technology in 3D printing. Also, he let me use his 3D printer to do research and prototype.

I am also grateful to my super spacer supplier EdgeTech in Germany and Jan Koudijzer for visiting FESTO in Delft. However, the project will not be the same without support from my parents and my girlfriend Livy. In the whole journey, they always listening and helping me when I feel stressed.

Without the help from all these people, this big project cannot be finished just by myself.

Contents

1. INTRODUCTION

1.1. Background:

In the last decades, the improvement of innovative solutions on windows to achieve sustainability within the built environment is considered as a principal issue. Windows have long been used in buildings for daylight and ventilation. From many studies, health, comfort, and productivity are improved by the well-ventilated indoor environment, because ventilation dilutes the indoor concentration of contaminations for indoor air quality. Also, too high indoor air velocity is perceived as draft or chilly, but too low air velocity may create stuffiness. Besides, natural ventilation is one of the most prominent issues of energy consumption within buildings. In summer, cooperated with chimney effect, natural ventilation can reduce the use of the cooling system. Even in winter, the openable window should dynamically adjust the ventilation rates based on actual population to control human CO2 emissions. Consequently, the use of heating, ventilation and air conditioning (HVAC) system will be reduced.

Windows influence the natural ventilation of a building directly and guarantee indoor comfort level, indoor air quality and minimize energy consumption. Windows can be opened manually, or center controlled mechanically. Unreachable windows for instance, in atriums or skylight, are opened by window actuators which are centrally controlled or passively controlled for the reason to optimize indoor comfort. There are advantages using window actuators in terms of controlled natural ventilation. Window actuators can make a significant contribution to a building's indoor environment and energy performance.

Today it should be easy for the window to control opening sizes for adapting wind direction and wind load, meanwhile, the inlet air velocity should be possibly manipulated to optimize indoor air velocity. In this thesis, the dynamic way of opening windows by using window actuators for the reason of manipulating inlet wind velocity and adapting wind direction and load will be developed. Inspired by that air velocity varies on a curved surface because of curvature changing, inlet air velocity can be manipulated continuously and smoothly by changing window curvature.

1.2. Problem statement:

Wind direction and load are difficult to predict, which gives challenges to window opening for desirable ventilation. Nowadays, cooperating with mechanical ventilation, the hybrid ventilation system is a relatively modern concept, which takes advantage of both natural and mechanical system. Even though, optimizing window opening direction and opening size for desirable natural ventilation still owns the potential to reduce mechanical ventilation usage. By using automatically openable windows, it is needed to implement complex mechatronics equipment, which increases cost because of producing and operating this equipment and enlarge load bearing on the structure. Additionally, because of maintenance and replacement, the low durability of motors will increase cost.

Nowadays, window opening directions and opening sizes are not dynamically adapt to unpredictable wind directions and wind loads for ventilated cooing. Automatically openable window and mechanical ventilation are becoming increasingly wide use due to the need and regulation of ventilation rates for the indoor environment. These mechanical systems have high produced, operating and maintenance demands.

1.3. Research question:

Main question:

How can soft pneumatic actuator(SPA) bend thin-glass windows structurally for natural ventilation?
Sub-question:

- How to prove curved window can decrease predict dissatisfied percentage due to draft
- Considering natural ventilation function, which window configuration can be developed
- What is the relationship between SPA geometry, air pressure and bending radius
- How to design window frame

1.4. Research objectives:

General objective:

Design a bendable window embedded with soft pneumatic actuator.

Sub-objectives:

- Exploring the benefit of using curved window instead of straight window on indoor comfort.
- Exploring the structure mechanism of using SPA to bending thin glass window
- Exploring relationship between SPA geometry, air pressure and bending radius
- How to design a window frame

1.5. Approach & methodology:

To be able to answer the research question and come to window detail design, the methodology of this research is proof of concept(POC). Two hypothesis is 'Soft Pneumatic Actuator can bend insulating ultra-thin glass window' and 'Curved window can improve predict dissatisfied percentage due to draft'. To prove both hypothesis, research, hand calculation, simulation, and experiment should be done.

The development of this research should start with normal window detail design. Research on indoor comfort due to draft should be done next. Followed by the thin glass and soft pneumatic actuator technology. And then structure mechanism and hand calculation need to be explained. FEM structure simulation will be verified by hand calculation results. Lately, detail design and comparison by benchmark will be discussed and evaluated. At last, one mock-up model will be made to illustrate how to bend thin glass window. The relationship in these steps is illustrated in Figure 1:

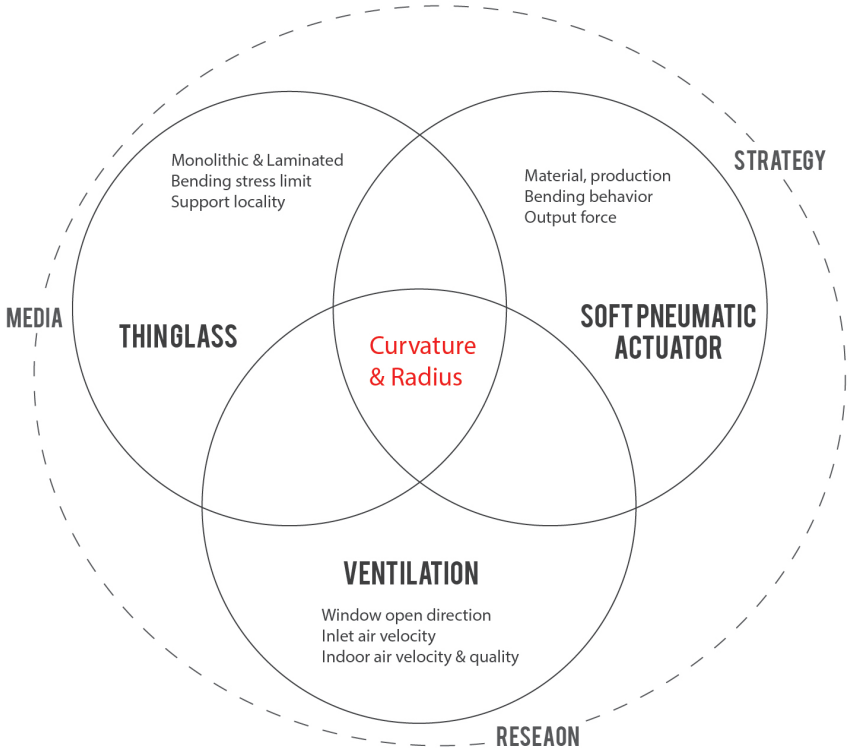

Figure 1:
research approach
Source: Own image

To explain the steps into detail. First, it must be discovered how windows are designed and opened for ventilation now, for which I can improve and illustrate why it needs to be improved, which will also demonstrate a strong reason why the curved window is needed.

Secondly, research on dissatisfied percentage due to draft will be introduced. Draught model from Fanger need to be explained, also, how curved window influence three main parameters: air temperature, air velocity, and turbulence intensity need to be illustrated.

Thirdly, based on a literature study on the thin glass production and prestressing peocess, possible alternatives will be explored. Some previous experiments about monolithic and laminated thin glass cold bending for discovering the relationship between bending stress and bending radius will be used as a reference for physical model and numerical model making. Abaqus CAE will be used as a simulation tool for geometric nonlinear analysis of thin glass bending and soft pneumatic actuator bending.

The next step, some specific technology related to pneumatic soft robotics must be discovered. Based on a literature study, besides material and production process, bending behavior and output force will also be explored. In this phase, whether output force is high enough to bend thin glass panel will be examined structurally by hand calculation and FEM analysis. Also, the relationship between air chamber geometry and bending curvature will be explored to fit thin glass bending curvature. The geometry simulated in Abaqus ACE will derive from a parametric model made in grasshopper. (Figure 2)

Then based on the result from above three steps, the optimal window curvature and movement will be achieved. In this phase, some window configurations designed before will be listed and compared with normal windows, like ventilation performance, cost, maintenance, durability and so on. The result will be discussed and evaluated. From the comparison and the result, one design will be picked and developed further into details.

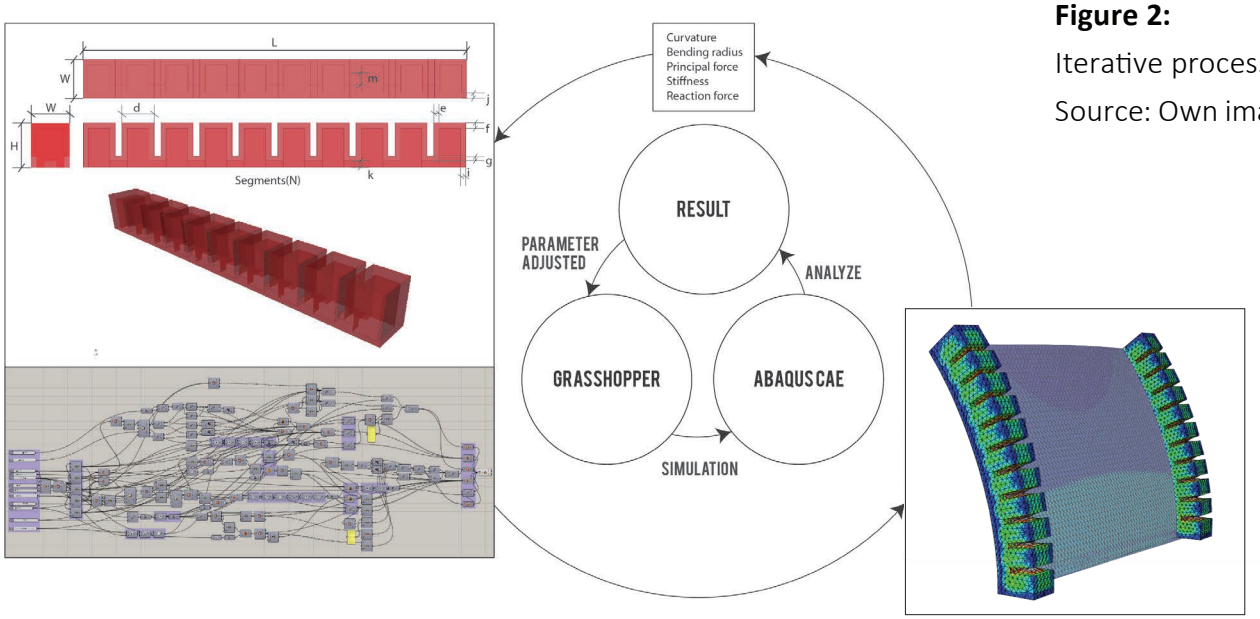

Figure 2:
Iterative process
Source: Own image

1.5.1 Proof of Concept(POC):

Hypothesis

A: Soft Pneumatic Actuator can bend insulating ultra thin glass window

B: Curved window can improve predict dissatisfied percentage due to draft

Hypothesis based Research

A: Soft Pneumatic Actuator, Ultra thin glass and Window detail

B: Aerodynamic theory and Draught model

Hand calculation based approximation

A: Structure mechanism, Soft Pneumatic Actuator morphology generation, Wind load, Window size, and Window detailing

B: Inlet air flow rate, Wind pressure and predict dissatisfied percentage

Simulation based approximation

A: Soft Fiber-Reinforced Bending Actuator, Soft Pneumatic Actuator, Assembling simulation

B: Mean air velocity and predict dissatisfied percentage due to draft

Experiment based evaluation

A: Model making by increase air pressure to test bending behaviour

1.6. Relevance:

Scientific:

Nowadays thin glass is applied only to electronic devices. Chemically tempered is the main characteristics of thin glass which improves tensile strength. Compare to regular glass, thin glass is lightweight, flexible, lower use of raw material, the higher impact resistance of its surface and good optical quality. (Özhan, 2017) Thanks to these properties, there will be a potential using thin glass in the building environment. Several graduate students at TU Delft have already studied on applying thin glass on buildings. So far, some research has been done on double skin facades and first skin facades. Özhan Topçu did a study on the feasibility of a water- and airtight kinetic façade with a bending-active thin glass element, which is cold bending on one thin glass layer. Iris van der Weijde designed ultra-lightweight insulating thin glass sandwich façade panel with a honeycomb structure in between. However, combing lightweight and flexible properties with the pneumatic soft robotic actuator to make a bendable thin glass window for ventilation is never being done before. There are several reasons for using a pneumatic soft robotic actuator which has already been given above.

Soft Robotics is one of the most promising frontiers for robotics research and technological innovation. The field of soft robotics is a multi-disciplinary, connecting material science, mechanical/ electrical engineering, control engineering, chemistry, physics, computer science, biology and many more. (Kim, Laschi, & Trimmer, 2013) However, there is rarely practice soft robotic technology using on building façade system. In ETH Zürich, Prof. Arno Schlüter used an adaptable façade system driven by a pneumatic soft actuator for solar tracking. This façade system aims to produce electricity and regulate light and heat generation and is a second façade system, which needs secondary structure. How to use soft robotic actuator as a high force frame to make an openable window still need to be studied.

This thesis is a study coupling thin glass window and soft robotics for natural ventilation, meanwhile, this thesis builds a bridge between thin glass façade in building environment and soft robotics in product design engineering to improve the solution of innovation in the sustainable design area.

Environmental:

In this thesis, the environmentally friendly issue is the main motivation to develop adaptable window. To reduce the usage of HVAC system, natural ventilation of buildings owns big potential. Especially in summer, well-controlled natural ventilation system can save energy from the cooling system and fan. Even in winter, this system can improve indoor air quality by manipulating window opening direction and size. Furthermore, the pneumatic soft robotic actuator will replace complex mechatronics equipment system.

2. CONCEPT HYPOTHESIS

2.1. Concept starting point

The concept comes from ultra-thin glass properties. One of the most important properties of ultra-thin glass is flexibility. There is some researchers designing facade by using ultra-thin glass. However, Ultra-thin glass is mostly used on the second facade by changing the geometry instead of used on the primary skin. Even though, ultra-thin glass on the primary skin is used as one part of the rigid sandwich panel by losing the flexible property. As a result, how to keep flexibility on primary skin becomes the starting point in my research.

2.2. Hypothesis of concept

The first hypothesis of the concept is that soft pneumatic actuator can bend double-glazing thin glass window. In this hypothesis, the main challenge is structure. The concept is to transfer inlet air pressure to bending behavior of window. Between the air pressure and bending behavior is a black box which needs to be discovered in my thesis. To simplify this process, the initial model has been made. Glass panel geometry will be rectangular shape attached with multiple soft pneumatic actuators. (Figure 3)

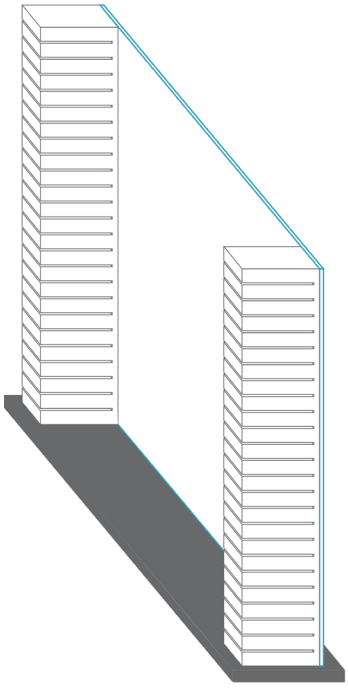

Figure 3:
Initial model
Source: Own image

The second hypothesis is that curved window can help to improve the indoor environment by decreasing predict percentage dissatisfied due to a draft. The basic knowledge of this hypothesis comes from aerodynamic theory, which illustrates that when wind hits on a curved surface and flat surface, wind from the curved surface can generate the laminar air flow, however, it from the flat surface will generate turbulent air flow.

3. HYPOTHESIS-BASED RESEARCH

3.1. Windows design

3.1.1. Water penetration:

Based on the design objectives, one of the biggest challenges of the bendable window is watertight and airtight. In this phase, getting to know the critical barriers in window frame will be the first step, followed be how to find out the leakage paths and water penetration. There are four critical barriers in window frame and wall interface. One of these barriers is water shedding surface. The slope of water shedding surface deflects liquid water and moisture to outside. The second barrier is called exterior moisture barrier, which prevents internal finishes or material from outside water. The last two barriers are the vapor barrier and air barrier, the function of these two barriers is to retard the migration of water and air. (**Figure 4**)

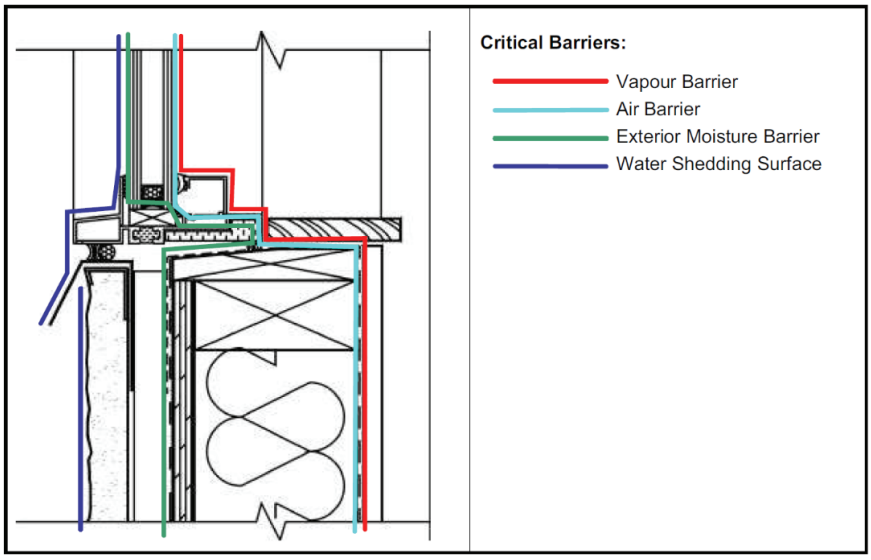

Figure 4: Critical barriers on window to wall connections
Source: (Limited, 2002)

To design a watertight window, primary leakage paths should be found out first. After knowing the normal leakage paths, details can be taken care of. There are six possible leakage paths from (Limited, 2002) the **Figure 5**.

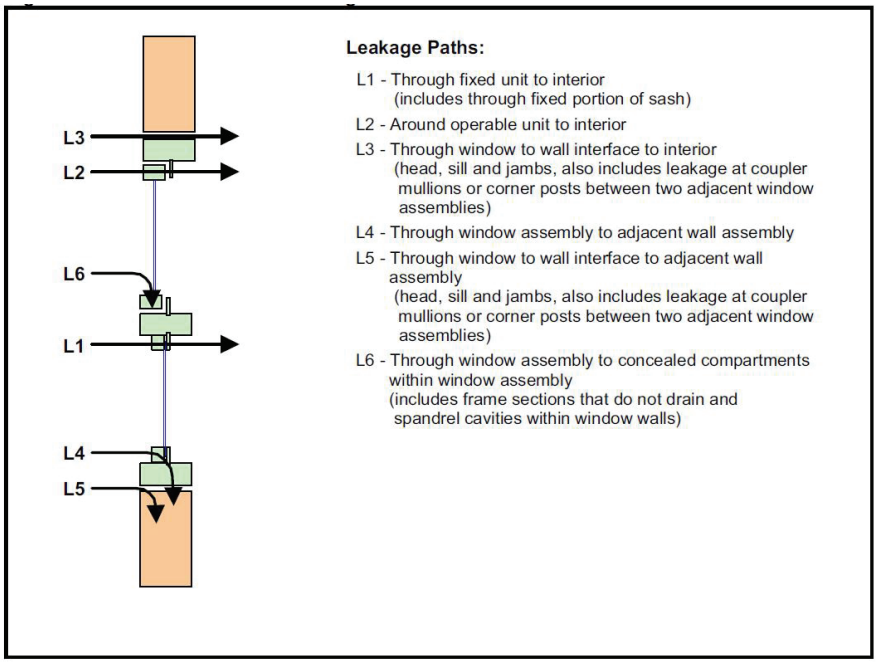

Figure 5: Critical barriers on window to wall connections
Source: (Limited, 2002)

3.1.2. Electric chain actuator:

ACK4 Chain actuator 230V or 24V (**Figure 6**) design by Rocburn is used widely in both domestic and commercial property. This chain actuator can be used on skylights and roof vents because of sealing in the motors to prevent rain. This product is popular because it can control room temperature by actuating window openings with control panels. Also, the rain sensors are useful when the weather changes. (Rocburn limited, 2014)

Figure 6: ACK4 Chain actuator
Source: https://www.tealproducts.com/product/actuators/chain-type/single-chain/topp-ack4-chain-actuator-400mm

Electric window opener:

This window actuator (**Figure 7**) is designed in Denmark and can be assembled for windows in difficult to reach space. It can be controlled by remote and connected with 5 windows. This actuator can be used in the home, school, office or in conservatories. (Rocburn limited, 2014)

Figure 7: Venset electric window opener
Source: http://www.window-openers.com/plug-opener-gallery/

3.1.3. Greenhouse or Conservatory Window Openers:

Natural ventilation in the greenhouse is the key to keeping plants growing healthy in warmer months. Using automatic greenhouse vents (**Figure 8**) is a way to ensure greenhouse stays at the right temperature year-round. The pistons contain a mineral wax that expands when heated. It will open the greenhouse vent when hot temperature let wax expand. When the temperature falls, the wax will contract to close greenhouse vent. The automatic greenhouse vent doesn't need electricity to motivate, instead, it is made from durable material.

Figure 8: Automatic vent opener for greenhouse
Source: https://www.drpower.com/power-equipment/lawn-and-garden/gardening/greenhouses/automatic-vent-opener.axd

3.1.4. Top-hung window

Top-hung window(**Figure 9**) is very common in window market. This types of the window can provide both smoke and natural ventilation. Compare to the double-hung window in the same size, the top-hung window can provide more fresh air. With the handle on the bottom, top-hung windows can provide a full sky view and sunlight. Also, the top-hung window is good at protecting rain going into rooms. (Markot Meghna, 2017)

Figure 9: Top-hung window
Source: https://www.quora.com/What-is-top-hung-window

3.1.5. Double Hung Double-Glazed Sash-less Window:

Sash-less windows use a double-hung system without sash frames climbing (**Figure 10**). This kind of windows is frameless to maximum the view to outside. To provide better ventilation, this window can be opened at both top and bottom. (**Figure 11**)(Aneetawindows. 2015)

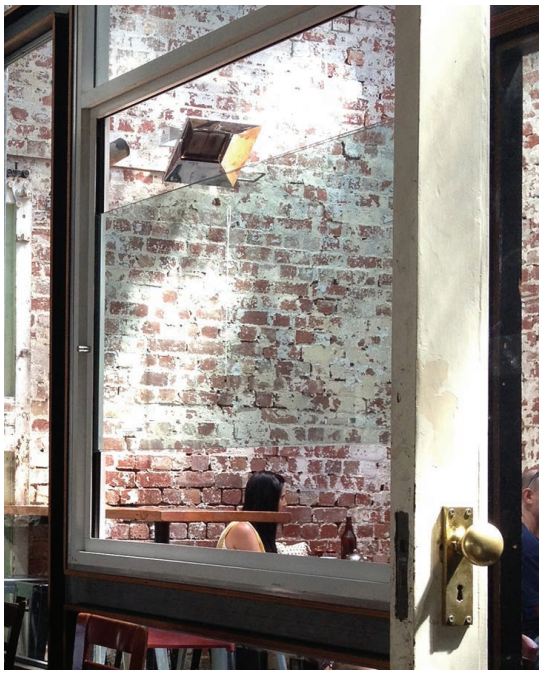

Figure 10: The auction rooms
Source: http://www.austview.com.au/portfolio-items/the-auction-rooms/

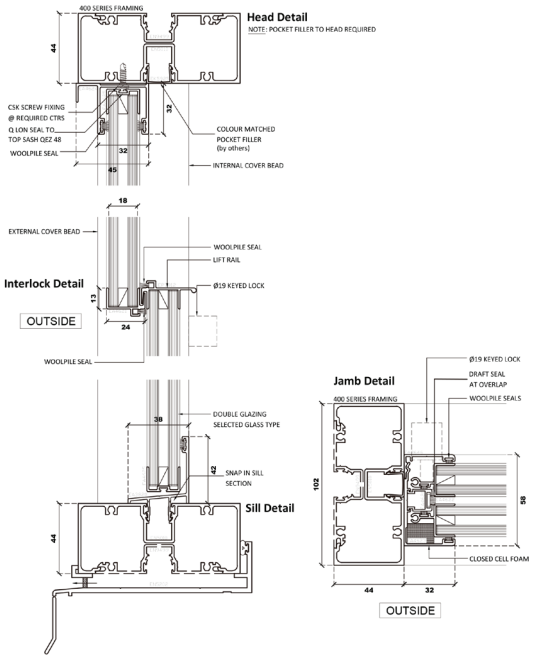

Figure 11: Austview Sash-less Double Glazed Double Hung
Source: http://www.austview.com.au/products/double-glazed-sashless-window/

3.1.6. Frameless sliding glass window:

Frameless sliding glass window can create a frameless view of the external environment. The minimalistic design of the large fixed and sliding window with slender profile geometry provide users large, light-flooded living spaces. Outer frames set into the floor should be integrated with sliding rail, which will create a barely perceptible, barrier-free threshold. (**Figure 12**) The sliding systems can achieve energy efficient through the optimized insulation of the profiles and the use of large thermal insulation glazing. The outer frame can be hidden around the wall, ceiling, and floor. (**Figure 13**)"Electric motors used by KELLER have the tensile force of 800 kg (KELLER MOT800) and 2,000 kg (KELLER MOT2000) moving the sliding leaves silently via toothed belts. They are controlled either automatically (remote control, home automation adaptations) or manually (dead-man or room switch). Window façades with several leaves can be opened telescopically at the push of a button." (KELLER, 2016)

Figure 12: Stainless steel sliding rail

Source: https://www.minimal-windows.com/en/downloads/

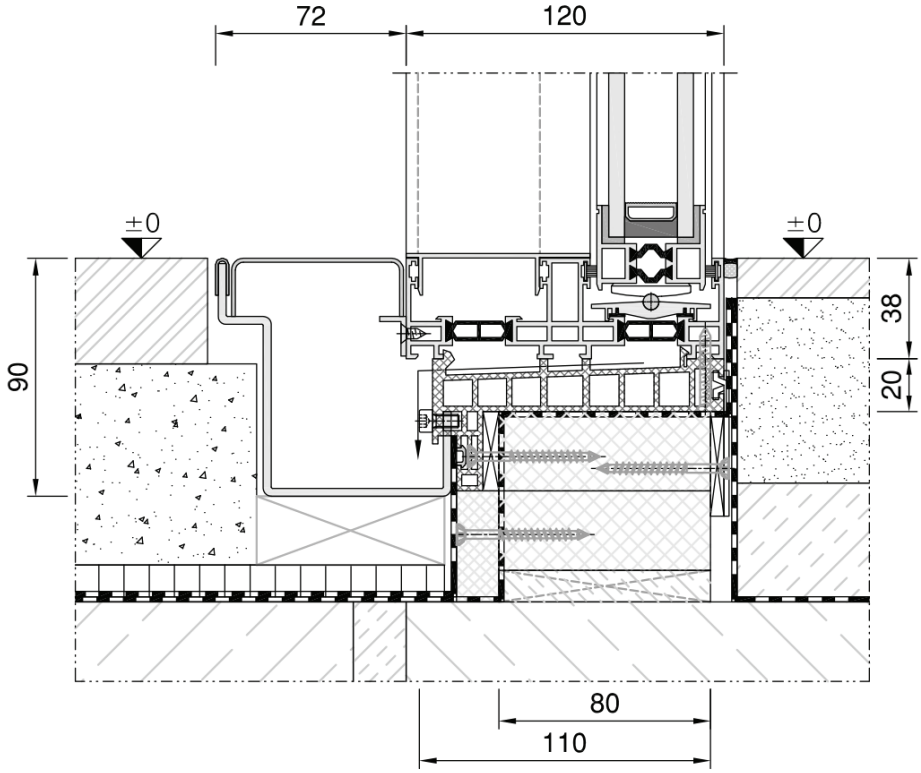

Figure 13: Detailing of sliding window

Source: https://www.minimal-windows.com/en/downloads/

3.1.7. Double glazing window effective flexural stiffness:

When the window is sealed, the pressure inside and outside is the same. Inside the insulation windows, the air- argon is not only responsible for window insulation, but also generate mechanical atmospheric pressure to against uniform pressure outside. (**Figure 14**)

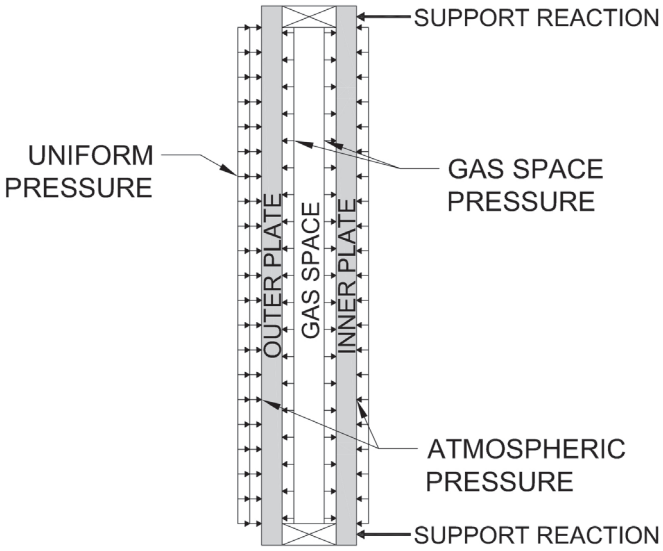

Figure 14: Pressure distributions acting on a double pane insulating glass unit
Source: (Mertens, 2015)

3. HYPOTHESIS-BASED RESEARCH

3.2. Soft robotics

The spread of soft robotics research in the world has bridged the gap between technologies in terms of rehabilitation, Minimally invasive surgery, building environment, producing, human-computer interaction and so on. More and more boundaries are pushed through by developing soft robot technology due to its abilities, such as squeezing, stretching, climbing, growing and morphing.

Using pneumatic actuators by pressurizing air has five advantages: 1) it provides fast inflation for actuators because of low viscosity of air. 2) it can be easily controlled and measured by using sensors. 3) it is almost available by using compressors or compressed gas tanks. 4) it is lightweight. 5) pressurized air can be used and discarded sustainably from and to the atmosphere around. (Mosadegh et al., 2014)

It has also been shown that soft bending actuators can generate inherent bending motion without requiring any rigid components. (Galloway, Polygerinos, Walsh, & Wood, 2013) It will reduce the weight of actuator and simplify assembling process. Soft robotic actuators can be made of flexible materials that take continuous forms when the pressure in the special chambers change. Such actuators are normally used mainly for prosthetic and biomimetic robots; I am now discovering and exploring possibilities to embedded with thin glass windows. With the inherent mechanical compliance, the soft pneumatic actuator(SPA) have unique advantages in environments requiring conformity and variable stiffness. In bending thin glass panels, soft robotic actuators could adapt to the curvature with thin glass panels. This character could reduce system complexity and cost. At the same time, it will improve bending performance and safety. (Zhou, Chen, & Wang, 2017) By using soft robotic actuator as window opener can make lightweight thin glass panel rigidly attached to building the facade, meanwhile, these panels can open in variable radiuses for natural ventilation. Without soft actuators, many complex mechanical parts need to be combined to achieve such functionality. There will be low durability and high expenditure leading to unlikely widespread use in facades. (Hofer, Groenewolt, Jayathissa, Nagy, & Schlueter, 2016) My result will demonstrate that there is promise for the development of multidisciplinary technology design between the pneumatic soft robotic system and the thin glass window that may be used in many applications based on an understanding of high-performance integrated façade design.

This chapter summarizes the results of the desktop research. During this phase, there are articles, books, and reports on the soft pneumatic actuator which is examined. Relating to the main research question in this thesis, this desktop research mainly focuses on some theoretical and practical results which have been done before.

In this phase, the simplified model with the single air chamber and fiber reinforcement will be used. A quasi-static analytical model and a finite-element method model can be used for finding the relationship of supplied air pressure, actuator bending angle, and interaction force at actuator tip. In the previous work, it has been proved that hemi-circular cross-section shape requires the lowest pressure to bend to the same angle. (Polygerinos et al., 2015)

3.2.1. Soft pneumatic actuator

To demonstrate the relationship of supplied air pressure, actuator bending angle, and interaction force at actuator tip, the effect of actuator morphology is significantly important. First, the comparison between PneuNets (pneumatic networks) bending actuators and fiber-reinforced actuators should be illustrated first. On the one hand, a wider range of motions and more robust can be achieved by the fiber-reinforced actuator. On the other hand, the fabrication time of PneuNets is much shorter than fiber-reinforced actuator, PneuNets actuator can be cast and assembled in less than one hour, however, casting a fiber-reinforced actuator will take 5 days. (Polygerinos et al., 2015)

The soft pneumatic actuator consists of an extensible layer on top and an inextensible but flexible layer on the bottom. Two inside walls are thinner and top walls are thicker. When air pressure rises inside air chamber, inside walls will expand first, pushing against each other to create bending behavior. Meanwhile, elongation of extensible layers can be controlled on a slight change in height.

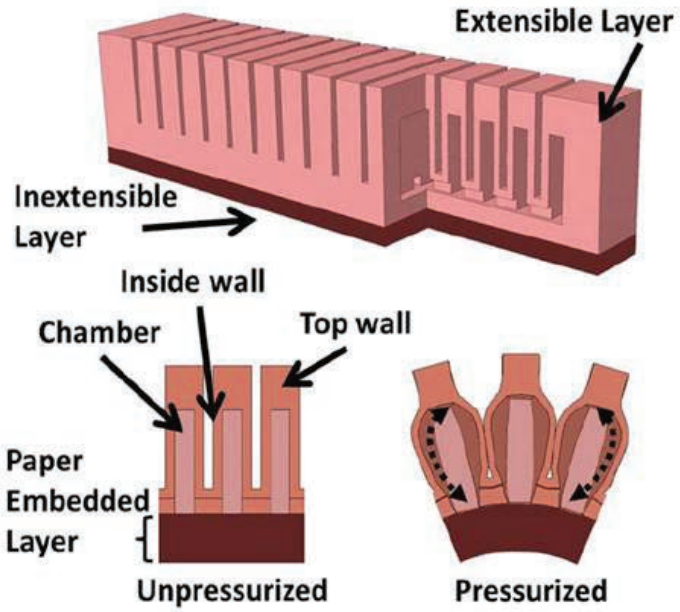

Figure 1: Actuator section unpressurized and pressurized
Source: (Mosadegh et al., 2014)

3.2.2. Structure mechanism

When the air pressure increases, actuators generate two behaviors in bending moments. First bending behavior comes from material stretching. When the top layer material stretches, bottom layer material is constrained by inextensible layer, which will generate bending behavior. (**Figure 2**) The other bending moment comes from side wall contacting. Previous segment contacts next segments and force come from the previous inner cavity. The next segment will be pushed to rotate around the connection between two segments. (**Figure 3**)

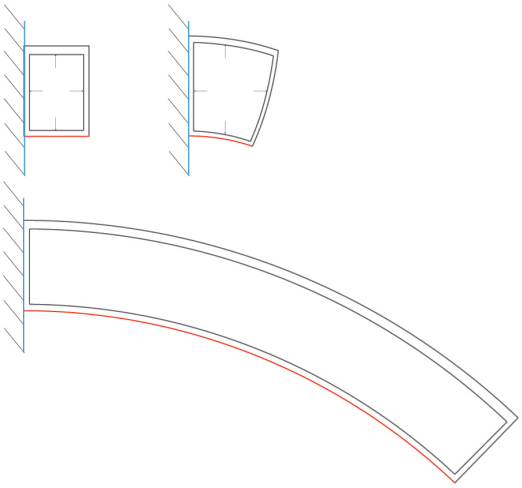

Figure 2: Stretching model
Source: Own image

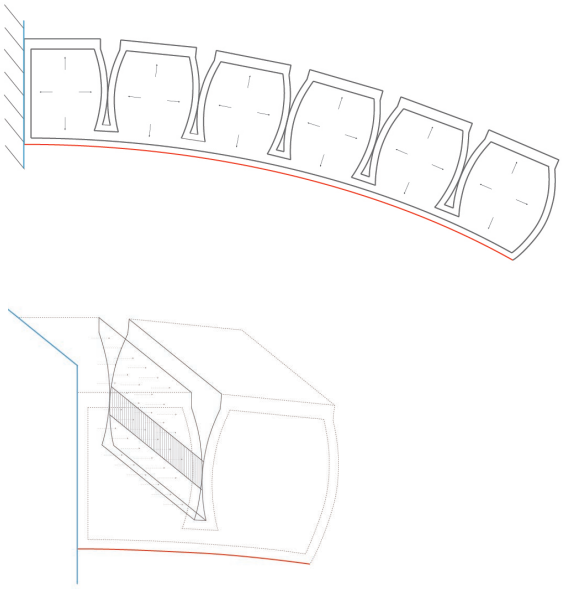

Figure 3: Contacting model
Source: Own image

The radius generated by two types of bending moment are different. However, the two types of radius are connected with each other, generating total bending geometry. (**Figure 4**)

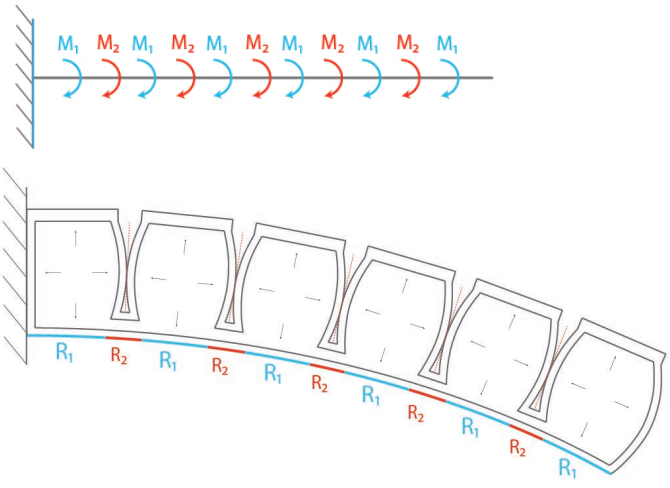

Figure 4: Bending behavior due to two types of bending moment.
Source: Own image

To make an approximation of bending moment, an analytical model should be built. The aim of building analytical model is to calculate bending radius in certain air pressure and have an approximation of soft actuator size. From the suitable formalization made by Raphael Deimel, as a previous researcher, the simplifications of the calculating bending moment is verified by his experiment. Figure 8 shows the small segment of the actuator. Length, width, and thickness can be defined as x, z, d. (Deimel & Brock, 2016)

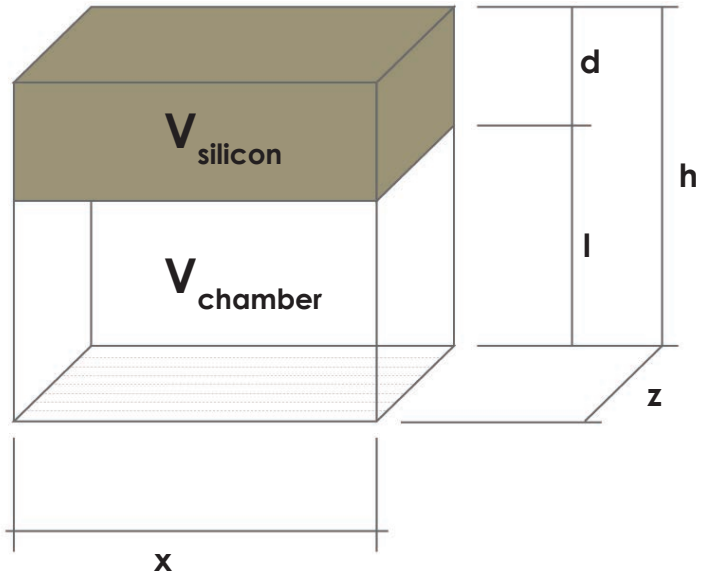

Figure 5: Actuator segment
Source: Own image

When the air pressure increase, the geometry will change. Outer layer will expand and inner layer will keep the same length but curving. From the figure $V_{silicon}$ will keep constant, $V_{chamber}$ will increase. Stretch λ_1, bending angle θ and bending radius r will be changed.(**Figure6**)

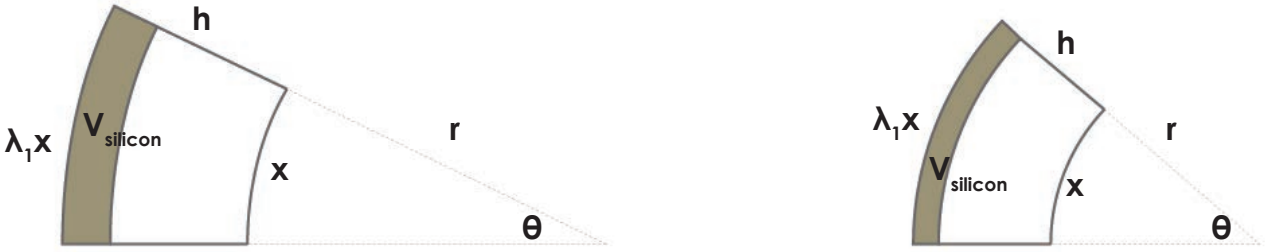

Figure 6: Actuator segment section and bending geometry
Source: Own image

The following equations show the relationship between curvature k, radius r, bending angle θ and stretch λ_1.

$$\theta = k*x$$

$$k_{top} = \frac{1}{\frac{1}{k}+h}$$

$$kx = \frac{1}{\frac{1}{k}+h} * \lambda_1 x$$

$$\lambda_1 = k*h+1$$

Volume of air chamber will change when air pressure increases. V_{actual} is the actual volume of the air chamber. After inflating, the total volume should be $V_{actual}+V_{silicon}$.

$$V_{actual}+V_{silicon}= V_{actuator}(1+\frac{h}{2}k)$$

$$\lambda_1 = 1+2*(\frac{V_{actual}-V_{chamber}}{V_{actuator}})$$

$$\frac{\delta\lambda_1}{\delta V_{actual}} = \frac{2}{V_{actuator}}$$

To calculate energy stored in the rubber, strain tensor invariants should be used which is related to the orthogonal stretches:

$$J_1 = \lambda_1^2+\lambda_2^2+\lambda_3^2-3$$

$$J_2 = \lambda_1^2\lambda_2^2+\lambda_1^2\lambda_3^2+\lambda_2^2\lambda_3^2-3$$

$$J_3= \lambda_1\lambda_2\lambda_3 -1$$

Because the incompressible property of rubbuer, λ_3 should be 1. Also, I assume the radial size of actuators will not change due to the thickness of side walls are larger than contacting walls.

$$\lambda_1\lambda_2\lambda_3 =1$$

$$\lambda_3 =1$$

$$J_1 =J_2=\lambda_1^2+ \lambda_1^{-2}-2$$

In the minimum total potential energy principle, the total potential energy is the sum of elastic strain energy and potential energy stored in the deformed body. In this system, the total potential energy of the actuator is the sum of energy from gas compression, elastic rubber deformation, and external load.

$$W= W_{air}+W_{sil}+W_{load}$$

The gradient of this equilibrium is zero if we make a differential by λ_1.

$$\frac{\Delta W}{\Delta\lambda_1} = 0$$

Energy of gas equals to pressure times volume. According to ideal gas equation: P*V=nRT. When the volume changes from V_1 to V_2, air energy should be:

$$W_{air} =W_{v1}-\int_{V_1}^{V_2} p(V)*dV$$

$$W_{air} =W_{v1}-\int_{V_1}^{V_2} p(V)*dV$$

$$\frac{\delta W_{air}}{\delta\lambda_1} = -p*\frac{V_{actuator}}{2}$$

The energy inside rubber $W_{silicon}$ is modeled as Neo-hookean solid model. G is the material's shear modulus.

$$W_{sil} = \frac{G}{2} * J_1 * V_{sil}$$

$$\frac{\delta W_{sil}}{\delta \lambda_1} = G*(\lambda_1 - \lambda_1^{-3})*V_{sil}$$

In this analytical model, I just considering stretching behavior, which means that external load generates rotary moments. Because of in this model, there is no contacting behavior, rotary moments from stretching is the only source. To calculate bending moments from stretching respect to energy equilibrium, stretching energy gradient w.r.t. λ1 should be:

$$\frac{\delta W_{load}}{\delta \lambda_1} = M * \frac{x}{h}$$

To sum up, by using the equilibriums above, I got the result of bending moment due to stretch.

$$M_{stretch} = \frac{h^2 * z}{2} * p - (\lambda_1 - \lambda_1^{-3}) * G * h * d * z$$

The other analytical model is contacting model. The bending moment due to contacting behavior can be calculated as belows: **figure 7**

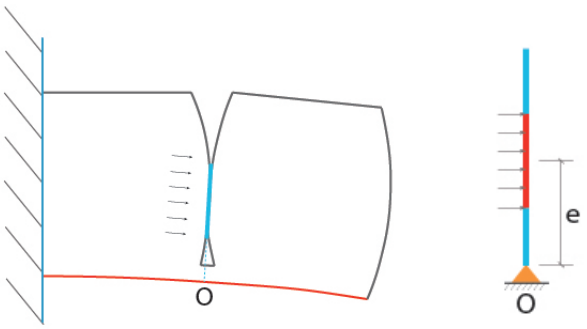

Figure 7: Actuator contacting behavior
Source: Own image

$$M_{contacting} = P*A*e$$

3.2.3. Actuator morphology

In this experiment, chamber numbers, heights, and wall thickness are the three important parameters. To investigate the impact of geometry on bending behavior, the experiments were supposed to make full bending and compare the air pressure. (Mosadegh et al., 2014) In the results of the experiments, a pneumatic actuator with more segments requires less air pressure. Also, Higher segments and thinner sidewall require less air pressure to generate full bending. (**Figure 8**)

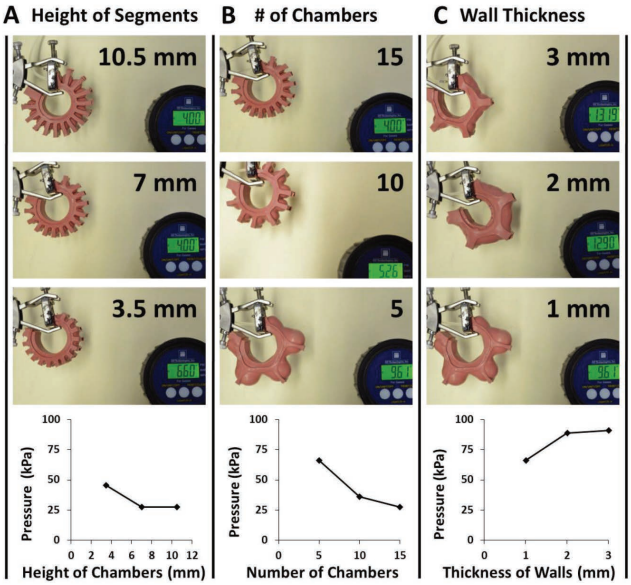

Figure 8: A) Different segements height B) different air chamber numbers C) different wall thickness
Source: (Mosadegh et al., 2014)

The experiment made in(Yap et al., 2016) illustrates how different actuator geometries influence the tip force under different air pressure. From the result below, it can be seen that bellow´s wall thickness and sidewall thickness decrease, as well as cross-sectional width increases, will result in increasing tip force. (**Figure 9**)

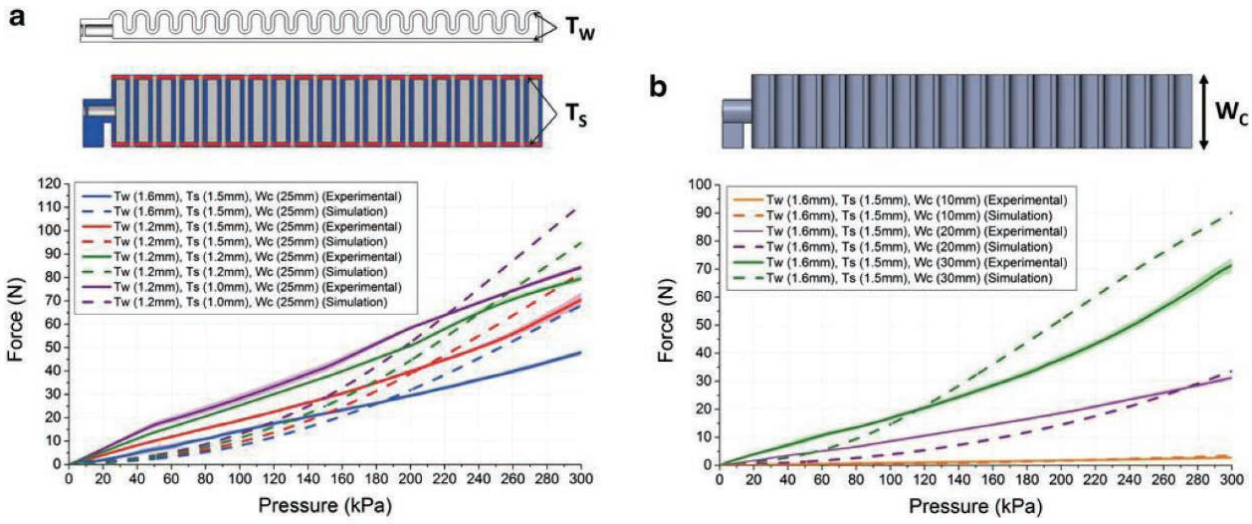

Figure 9: Relationship between tip force and air pressure from experiments and simulation
Source: (Yap et al., 2016)

3.2.4. Hyper-elastic models

When the soft pneumatic actuator is inflating, the strain happens on longitudinal direction, the constitutive model is considered to fit for the hyperelastic material. Ogden, Yeoh, Mooney Rivlin and Arruda-Boyce Models as four hyper-elastic models fit for longitudinal direction on strains. (Yap, Ng, & Yeow, 2016) The strain energy equation for each model is summarized below: (**Figure 10**)

Hyperelastic model	*Strain energy function*
Ogden	$W = \sum_{i=1}^{3} \frac{\mu_i}{\alpha_i}(\lambda_1^{\alpha_i} + \lambda_2^{\alpha_i} + \lambda_3^{\alpha_i} - 3)$ μ_i and α_i are empirical parameters, and λ_1, λ_2, λ_3 are deviatoric principal stretches
Yeoh	$W = C_{10}(I_1 - 3) + C_{20}(I_1 - 3)^2 + C_{30}(I_1 - 3)^3$ I_1 is the first deviatoric strain invariant, and C_{10}, C_{20}, C_{30} are material specific parameters
Mooney–Rivlin	$W = C_{10}(I_1 - 3) + C_{01}(I_2 - 3)$ I_1, I_2 are the first and second deviatoric strain invariant, and C_{10}, C_{01} are material-specific parameters
Arruda–Boyce	$W = \mu \sum_{i=1}^{5} \frac{c_i}{\lambda_m^{2i-2}}(I_1^i + 3^i)$ $C_1 = \frac{1}{2}, C_2 = \frac{1}{20}, C_3 = \frac{11}{1050}, C_4 = \frac{19}{7000}, C_5 = \frac{519}{673750}$ μ and λ_m are empirical parameters

Figure 10: Hyper-elastic strain energy functions
Source: (Yap et al., 2016)

3.2.5. Variable stiffness at different localities to conform to the shape:

Air chamber locations can also be changed. The hand rehabilitation glove below shows the possibilities. With variable air chamber location, the glove can generate different stiffness and different curvature to meet human finger bending behavior. (Yap, Lim, Nasrallah, Goh, & Yeow, 2015) When air chambers are inflated, different stiffness is assigned to different localities, as a result, actuators can conform to variable geometries. (**Figure 11**)

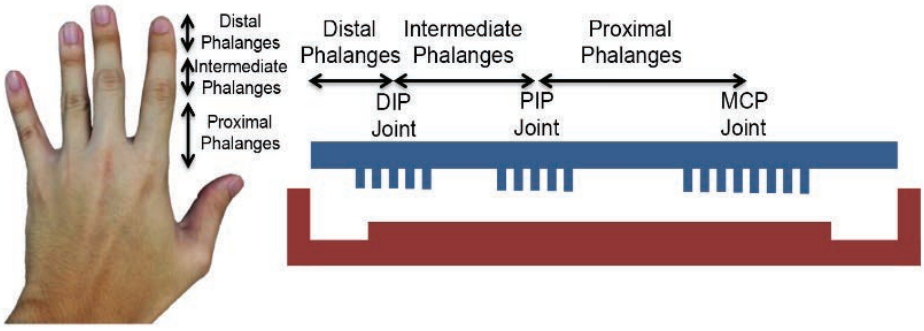

Figure 11: Finger joint size and locations have to be known before designing.
Source: (Yap et al., 2015)

3.2.6. Advanced soft pneumatic actuators:

In the following examples, more advanced and efficient applications will be discussed. Combining with flexible material and complicated geometry, soft robotics are widely used in a different research area. Well-designed air chamber can achieve different bending behavior in a controlled way. (Laschi, Mazzolai, & Cianchetti, 2016)

This example below combines flexibility with a rigid component to achieve accuracy movements. Minimally invasive surgery is the example which can be used in the medical section. In general, it is the use of the antagonistic arrangement of soft actuators and the use of semi-active actuators with variable stiffness ability. The STIFF-FLOP (**Figure 12**)manipulator matches all these requirements. It is based on three identical modular, and each modular is composed of three chambers and one central channel with a granular jamming system for stiffening the arm in the right direction. (Laschi et al., 2016)

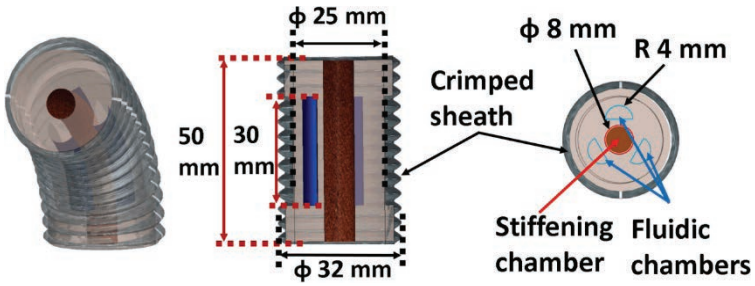

Figure 12: Section and dimensions from single modular.
Source: http://iopscience.iop.org/article/10.1088/1748-3190/10/3/035008

To make the actuator stiffer, a granular jamming system can be a good solution. (**Figure 13**) In the unjammed state, the actuator keeps the highly flexible property. When the air chamber is vacuumed, stiffness increases fast(**Figure 14**). Coffee powder is often used as the granular material, by controlling vacuum level, the stiffness can be manipulated. (Cianchetti et al., 2013)

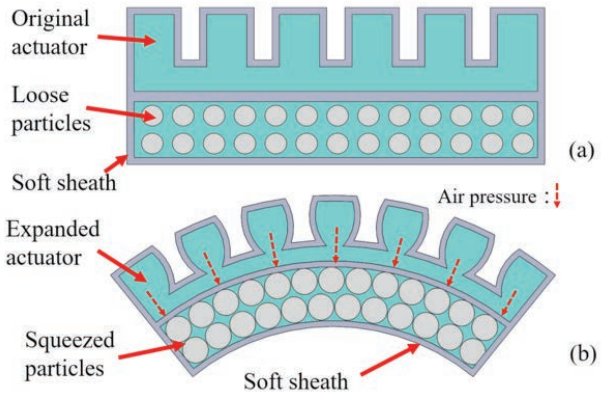

Figure 13: Passive particle jamming mechanism
Source: Cianchetti et al., 2013

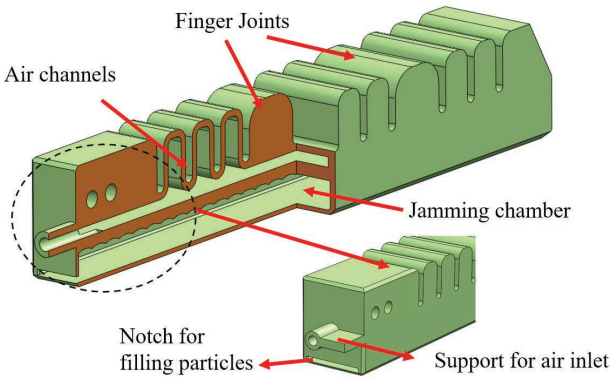

Figure 14: 3D model for the proposed finger
Source: Cianchetti et al., 2013

3.2.7. Soft pneumatic actuators used in facade system:

Since robotics are more and more used in the building environment, there are some pioneers implementing soft robotics in building technology. In this paragraph, two examples will be discussed.

Students Nasser Ghannam, Guoliang Zhang, Mohamad Al Chawa and Dongliang Ye from Institute for Advanced Architecture of Catalonia created a responsive facade system by using soft robotics which passively adapts to the environment around (**Figure 15**). There are two challenges of this project: first is that if the passive power is enough to activate this system; second is that if the scale of this actuator is possible to be manufactured (**Figure 16**). To answer both questions, this group did some research on passive technology and soft robotics production technology. This passive system is based on air pressure from low boiling points liquid (**Figure 17**). By using the air pressure to activate soft robotics. They also plan to test this system in different scales and different performances. (Nasser Ghannam, Guoliang Zhang, Mohamad Al Chawa, Dongliang Ye, 2016/2017)

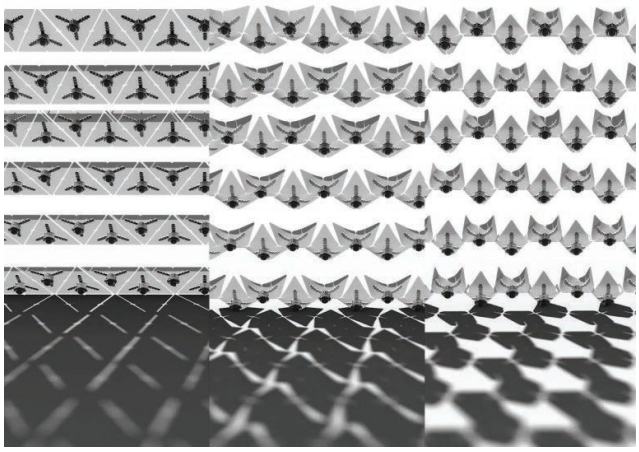

Figure 15: Passive sun shading system
Source: http://www.iaacblog.com/programs/soro-lightweight-passive-shading-system/

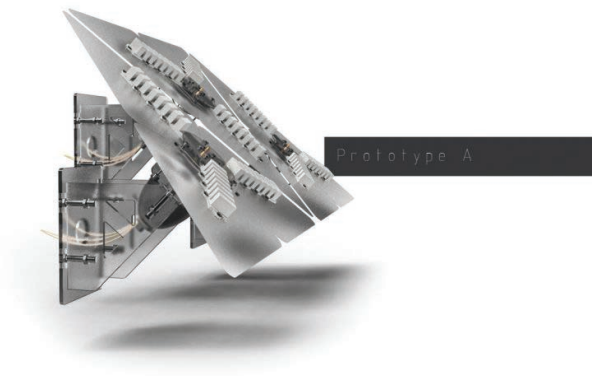

Figure 16: Prototype 3D model
Source: http://www.iaacblog.com/programs/soro-lightweight-passive-shading-system/

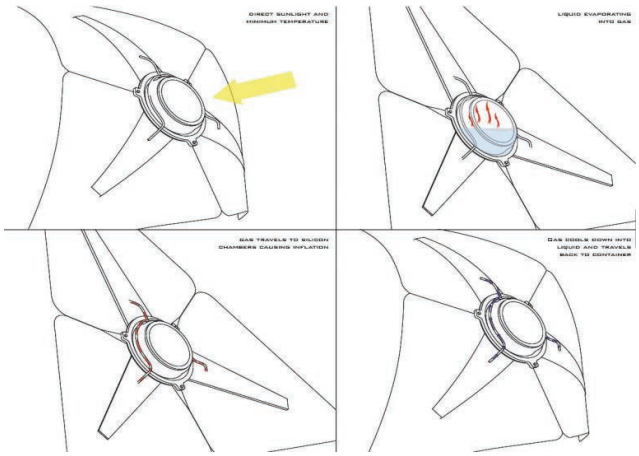

Figure 17: Passive system principle
Source: http://www.iaacblog.com/programs/soro-lightweight-passive-shading-system/

The second example is photovoltaic sun shading system activated by soft robotics. (Figure 18) This adaptive facade has been used on House of Natural Resources (HoNR). This facade can generate electricity by rotating its angle. On the back of the PV panel is soft robotics, by inflating air chamber, soft robotics helps PV panel rotate in different angles. To increase the effectiveness of this facade, soft robotics rotate towards the sun. This facade can also control indoor thermal comfort by controlling light coming in. This adaptive solar facade is lightweight and can be placed almost anywhere. (Hofer et al., 2016)

Figure 18: photovoltaic sunshading system embeded with soft robotics
Source: (Hofer et al., 2016)

3.2.8. Material:

Material stiffness will influence how much air pressure it can resist failure. Stretchy materials will deform more than rigid materials but have lower stiffness. For example, by using fused deposition modeling technology, a commercial thermoplastic elastomer filament NinjaFlex can be used. (Yap et al., 2016) The nozzle diameter of the printer is 0.4mm. In the figure below, actuator started to leak under pressure 440kPa. (**Figure 19**) Instead, material elastosil M4601 silicon starts to leak around 50kPa.

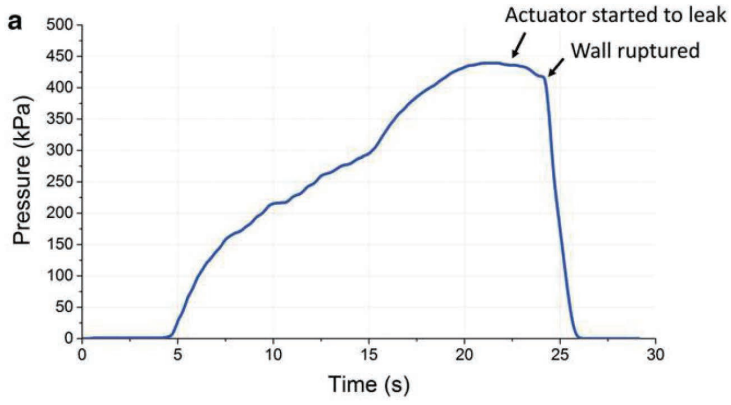

Figure 19: 3D printed SPA leakage test
Source: (Yap et al., 2016)

Also, compare to Elastosil M4601 silicone with paper as strain constraints, Ecoflex silicone with PDMS silicone performs differently. From the comparison experiments below, to achieve the full bending, material eco flex 30 inflates under 8 kPa compared to 60 kPa by elastosil. This experiment shows material stiffness will influence air pressure needed. (**Figure 20**)

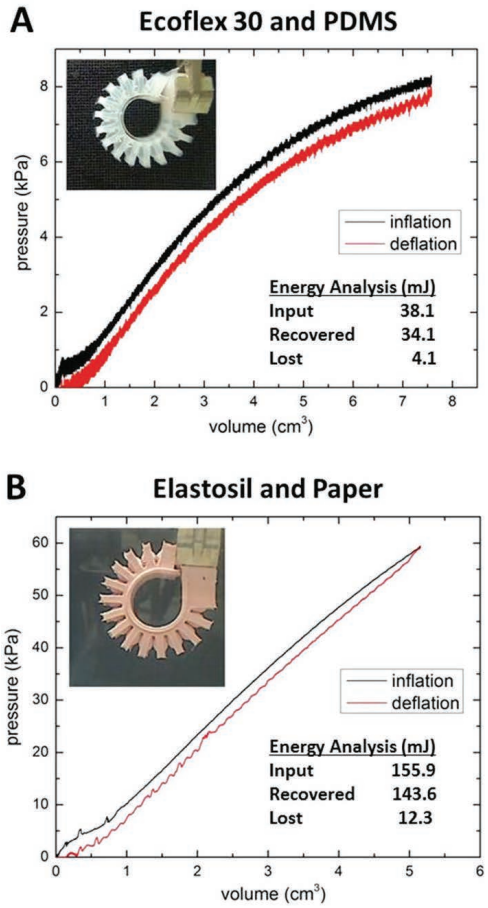

Figure 20: Effect of defferent materials in supplying different air pressure to achieve the same bending. (A) extensible layer ecoflext 30 with inextensible layer PDMS (B) extensible layer elastosil with inextensible layer paper
Source: (Mosadegh et al., 2014)

3. HYPOTHESIS-BASED RESEARCH

3.3. Thin glass

3.3.1. Manufacturing glass

Today, it is very common to use float glass method to produce flat glass. This method is effective and can provide a smooth surface without additional treatment. In **Figure 1**, it shows the process of producing flat glass. The first step is to melt raw material at 1550oC to make sure the molten material is homogeneous. And then, the molten material flows onto floating bath to cool down until 600oC. The next step is to cool the glass sheet into 100oC over the length of 150m to give the glass sufficient inherent strength. In this process, the flat plate gets gained optimum flatness and solidity. After this step, the glass will be cut into pieces and be transported. (Özhan, 2017)

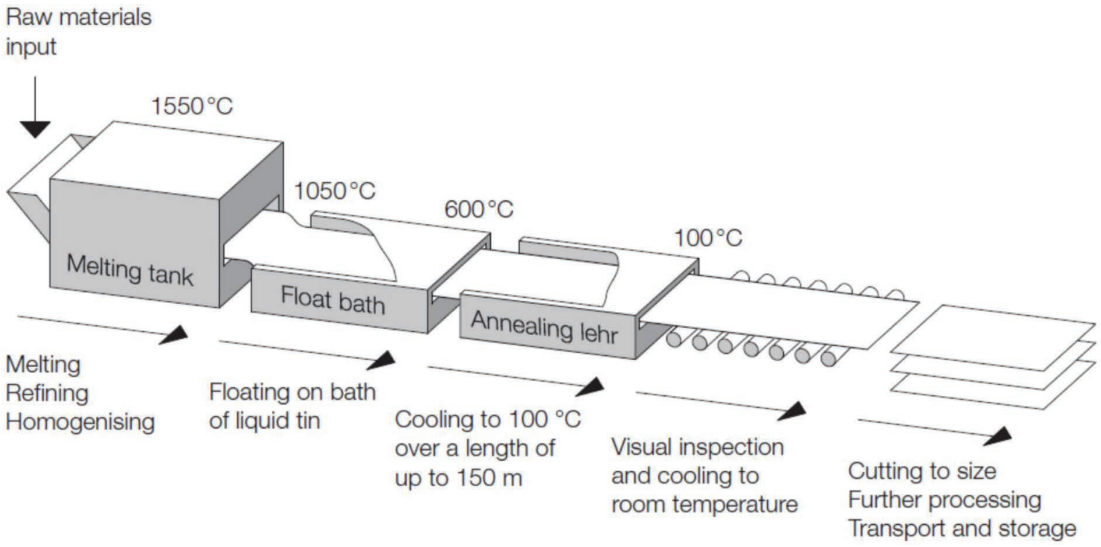

Figure 1: Flat glass producing process
Source: (Özhan, 2017)

Overflow fusion method (**Figure 2**) is first used by Corning as its big key to the innovation in the past two decades. At first, the raw material is merging and melting in a tank above 1000oC. And then the molten glass is released and flow down through V-shaped isopipe to merge into one single plate. The next step is to cool down the glass plate and cut into pieces for packaging and transport. Unlike the other process, overflow fusion can forgo the surface polishing and many other post-process. (Corning Inc., 2017).

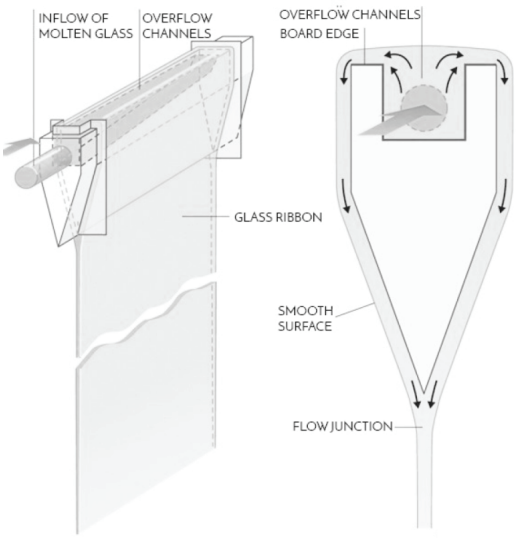

Figure 2: Overflow fusion producing process
Source: (Corning Inc., 2017)

3.3.2. Glass bending radius

Because of in this project, bending thin glass panel is the main goal. Research on bending radius and tensile stress is important. **Figure 3** shows the relationship between bending curvature and stress on the glass top under different glass thickness configurations. From this figure, it is not difficult to give an assumption about the relationship between window opening size, bending radius and tensile stress on the thin glass surface. Also, the tensile strength of chemically prestressed thin glass panel is the threshold of the whole assumption process. These will be discussed in the later chapter. (Nippon Electric Glass Co., 2007)

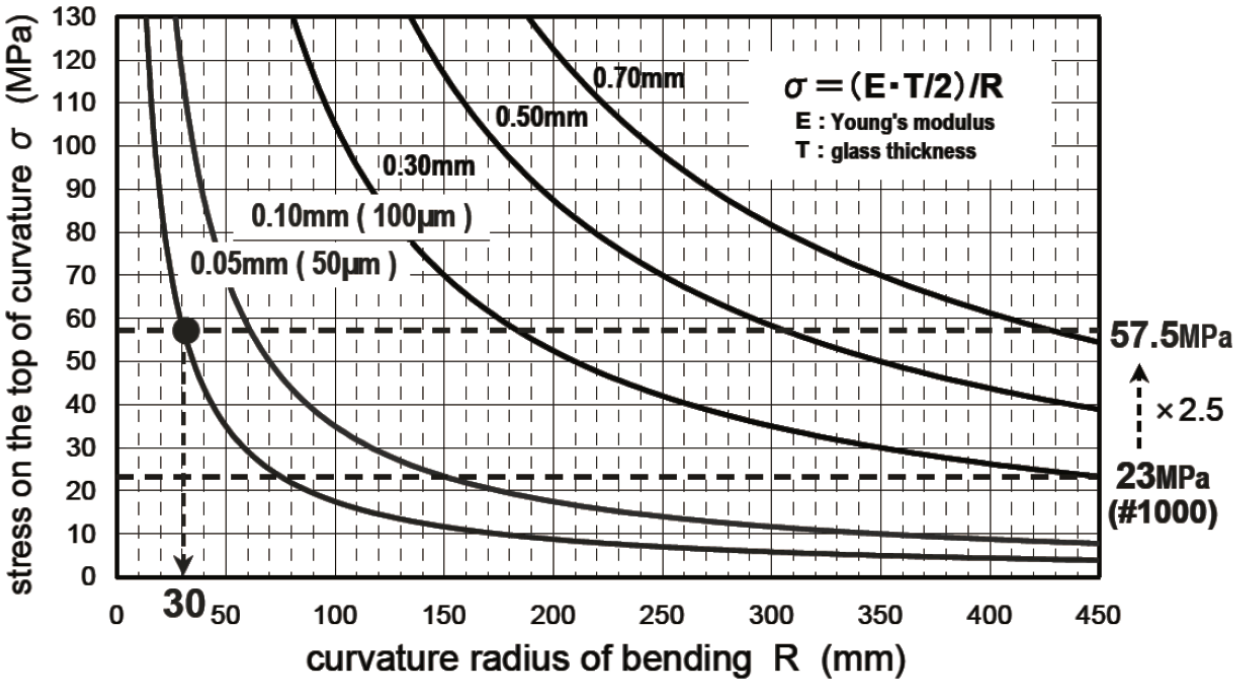

Figure 3: Glass bending radius and stress relationship
Source: (Nippon Electric Glass Co., 2007)

3.3.3. Recent research and practice on thin glass

In this section, I will discuss the thin glass applications in the building environment. First I will list all thin glass master thesis from TU Delft and have a short introduction of what they have done.

First one is Thin Glass Adaptive Facade Panels made by Rafael Ribeiro Silveira 2016. This design focused on how can thin glass second facade be made adaptive. Rafael did some research on thin glass bending behavior in single and double curvature, also how stress will generate by bending thin glass panels. (**Figure 4**)

Figure 4: Thin Glass Adaptive Facade Panels
Source: (Rafael Ribeiro Silveira 2016)

Özhan Topçu´s report about Kinetic Thin Glass Facade focuses on how can kinetic thin glass facade be designed airtight and watertight. Özhan did some research on bending laminated thin glass and simulated the bending behavior. The further design is about detailing the window open system which is very practical. (**Figure 5**)

Figure 5: Kinetic Thin Glass Facade
Source: (Özhan, 2017)

Iris van der Weijde uses thin glass to make a insulating facade panel with honeycomb structure in between. In her research, she not only calculate structure behavior of composite plate, but also, she calculates thermal insulation of her product. In her research, she compares the weight and thermal performance with existing facade system. (**Figure 6**)

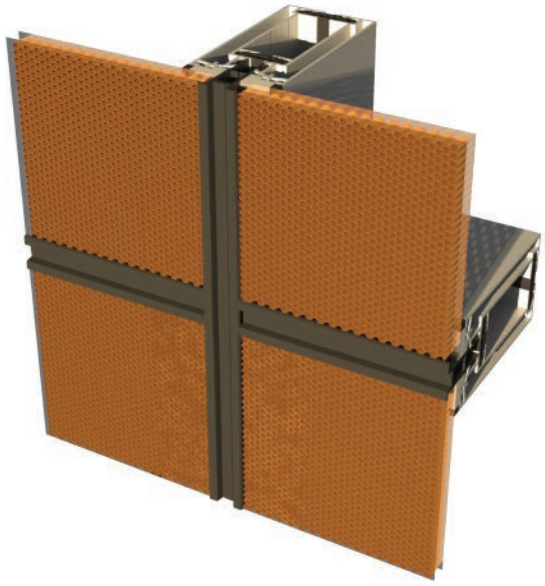

Figure 6: Ultra lightweight, insulating thin glass facade panel
Source: (Iris van der Weijde, 2017)

3.3.4. Prestressing glass:

The main reason of prestressing glass is basic float glass can not resistant environment surroundings. Also, compare to compressive strength, glass tensile strength is significantly lower. The basic float glass cannot avoid exposing itself in tensile circumstance, so prestressing process is very important to protect the glass. Prestressing glass is to give compressive layer on the surface to overcome tensile stress.

In cold bending behavior, glass plates are deformed temporarily and released to spring back. On the surface of basic floating glass, tensile stress will be generated. To prestress the glass and give compressive stress on the surface to compensate tensile stress is necessary. There are some ways to prestress glass: heat strengthened, thermally toughened safety glass and chemically strengthened glass.(Wurm, 2007)

Heat strenthened glass:

Heat strengthened glass is been heat- treated to have a surface compression and is twice as much strength as annealed glass of the same thickness and configuration. (**Figure 7** and **Figure 8**) Heat strengthened glass can resist more thermal load than annealed glass and the fragments are larger than fully tempered glass.(Wurm, 2007)

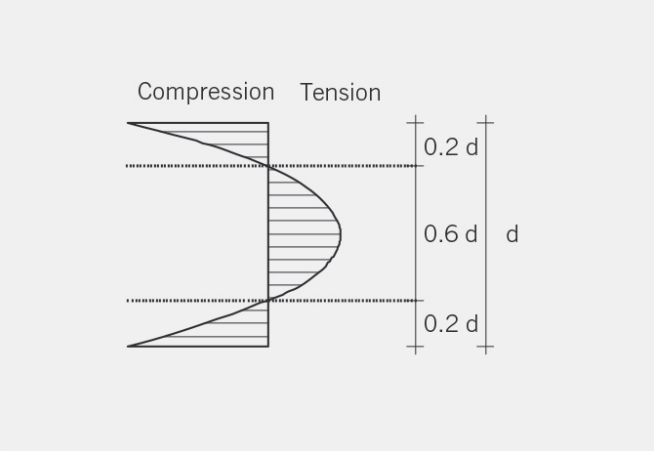

Figure 7: Stress cross-sectional diagram of heat-strengthenedglass
Source: (Wurm, 2007)

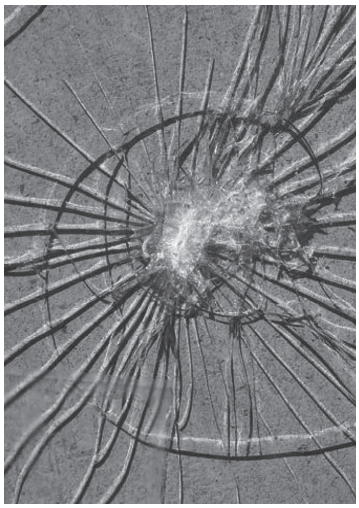

Figure 8: Fracture pattern of heat-strengthened glass
Source: (Wurm, 2007)

Thermally Toughened Safety Glass:

In production, tempered glass cooled more quickly than heat- strengthened glass. This glass is heated to 100 °C higher than transformation point and cooled down fast. In this way, the surface is already cooled down and the inner layer has to expand resulting in compressive stress on the surface and tensile stress in glass core. (**Figure 9-10**)

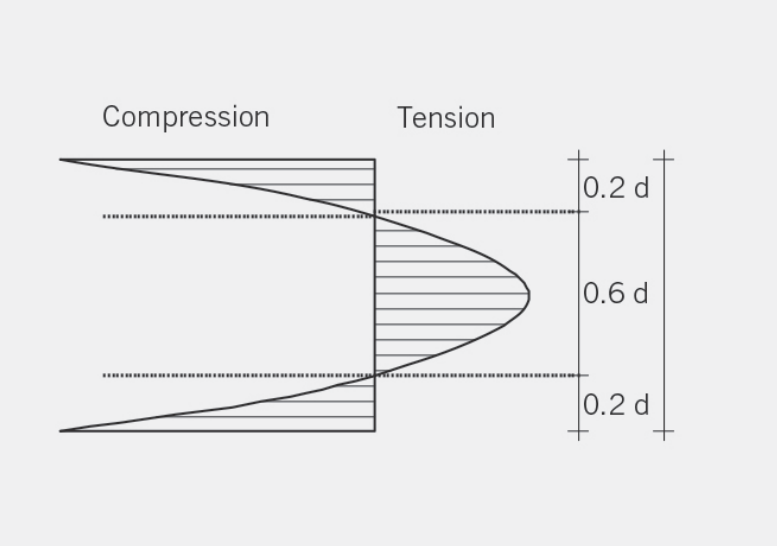

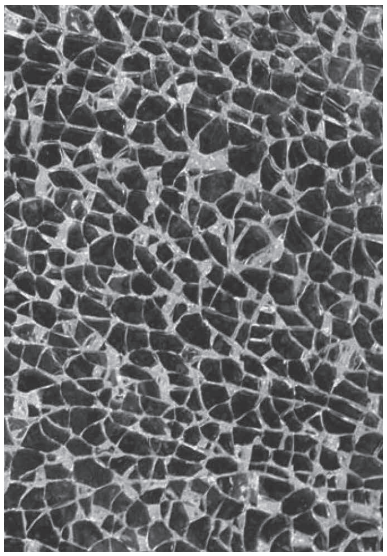

Figure 9: Stress cross sectional diagram of fully tempered glass
Source: (Wurm, 2007)

Figure 10: Fracture pattern of tempered glass
Source: (Wurm, 2007)

Chemically strengthened glass:

In glass material, there are huge numbers of defects distributed through the glass. Actually, the size and numbers of the defects determine how strong the glass is. If the glass is treated without defects, this glass will be 100 times stronger than the glass nowadays. With the current technology, we can not reduce the numbers of defects. But with chemical treatment, we can eliminate the tension force and make the material stronger. Most glass in the world has sodium added to lower the melting temperature. The chemical process is to submerge glass in a potassium salt bath, and through the natural process of diffusion, larger potassium atoms are shoved into space between sodium atoms at a lower temperature than glass softening. The glass is still hard when this process happens. So on the surface of the glass is under compression. (**Figure 11**) The center of the glass will not be effective because the potassium atoms cannot be into glass core fast. So after the process, the surface will be in compression and center will be in tension. (Wurm, 2007)

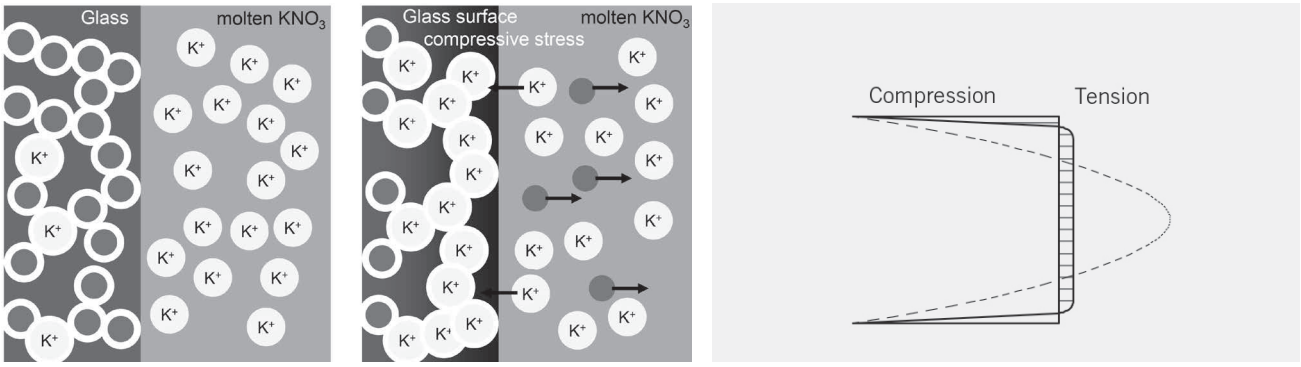

Figure 11: Stress distribution over the thickness of chemically toughened glass.
Source: (Wurm, 2007)

Cold bending laminated glass:

Two thin glass layers laminated with polyvinyl butyral(PVB) results in a composite material. Under bending load, different layer acts differently and influences each other resulting from the linear-elastic behavior of thin glass and viscoelastic behavior of PVB. The nonlinear elastic behavior of laminated glass panel is mostly learned from experiments and verified by numerical analysis. (Molnár, Vigh, Stocker, & Dunai, 2012)

Two-layer laminated glass plates behave structurally in between two states. (**Figure 12**) When there is no bonding between thin glass and PVB, compressive-tensile stress is the same as the stress in the monolithic panel. The second state is that when thin glass completely bond with PVB, compressive-tensile stress changes to single transition with the lower peak. (**Figure 13**) In reality, the compressive-tensile stress stays between these two states. (Molnár et al., 2012)

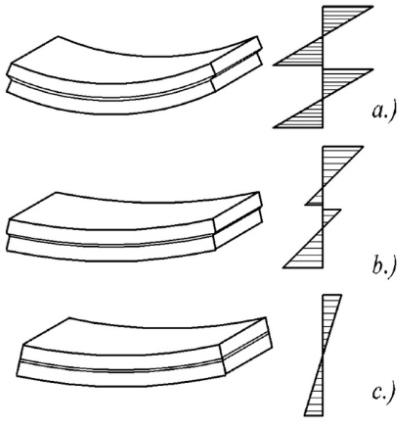

Figure 12: Interaction between two glass layers.
Source: (Molnár et al., 2012)

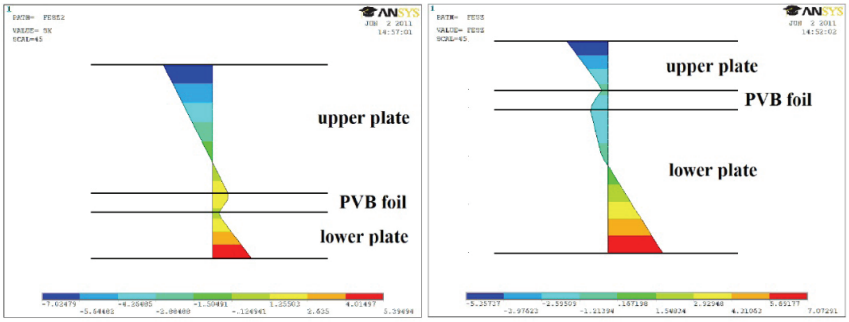

Figure 13: Stress distribution from different lamination configuration.
Source: (Molnár et al., 2012)

The relationship between bending, stress and reaction force was illustrated by Özhan Topcu through comparison from numerical results. (**Figure 14-17**) The size of the panel is 1000mm*2070mm. In this comparison, parameters are glass thickness, PVB thickness, and effect of an asymmetric configuration. (Özhan, 2017)

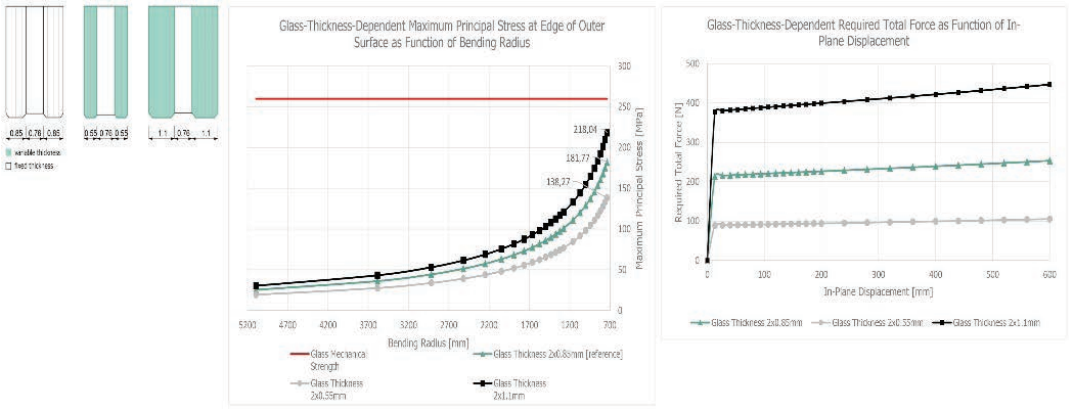

Figure 14: Different glass thicknesses influence relationship between maximum principal stress, bending radius and required force

Source: (Özhan, 2017)

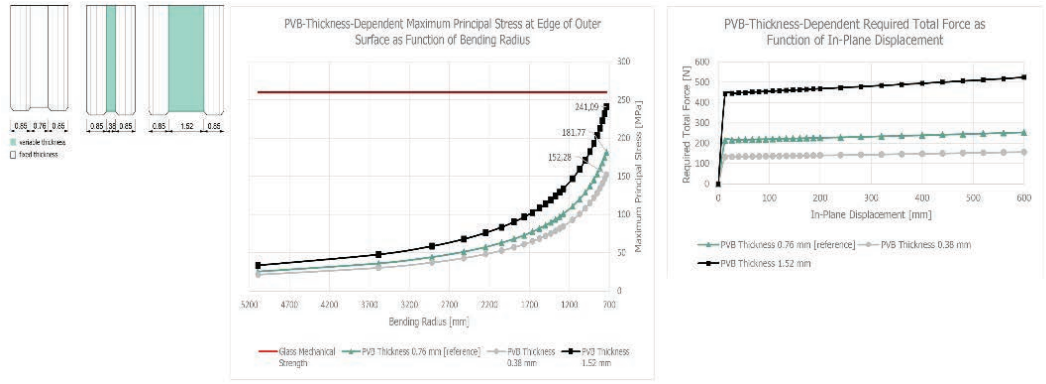

Figure 15: Different PVB thicknesses influence relationship between maximum principal stress, bending radius and required force

Source: (Özhan, 2017)

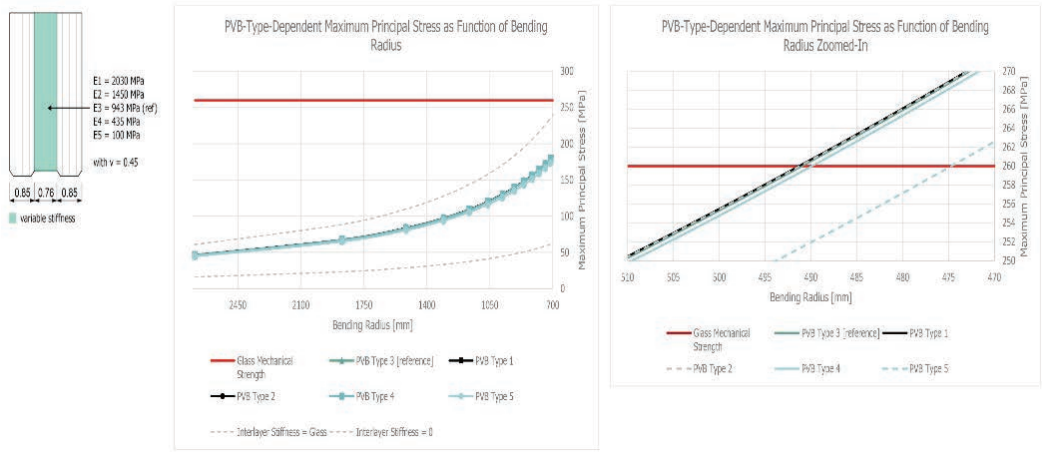

Figure 16: Different PVB stiffness influences relationship between maximum principal stress, bending radius and required force

Source: (Özhan, 2017)

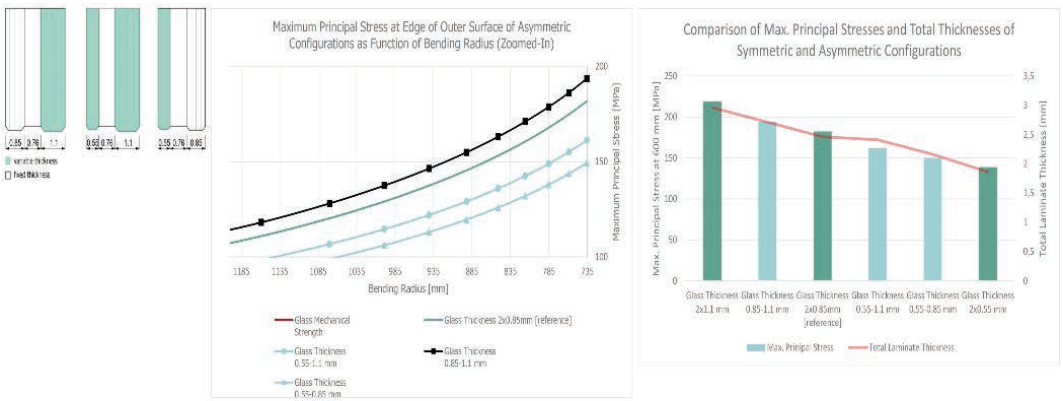

Figure 17: Asymmetric configurations influence relationship between maximum principal stress, bending radius and required force

Source: (Özhan, 2017)

In any case, the constant-curvature shape by cold-lamination-bending creates more stress concentration in PVB layer than sinusoidal-curvature shape which provides a much smoother shear stress distribution.(Galuppi & Royer-Carfagni, 2015) (**Figure 18-19**) Gradually releasing the bending movement can result in softening the stress concentration in PVB inner layers.(Galuppi & Royer-Carfagni, 2015)

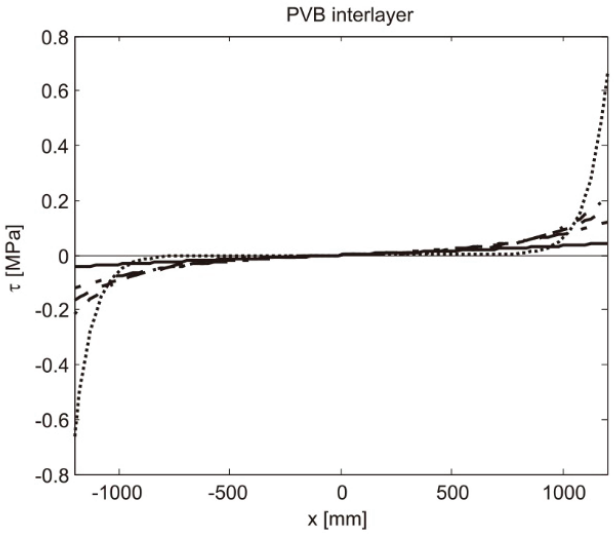

Figure 18: Constant-curvature cold-lamination-bending Shear stress in the interlayer for various times t

Source: (Galuppi & Royer-Carfagni, 2015)

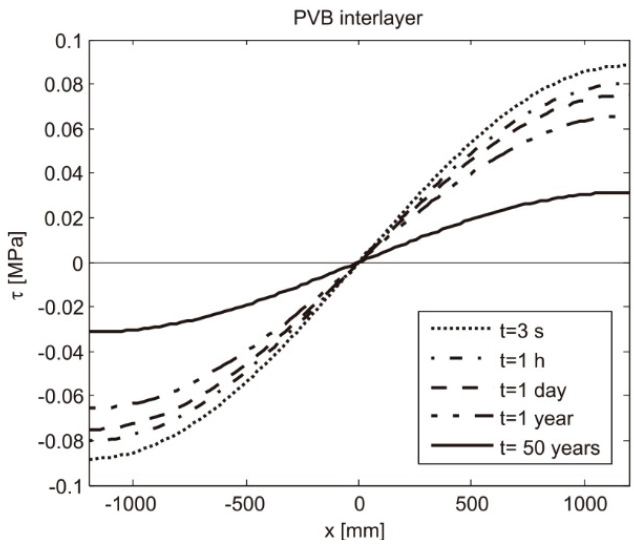

Figure 19: Constant-curvature cold-lamination-bending Shear stress in the interlayer for various times t

Source: (Galuppi & Royer-Carfagni, 2015)

3. HYPOTHESIS-BASED RESEARCH

3.4. Indoor comfort

3.4.1. Fanger's drought model:

People feel uncomfortable when draught happens. Draught is caused by unwanted cooling air movement, which makes people feel cold. When draught happens, People in the room may stop ventilation systems or close windows. In the winter time, draught may cause energy assumption increasing due to a usage of a radiator. According to Fanger's experiment (Fanger, Melikov, Hanzawa, & Ring, 1988), air temperature, air velocity, and turbulence intensity are the three main aspects influencing human's feeling about draught (**Figure 1**). From Fanger and Pedersen's experiment, fluctuating air flow causes human more uncomfortable than laminar airflow does. The experimental conditions are valid for the air temperature of 20-26 oC, air velocity of 0.1-0.4 m/s and turbulence intensity of 10-70%.

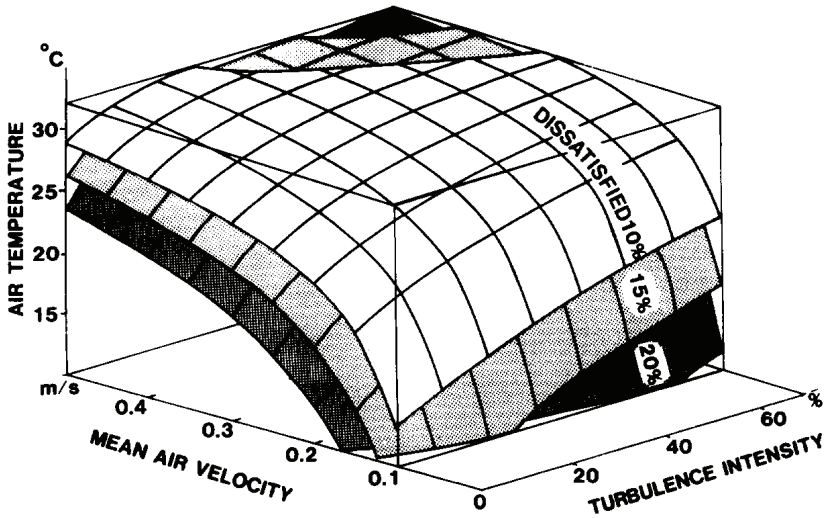

Figure 1: Three dimensional draught-risk model.
Source: (Fanger, Melikov, Hanzawa, & Ring, 1988)

The equation from the experiment is :

$$PD = 3.143*(34-t_a)(\bar{v}-0.05)^{0.6223}+0.3696\bar{v}Tu(34-t_a)(\bar{v}-0.05)^{0.6223}$$

for $\bar{v}<0.05$ m/s insert $\bar{v}=0.05$ m/s
for PD>100% use PD=100%

As the model and equation showed above, airflow with higher turbulence intensity will make people in the room more uncomfortable when the temperature and air velocity are the same. The lower temperature of the air flow will increase more complaint than warmer air when the velocity and turbulence intensity keep constant. (Fanger, Melikov, Hanzawa, & Ring, 1988)

This investigation shows the complexity of human mental performance and indoor environment. In many fields, measurements have illustrated that thermal comfort is different in air-conditioned and naturally-ventilated situations. The comfortable temperature range and acceptable mean velocity are much higher in naturally ventilated rooms. (Cui, Cao, Ouyang, & Zhu, 2013) To simulate air flow from natural ventilation, the experiment has been done to use the fan for airflow supplying. However, airflow from fans is different from natural ventilation because of turbulence intensity and spectral characteristics. (Ouyang, Dai, Li, & Zhu, 2006)

3.4.2. Aerodynamic theory:

Aerodynamics is the about studying liquids and gases movement. In aerodynamic theory, when objects move through the still fluid, the science is the same when fluid moves through a still object. No matter which situation happens, air resistance occurs. When air resistance happens, airflow will become turbulent flow or laminar flow. The surface geometry and surface properties will influence airflow type. For instance, when sports car drives through the stationary air, the air remains laminar, however, when a truck moves through the air, it will generate turbulence air flow. Air resistance also calls drag, which is the force that moving objects resist. Drag increases according to the square of speed. When the wind passes through the curved surface like a sports car, the air particles don't move at all, but the adjacent air layer moves faster. All layers move faster than previous layer, which causes friction drag. On the other hand, when the surface is rougher, there will be more friction drag and turbulent. The drag is called form drag. (**Figure 2**)

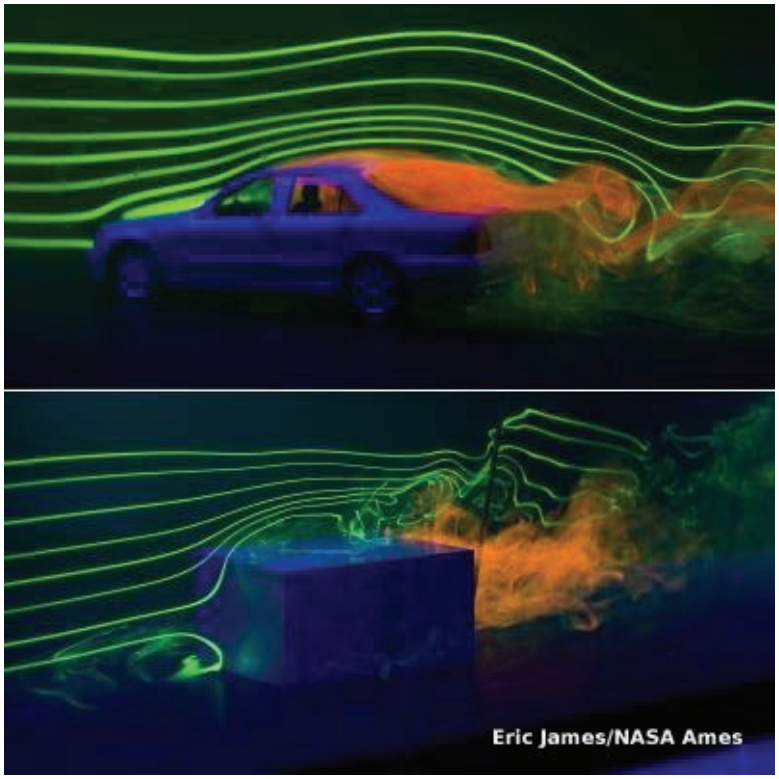

Figure 2: Friction drag on sports car and form drag on obstructive the object
Source: Eric James courtesy of NASA Ames Laboratory

3.4.3. Laminar, turbulent air flow and Reynolds number:

Because of the friction on object surface influences airflow type, there is an important parameter called Reynolds number which determines the type of airflow. In the case of the sphere, the equation is:

$$R_e = \frac{\rho d v}{\eta}$$

d is the diameter of the sphere, ρ is the density of the air, v is the air velocity, η is the viscosity of the air.

4. DRAFT DESIGN

4.1. Idea generation:

Based on previous research, how to use the knowledge to make draft designs is the main goal of this chapter. The idea generation process and methods will be discussed here. The result of idea generation will be a list of designs and analysis of the feasibilities. After explaining the list of designs, selection will be the next step in this chapter. Feasible design concept will be selected and put into next chapter to analyze.

To simplify next step which is to build up mathematical model, an idea generation phase, just single curvature behavior will be discussed. First of all, some sketches will be discuss below:

Bi-direction window actuator:

SPA can be fixed on the top or bottom, and the pipe can be inserted into SPA. There can be two separate actuators outside and inside. When the outside actuator is inflated, the window will open towards inside, when the inside actuator is inflated, the window will open towards outside.

However, if outside and inside actuators can work at the same time, both actuators will make two glass panels bend more effective. For example, in the **Figure 1** and **Figure 2**, when inputting air from the red line, inside actuator and outside actuator will both bend towards inside. When inputting air from the blue line, inside and outside actuator will bend towards outside. In this design, bi-direction actuator needs to be used. The problem with this design is SPA extensible layer connecting inextensible layer which makes shear movement difficult when the window is bending. The way to solve this problem is using sliding equipment connecting SPA and thin glass.

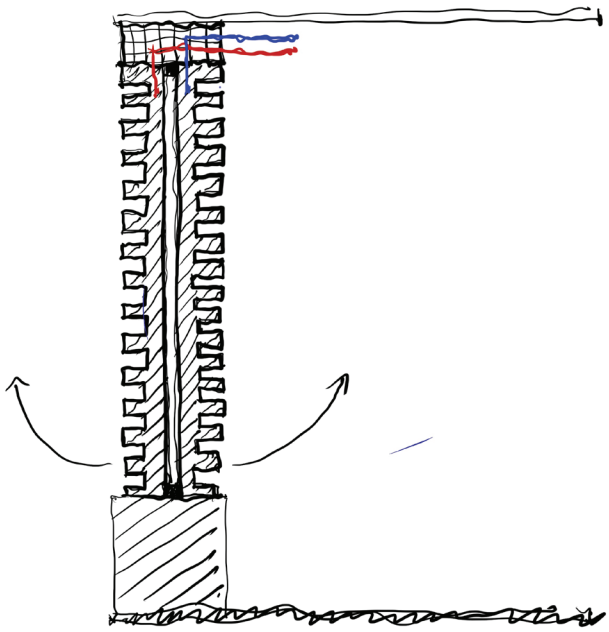

Figure 1: Bi-direction top-fixed window actuator
Source: Own image

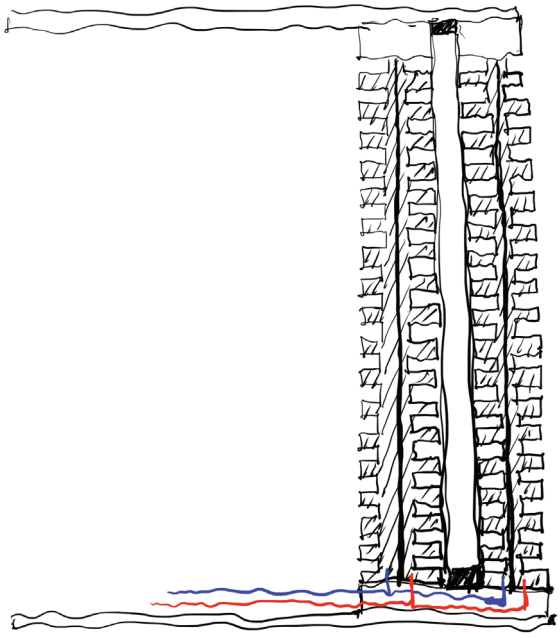

Figure 2: Bi-direction bottom-fixed window actuator
Source: Own image

Jamming chamber embedded actuator

In this design(**Figure 3**), I combine the jamming chamber idea with SPA idea for making the actuator stiffer. In the sketches, the jamming chamber can be located near the SPA chamber. The jamming chamber just needs to be vacuumed when inflation of SPA is finished. The reason to vacuum jamming chamber is to increase the stiffness to resist wind load.

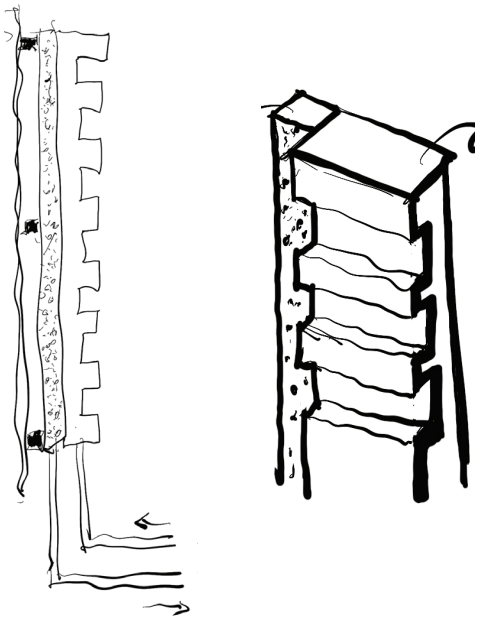

Figure 3: Jamming chamber embedded actuator
Source: Own image

Single direction opening actuator:

Instead of the opening window in two directions, this design will be much simpler. To avoid the complicity of engineering the first design, I attached SPA on the window surface and hung the top edge to the window frame. When input air into the cavity, the window will bend along the curvature generated by SPA. The other option is to fix SPA on the edge beam and use to beam to bend the window (**Figure 4** and **Figure 5**).

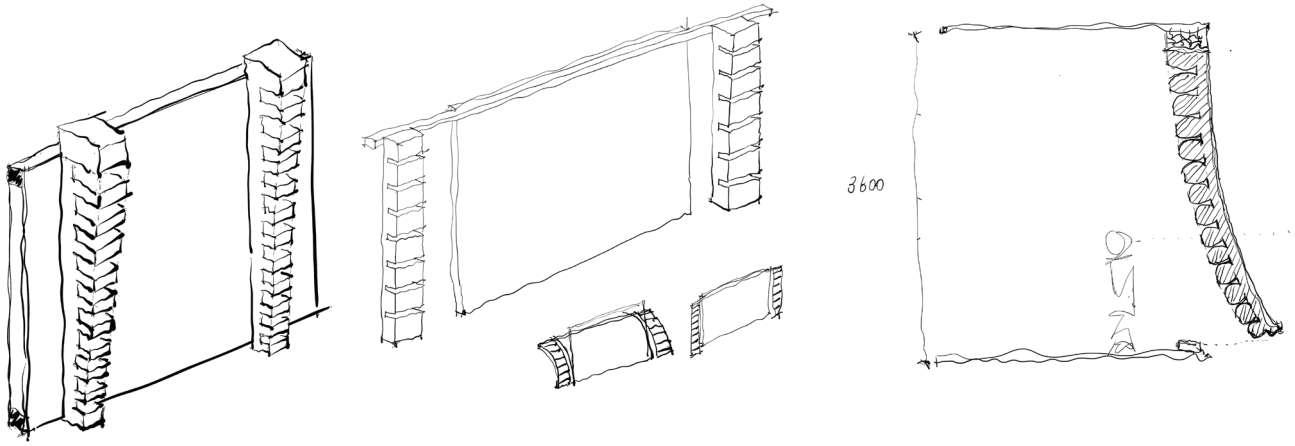

Figure 4: Single direction opening actuator
Source: Own image

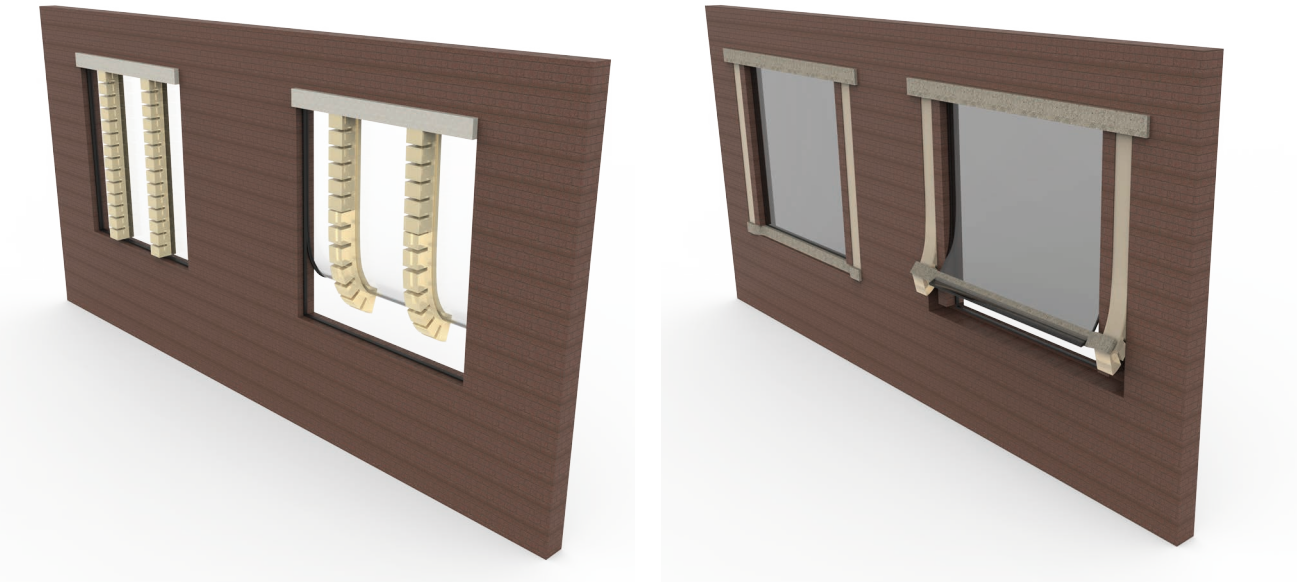

Figure 5: Single direction opening actuator rendering
Source: Own image

Four opening directions window

To make the window more adaptable to outside environment, mainly to wind direction and wind load, I design the four opening directions window which can be opened in four edges. In the middle, there is one fixed point with glass panel by using cable fixing on the four corners. In the middle, four SPA beams attached to glass panel can be controlled separately. (**Figure 6** to **Figure 10**)

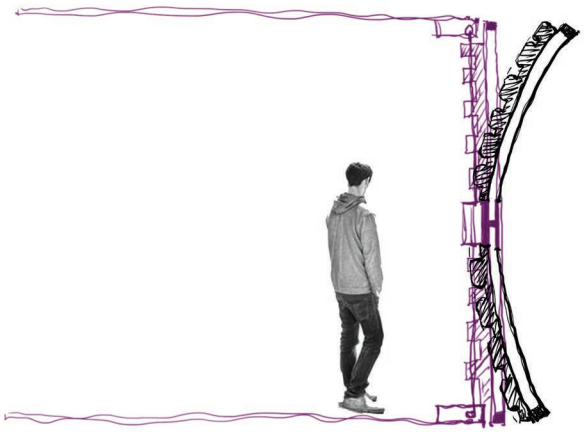

Figure 6: Four opening directions window
Source: Own image

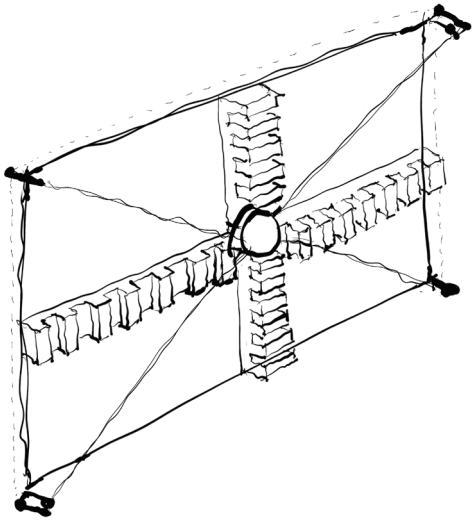

Figure 7: Four opening directions window
Source: Own image

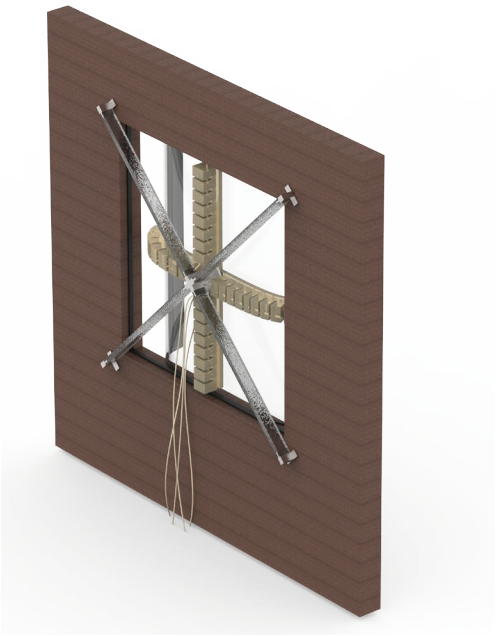

Figure 8: Four opening directions window rendering
Source: Own image

Figure 9: Four opening directions window rendering
Source: Own image

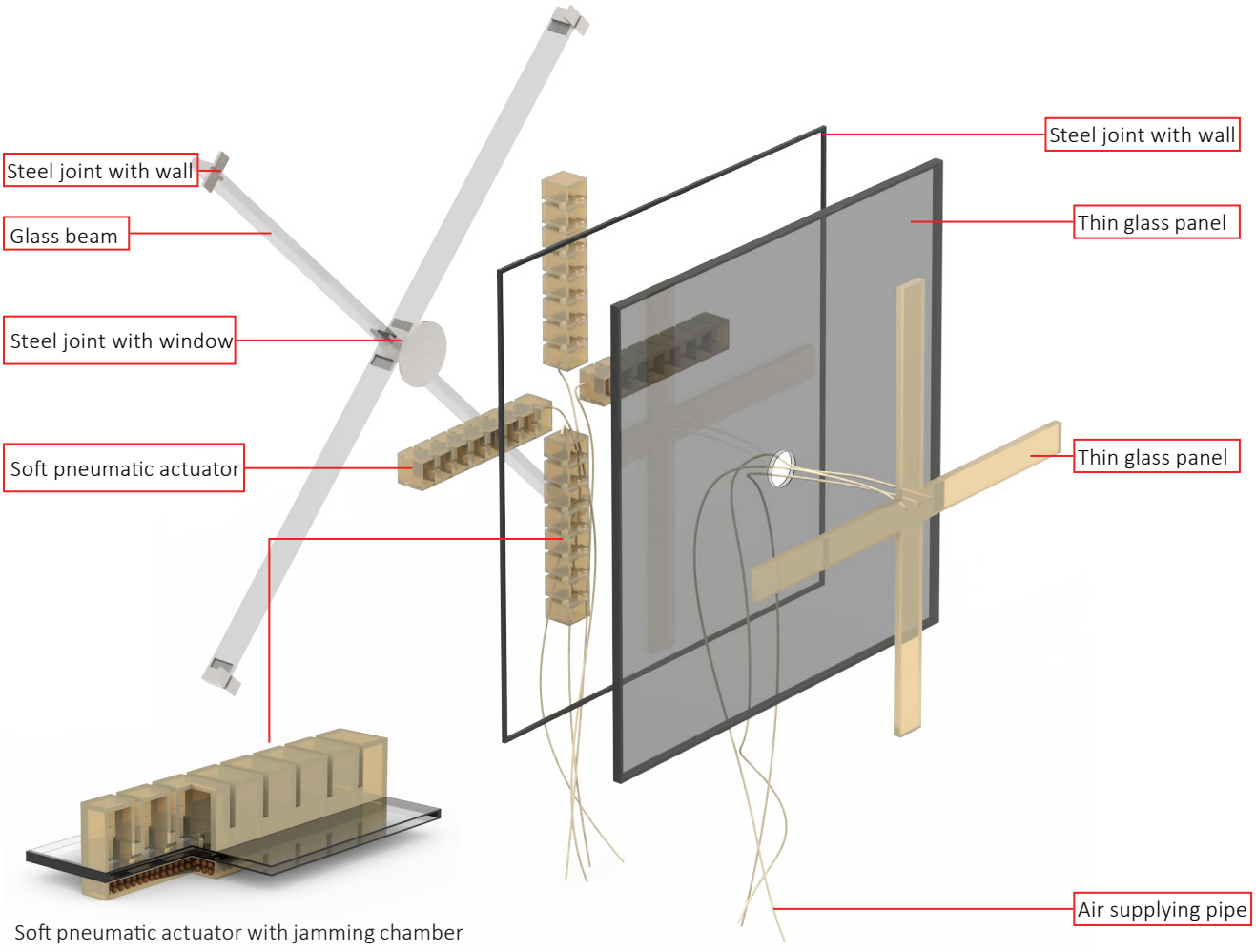

Figure 10: Four opening directions window rendering
Source: Own image

When the window is closed, ΔP1=0, ΔP2<0, the outside jamming chamber is vacuumed for increased stiffness. The second step is preparing to open the window, the jamming chamber needs to be released and input air pressure into SPA chamber. When a window opens into desirable status, SPA cavity pressure needs to be kept the same, meanwhile, the jamming chamber needs to be vacuumed to increase stiffness. (**Figure 11**)

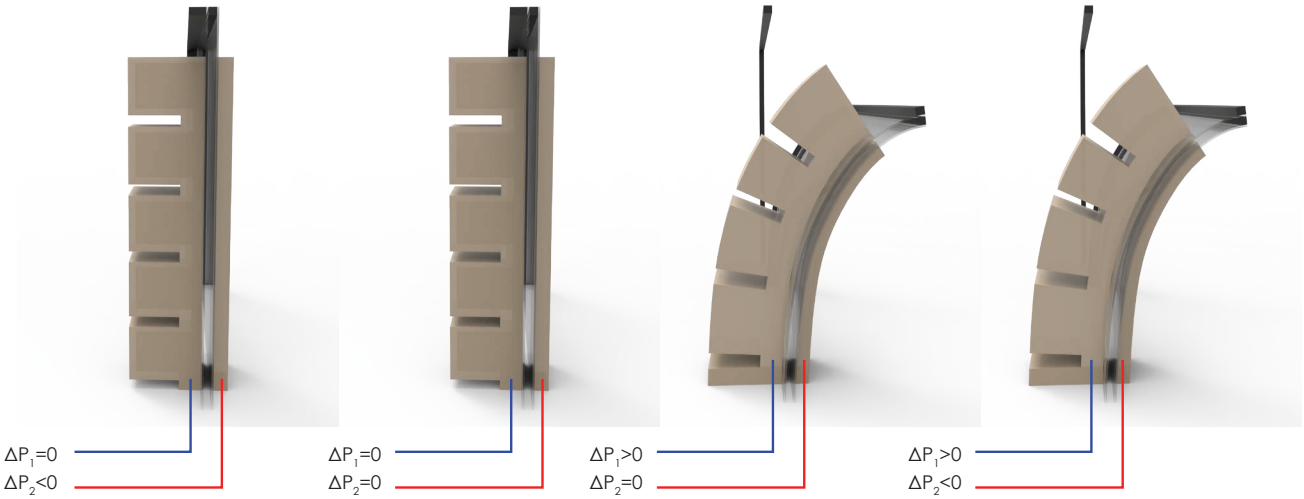

Figure 11: Inflating air chamber and jamming chamber opening process
Source: Own image

Single direction opening window

To simplify the design process, and not to make the system too complicated, I designed a window just opening in one direction. The window frame is made of aluminum, and SPA ends are fixed on the metal supports. Pipes go through the hollow profile and connect with SPA. (**Figure 12**)

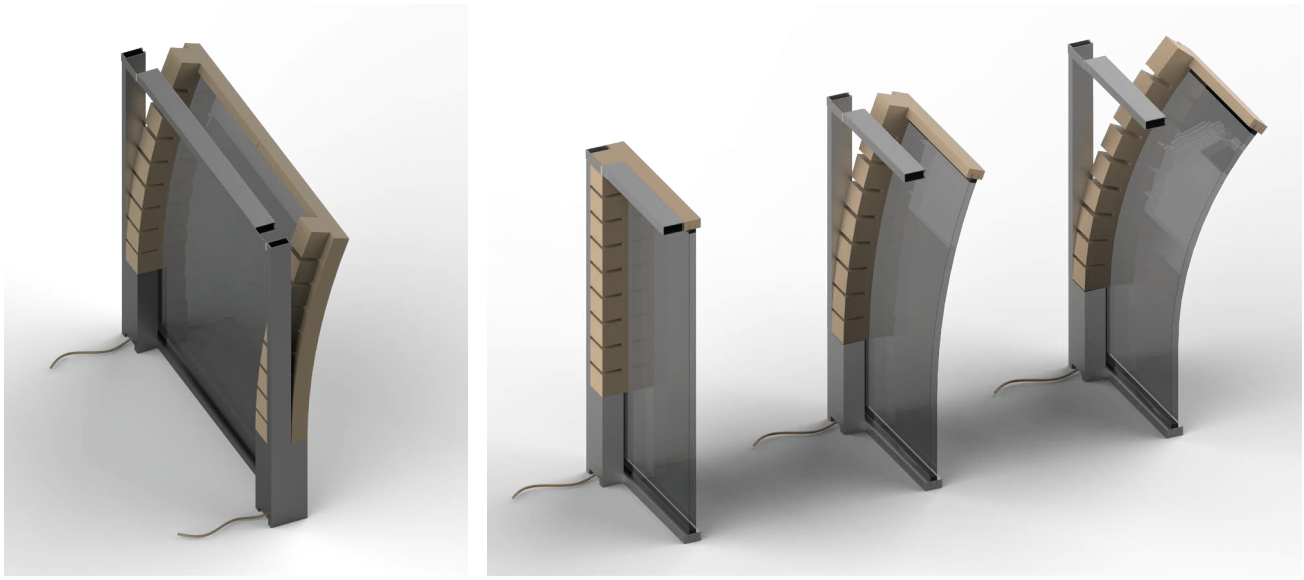

Figure 12: Single direction opening window
Source: Own image

In grasshopper, I make a parametric geometry script by changing the segments number, hight, width, wall thickness and air chamber size. The reason I made this model is for the simulation next step. In FEM simulation, the geometry cannot change at the same time when the result is not what we want. So if I make a new model by changing the geometry, it will take a long time. So in grasshopper, the geometry can be changed and baked into Abaqus CAE for simulation. This iterative process can help to save time.

At first, I make a center box and deconstruct the brep into different items. Because the sidewall thickness is different, the contacting part needs to be thinner for large deformation but the other side needs to be thicker for robust. (**Figure 13**)

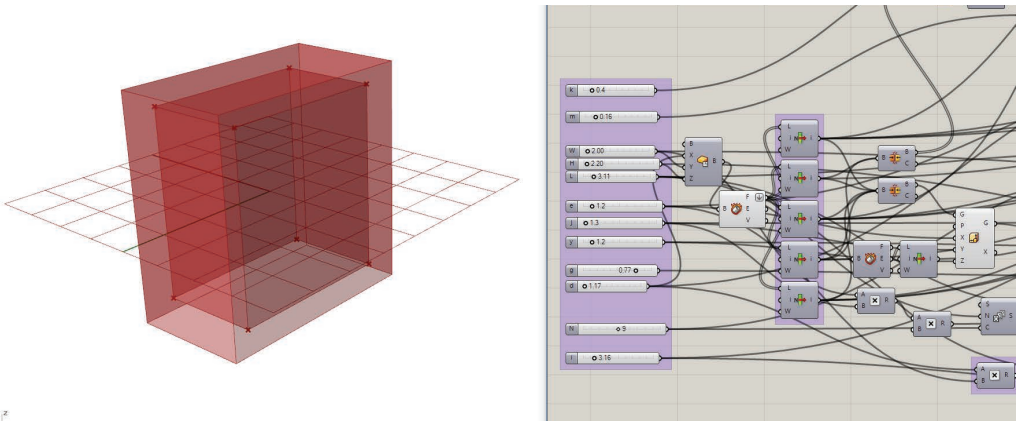

Figure 13: Center box and script
Source: Own image

The second step is to move the outer layer up and build the connection between two segments and manipulate the contacting wall thickness by the slider. The important part is to separate sliders into controlling contacting wall thickness and controlling other sidewall thickness. The segments number can be controlled by a separate slider. (**Figure 14-16**)

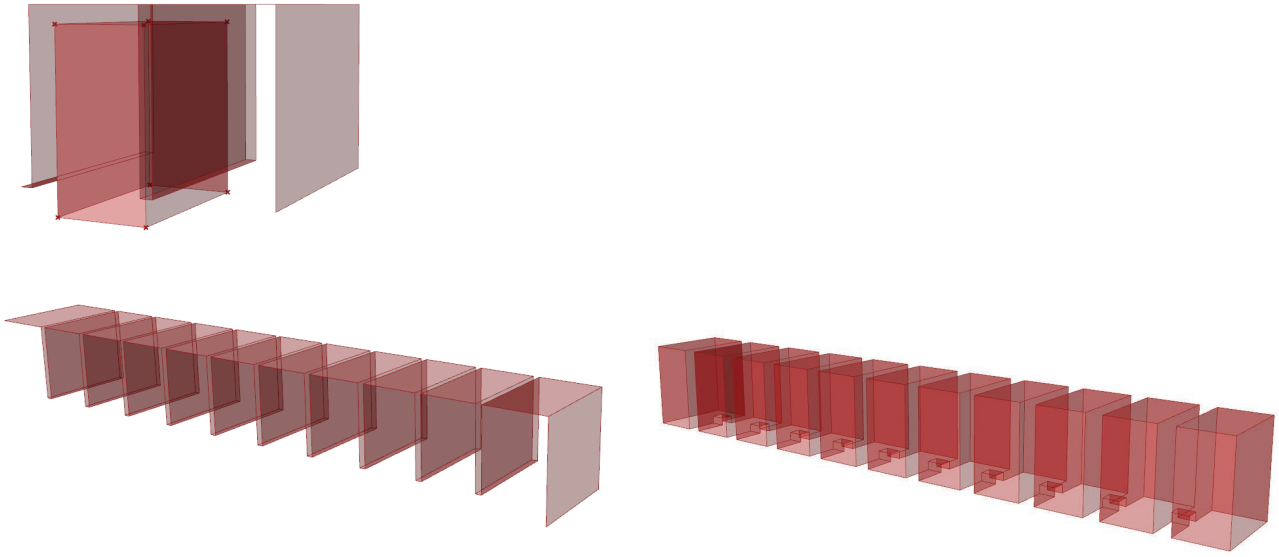

Figure 14-16: Wall thickness setting
Source: Own image

The last step is to assemble the model and separate the end wall thickness from contacting wall thickness. Because in the final product, the end surface will not expand too much also, the end surface will connect to the window frame. Keeping it robust will make the actuator more stable. (**Figure 17**)

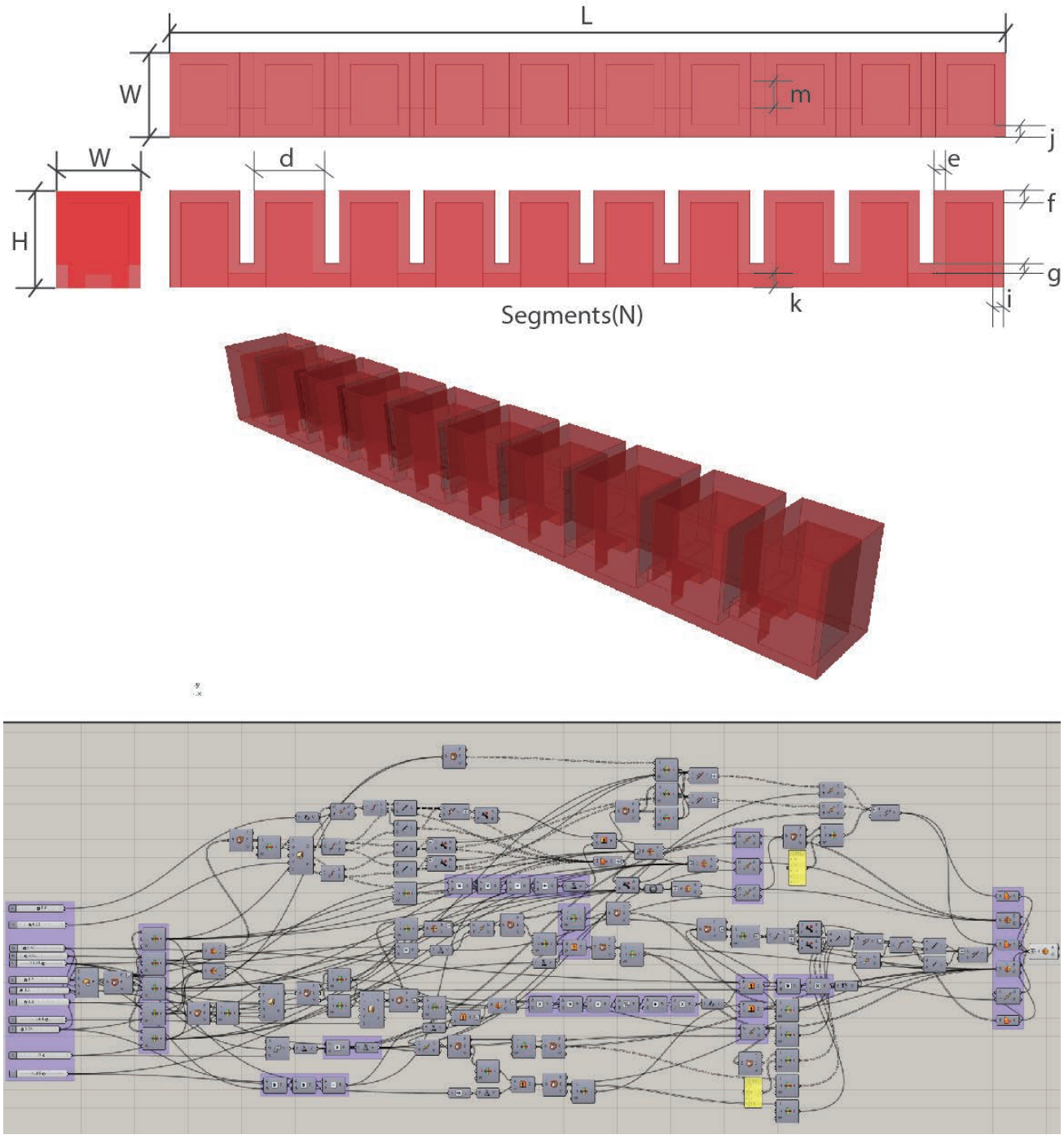

Figure 17: Final geometry and script
Source: Own image

In this project, except for the regular SPA shape, I also think about how the curve will be generated if the geometry is different. To keep it simple, I still use the regular block shape as SPA segment, but the segments are different from each other. In grasshopper, I make the similar concept by connecting each air cavity geometry to each slider. I will explain how it works below.

At first, I start with locating points, which can be changed separately. Every two adjacent points are connected into lines, and by changing numbers in sliders, the length of lines can be changed at the same time. The tricky part is the distance between each two-line should be the same and but changing sliders, the lines cannot overlap with each other. So I use maximum and minimum components. The reason I use points for location is the lines can be extruded into boxes. (**Figure 18**)

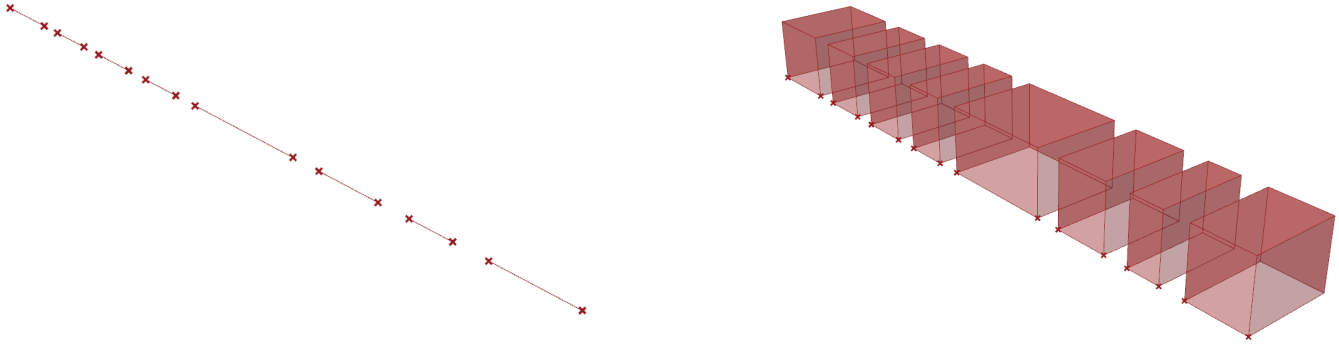

Figure 18: Seperate box size control
Source: Own image

The second step is the similar step like the first model, exploding the geometry and separate the contacting wall thickness and other walls thickness. And the last step is to assemble the model. (**Figure 19**)

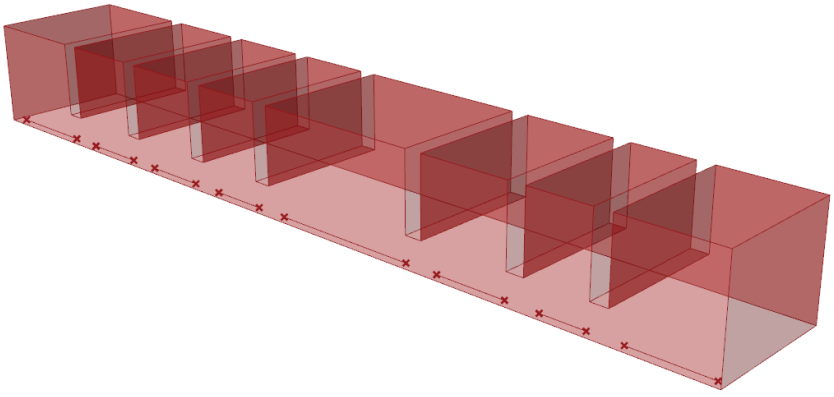

Figure 19: Wall thickness setting
Source: Own image

In this model, I use the same method as the first one. But the numbers of segments cannot be changed by sliders, the only way is to add another point and plug into the script. When the model is finished, the next step will be the simulation in FEM. Because of the time limitation, this model will not be simulated in this project, but this option could give some inspiration to the next researchers in the future. (**Figure 20**)

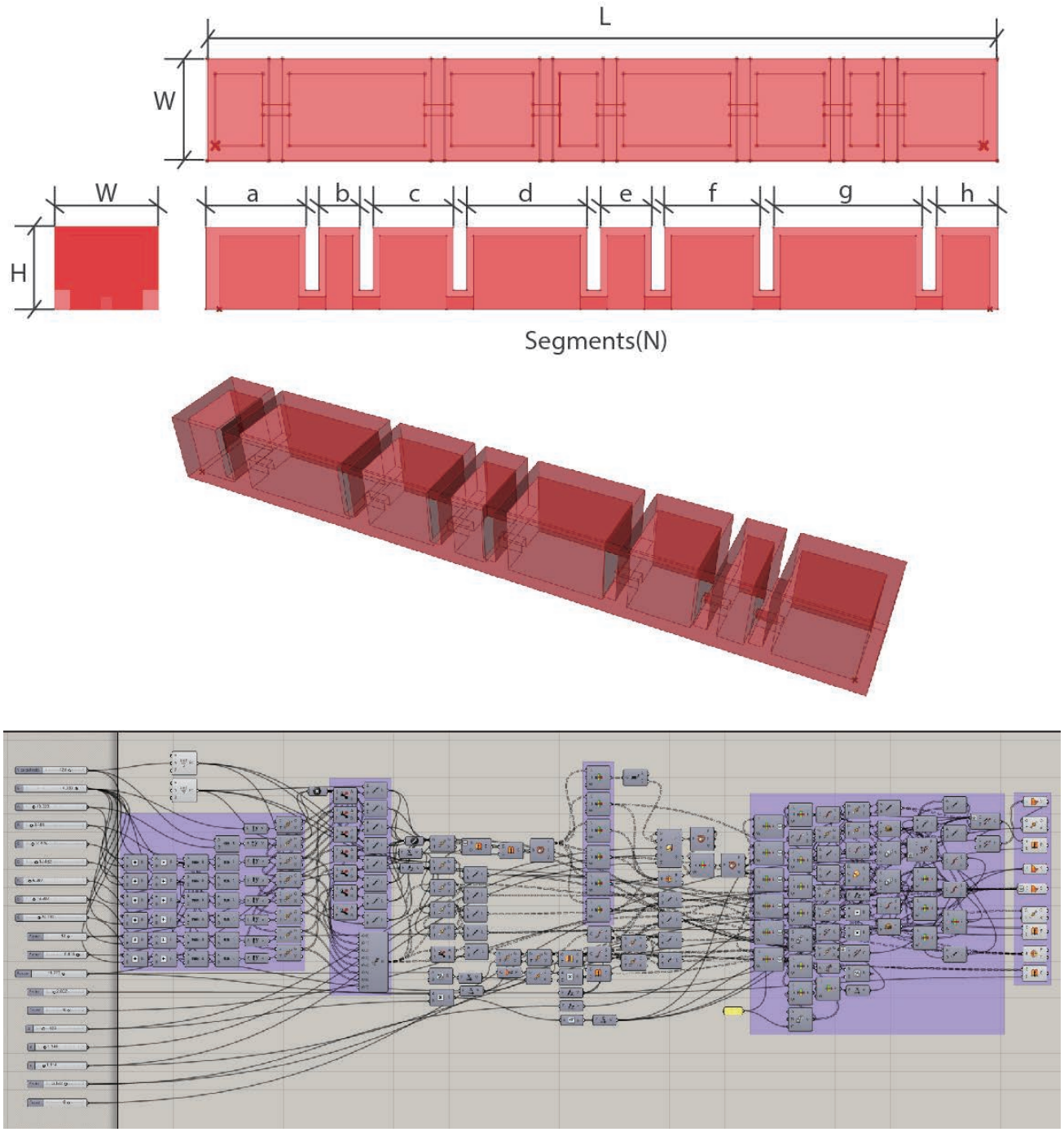

Figure 20: Final geometry and script
Source: Own image

5. MATHEMATICAL MODEL AND ASSUMPTION

The main goal of this chapter is to build up the mathematical model and develop feasible configurations. Based on previous research, there are three main mathematical models which need to be connected by the same parameters. The three main mathematical models are a soft pneumatic model, insulated thin glass model, and natural ventilation model.

First is the soft pneumatic model, as explained by the mechanism before, the most bending behavior comes from contact. And stretching can be neglected. (**Figure 1**)

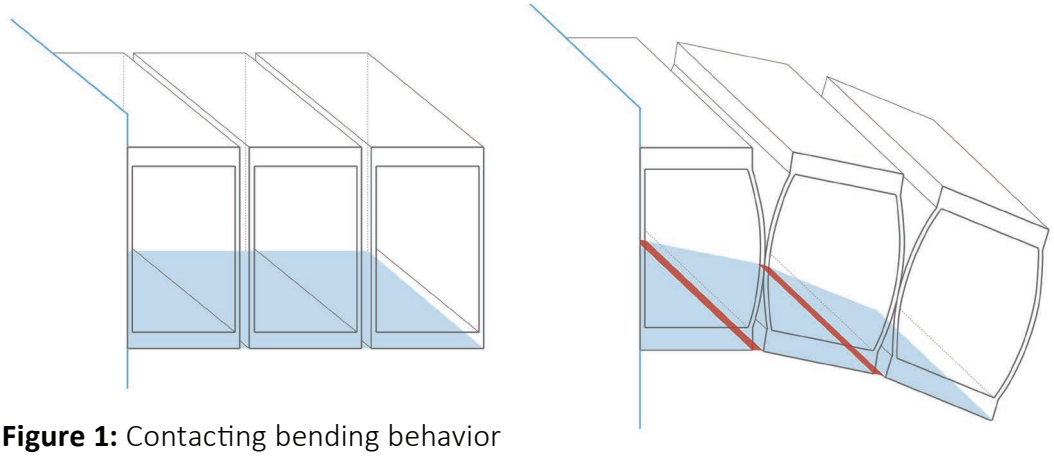

Figure 1: Contacting bending behavior
Source: Own image

The second model is insulated thin glass model. Even though thin glass is flexible and can be bent into the small radius, the composite insulating window will be much more rigid. This also depends on the thickness of composite window. If the spacer is made of rigid material, from the equations,

$$I_1 = \frac{b_1}{12}(h^3 - h_c^3)$$

$$I_2 = \frac{b_2}{12} h_c^3$$

$$EI_{effective} = EI_1 + EI_2$$

As the thickness increasing, moment of inertia increase rapidly. EIeffective will also increase rapidly because (h3-hc3) is large. However, with the high stiffness, will the SPA bend this composite window? This can be answered by calculating. (**Figure 2**)

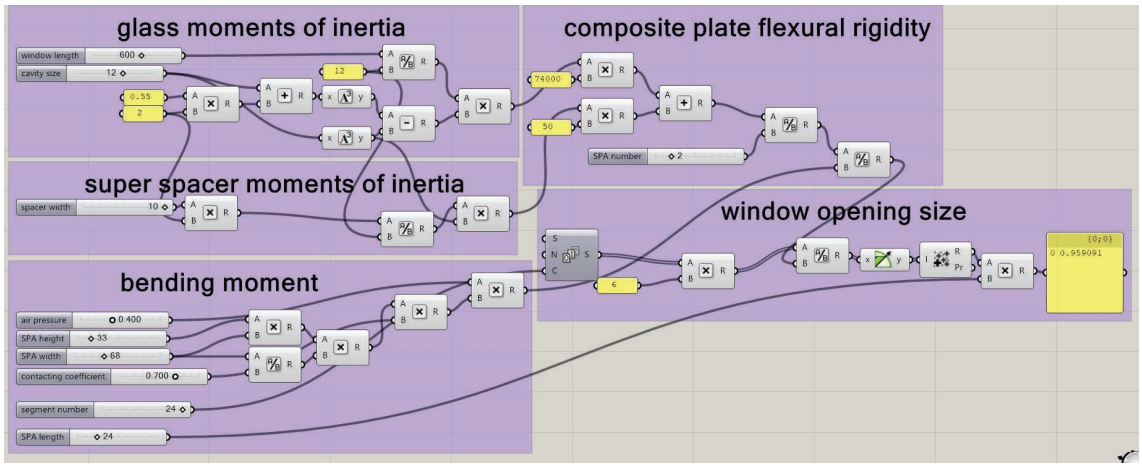

Figure 2: Window opening size calculation
Source: Own image

From the result in grasshopper, the length of window 600mm, cavity 12mm, 0.4MPa air pressure, and 33mm*68mm*0.7 contacting surface area, the window opening size is just 0.96mm. It is obvious that the window is not open at all. There are two ways to open the window, one of them is increasing bending moment from SPA by enlarging SPA size and increasing SPA number. The other way is to decrease the stiffness of windows by changing adhesive between thin glass and spacer. (**Figure 3**)

Method 1:

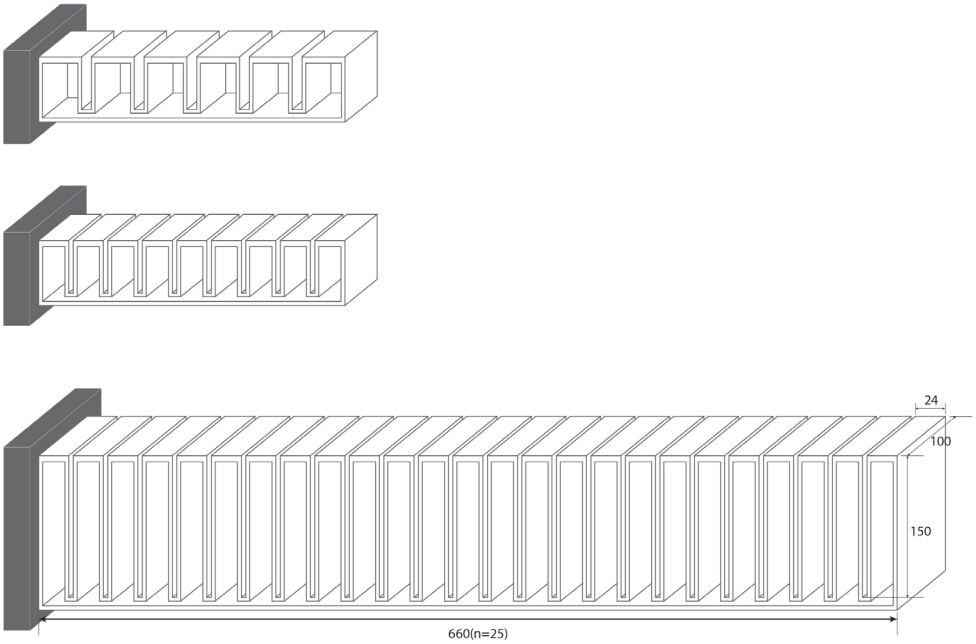

Figure 3: Changing SPA geometry
Source: Own image

Method 2:

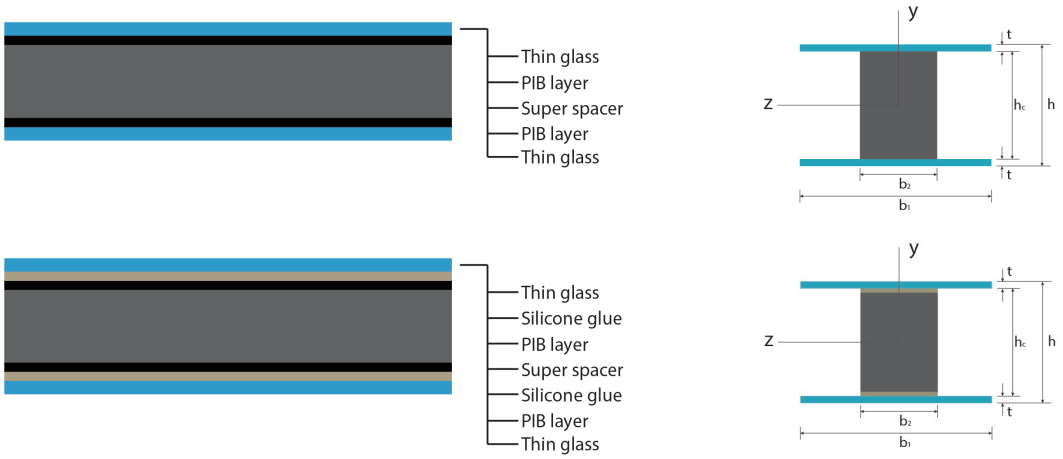

Figure 4: Decrease insulating window stiffness
Source: Own image

The second method is more feasible by using silicone adhesive between thin glass and spacer. Also, the aluminum spacer cannot be used in this product. Super spacer from Edgtech will be used here. Connecting thin glass and super spacer with silicone adhesive will decrease the stiffness of composite window. (**Figure 4**)

$$I_1 = \frac{b_1}{12} t^3$$

$$I_2 = \frac{b_2}{12} h_c^3$$

$$EI_{effective} = EI_1 + EI_2$$

It is difficult to compare the results just from the fomulas. So, in this project, the thickness of the thin glass and super spacer is 0.55mm and 12mm respectively. Without silicone layer, $EI_{effective}$ is 1.9*109 Nmm2. With silicone layer, $EI_{effective}$ is 1.3*106 Nmm2, which is much lower than the previous composite plate. Also from the experiment, it is obvious that under the same weight, silicone lamination window will deform more than PIB lamination window.(**Figure 5** and **Figure 6**)

Figure 5: PIB lamination window
Source: Own image

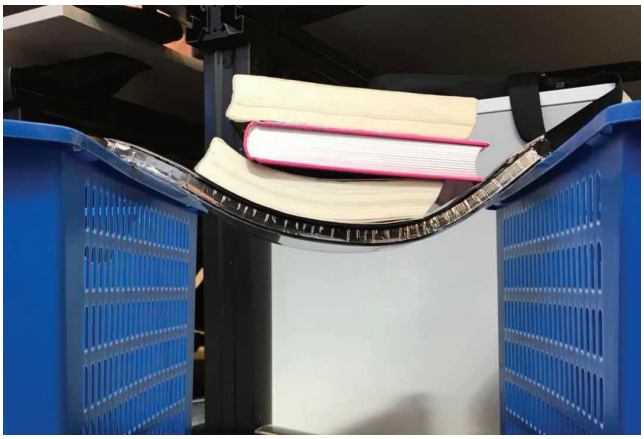

Figure 6: silicone lamination window
Source: Own image

Parametric control:

Since the three mathematical models are too complicated and by changing one parameter will lead to many results change. So based on grasshopper platform, I use sliders for important parameters and highlight the results I need. I will discuss the process in this chapter below. In this figure, parameters are window size, spacer size, air pressure, SPA geometry, segment numbers and segments distance. The outputs are stress on thin glass, SPA total length, window opening size, numbers of persons for fresh air.

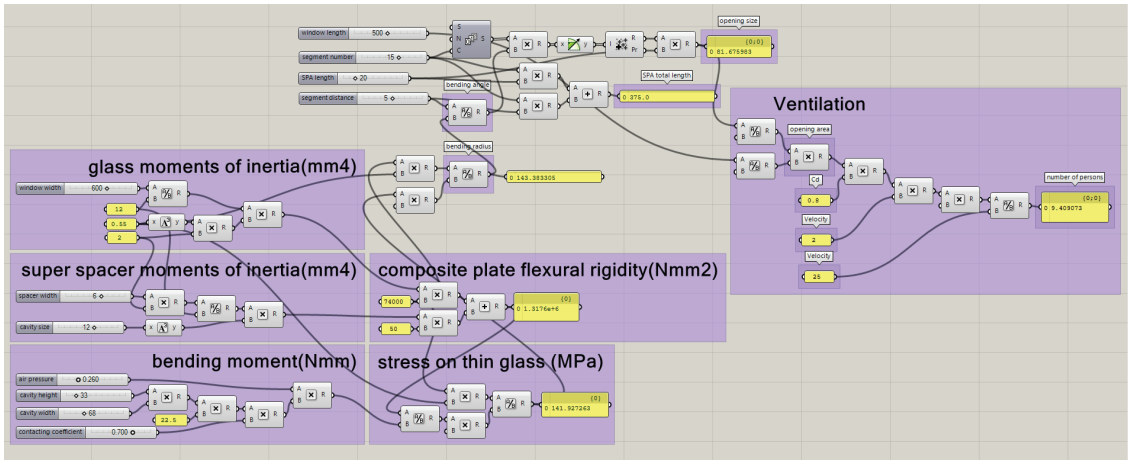

Figure 5: Grasshopper integrated calculation
Source: Own image

The equation of insulated window stiffness with soft adhesive is the sum of separate stiffness. So the effective stiffness of this insulated window should be thin glass stiffness multiplies super spacer stiffness. (**Figure 6**)

$$EI_{effective} = 2E_1I_1 + 2E_2I_2$$

$$I_1 = \frac{b_1}{12} t^3$$

$$I_2 = \frac{b_2}{12} h_c^3$$

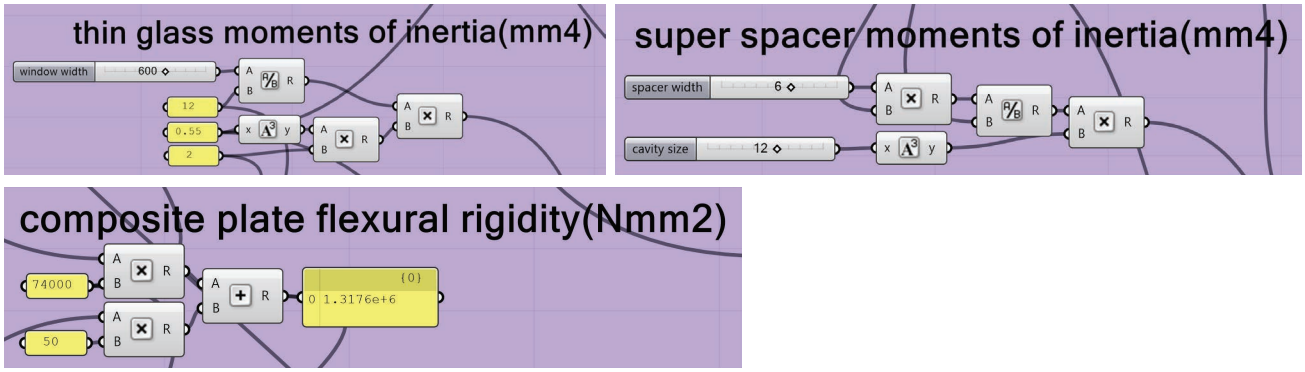

Figure 6: Insulated window effective stiffness calculation
Source: Own image

In the previous chapter, I did some research on structure mechanism of SPA and compared bending moment due to stretch and contacting. In the bending process, contacting bending moment is near 20 times more effective than stretching bending moment. As the result, to simplify the mathematical model, stretching bending moment need to be neglected. (**Figure 7**)

$$M_{contacting} = P*A*e$$

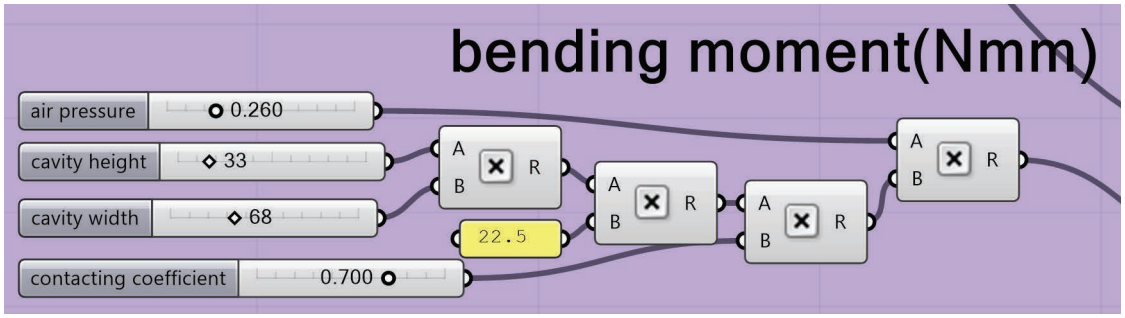

Figure 7: Contacting bending moment calculation
Source: Own image

Also, in the previous research about thin glass chemical strengthened process, the maximum stress of 0.55mm thin glass can reach to 260MPa. So to prevent thin glass from breaking, controlling stress result under 260MPa is important. (**Figure 8**)

$$\theta = L/R = \frac{LM}{EI}$$

$$\sigma = \frac{ET}{2R}$$

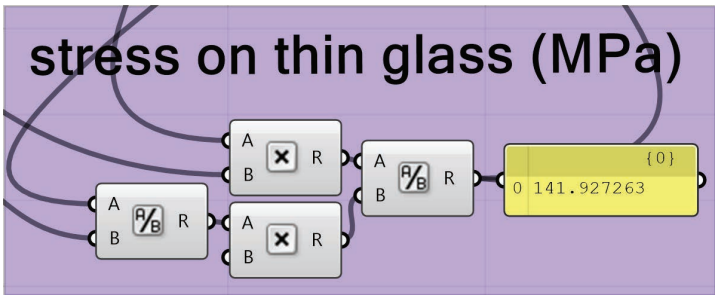

Figure 8: Tensile stress on thin glass surface calculation
Source: Own image

To bend a thin glass panel by contacting bending moment will not generate a circle. The structure mechanism of curving behavior is like the figure below. Neglecting stretching behavior, each gap between segments will bend the same radius R2. L is the thickness of SPA segments. To sum up, each segments bending, the opening size of the window can be calculated below: (**Figure 9-11)**

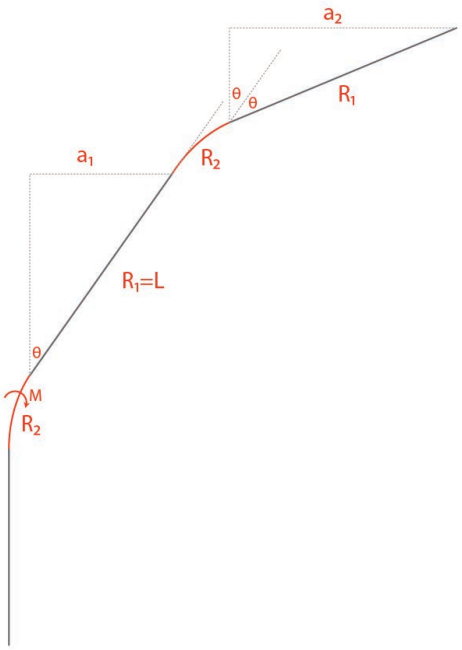

Opeing size=L(sinθ+sin 2θ+sin 3θ+.....+sin nθ)

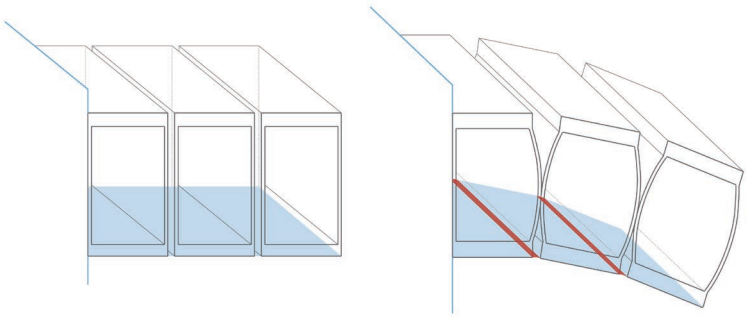

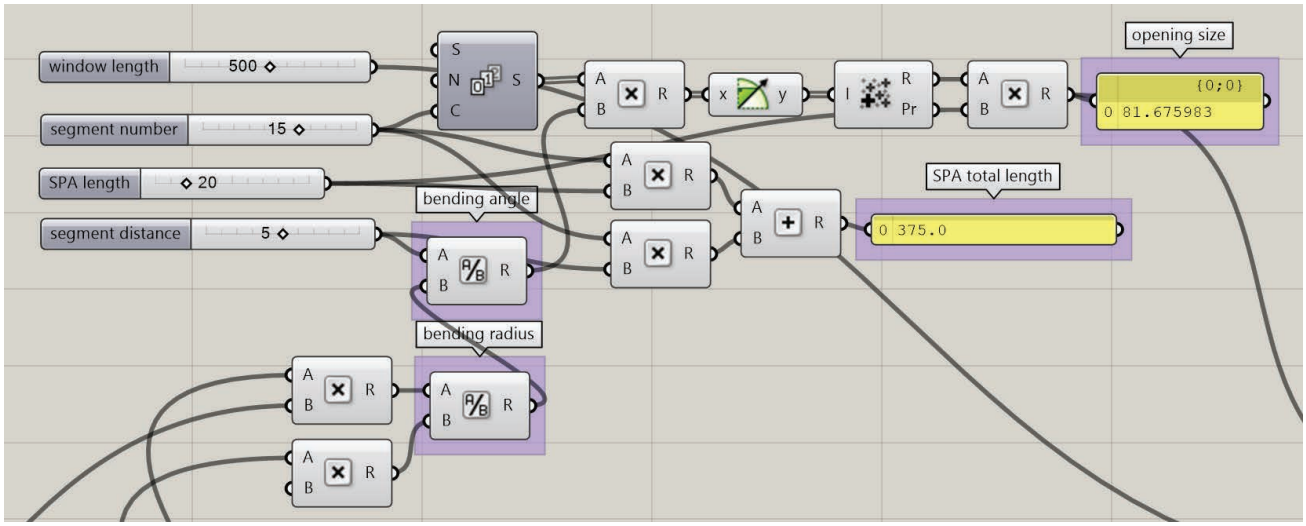

Figure 9-11: Thin glass window opening size calculation
Source: Own image

The last step is to calculate if the opening size is enough for people sitting in the room to breathe. Normally, one person in the room needs 25m3/h fresh air. I can calculate air flow rate by knowing the opening area and wind velocity. From the equation, I can find the relationship between air flow rate and numbers of people to breath fresh air.(**Figure 12**)

$$Q = C_d * AV$$

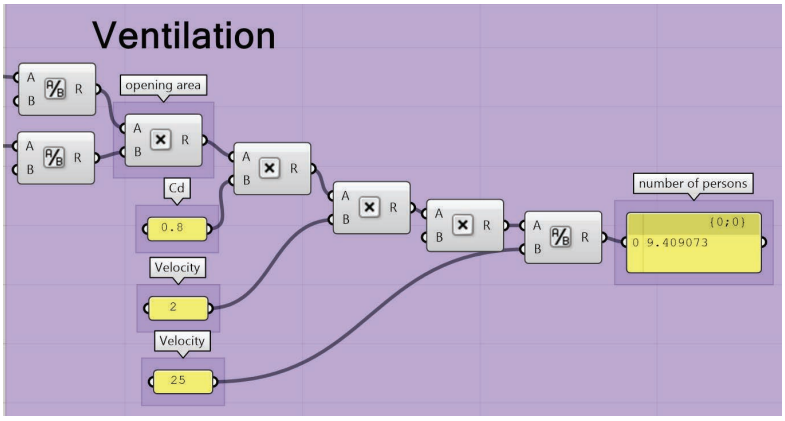

Figure 12: Ventilation calculation
Source: Own image

To sum up, by changing parameters in grasshopper, cavity size can be limited around 33mm*68mm, air pressure can be from 0.2MPa to 0.5MPa, window width is 600mm and segments number can be as much as 20. From the script in grasshopper, segments number will just influence window opening size. To keep the cavity size smaller will help decrease window frame size to make glass panel ratio lager. The contact coefficient value is the percentage of contacting surface area. When the pressure increases the value will be increased, as well as if the segments gap decrease, in the same pressure situation, the contacting coefficient value will be increased but the air inside the chamber will be squeezed, at the same time the pressure will increase.

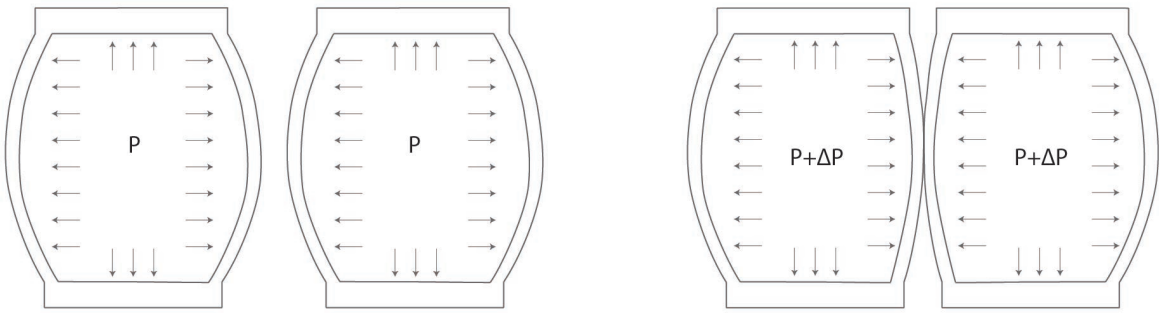

Figure 13: Air pressure increasing under air chamber squeezing
Source: Own image

We can see one side wall as a plate with the uniform load on the surface. (**Figure 14**) The reason to calculate the deformation is to find out the maximum gap between two segments. But the limitation of this method is the material property. The equation I use is about rigid material like steel, but this calculation can also give me the feeling of how much it will be deformed approximately under certain air pressure.

$$\Delta_{max}(center) = \frac{0.0284wa^4}{Et^3(1.056+1)}$$

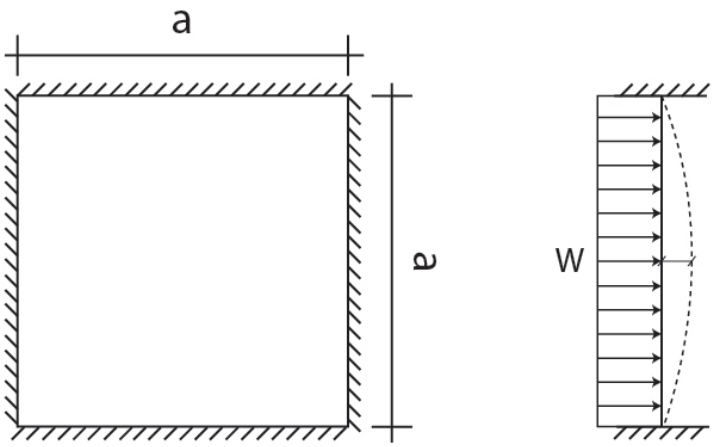

Figure 14: Inflated rubber deformation
Source: Own image

6. DRAFT EXPERIMENT

After building up the mathematical model and having an assumption of the window actuator size, the experiment is very important part of engineering the window and verify the hand calculation result. In this chapter, based on the previous chapters: draft design and mathematical modeling, starting to build up the prototype and doing some research on material and feasibility are important to finalize and design further.

Firstly, in the research chapter, I already discussed the SPA production process. There are two methods to produce. One is casting which is already introduced in the previous chapter. In this chapter, I will discuss the material properties and which material is feasible for this project.

In the research, Elastosil M4601 silicone rubber is used. The tensile strength of this material is 6.5MPa and elongation at break is 700%. The main goal of this chapter is to discover material resistant to air pressure and production process.

Elastosil M4601 silicone rubber (**Figure 1**) has to mix two components addition curing silicone material together, and also vulcanize at the room temperature. It is flexible and stretchable with high elasticity and optimum durability. This material can be cast into all molds of models because it is low shrinkage and easy to produce manually. The disadvantage of this material is the low tensile strength. In theory, the tensile strength is 6.5 MPa, however, in producing process, air cannot be vacuumed totally, which will affect the tensile strength. If the product made of this material is inflated, the maximum air pressure input will around 1 bar. This result can not be used in practice because, in my previous assumption, the minimum pressure needs to achieve 2 bars.

Figure 1: Inflated rubber deformation
Source: https://softroboticstoolkit.com/book/pneunets-modeling

3D printing

3D printing is the other way to produce soft robotics. Since 3D printing technology is widely used nowadays, in soft robotics area, the inner air cavity is difficult to cast, as the result, 3D printing technology can solve this problem. In this project, 3D printing technology is based on fused deposition modeling(FDM). As we discussed before, by casting soft pneumatic actuator needs many steps to produce, also, the process will take a long period of time manually. Even if the SPA geometry is as simple as the box, still the inner cavity increase the producing steps to cast and seal.

3D printing technology can directly print SPA geometry airtight to simplify the fabrication process. In this work, I propose to use Ultimaker 3 with TPU 95A as the flexible material. Ultimaker 3 is the new 3D printing machine comes from Ultimaker, compare to Ultimaker 2, Ultimaker 3 auto nuzzle-lifting system ensures a smooth and professional finish. Also, it can generate better cooling and high-quality bridging. In Utimaker 3 printing system, TPU 95A is the flexible material which can be used in SPA 3D printing. By using this material, Ultimaker 3 (**Figure 2**) can choose the suitable setting for TPU (**Figure 3)** and users do not need to set the temperature and speed by themselves. This will also increase the production speed. The maximum printing size is 342*380*389mm.

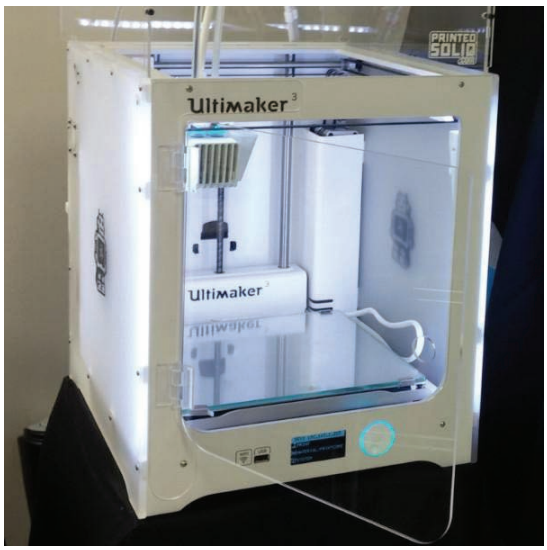

Figure 2: Ultimaker 3
Source: Own image

Figure 3: TPU 95A
Source: Own image

However, to 3D print air cavity inside is a big challenge. As the **Figure 4** I showed below, this is half SPA 3D printing product without support inside. If I continue printing this product without support, on the top layer of this product cannot be printed because there is no support under the cover layer. But if I print it with support, like the process simulation in Cura, when printing is finished, there will be no possibility to remove the supports. However, if decrease the air cavity thickness into 2mm, 0.4mm nozzle can bridge the cavity gap and close the geometry. To make a window actuator by 300mm length needs to print over 150 air chambers on both edges, which is time assuming and less effective. (**Figure 5**)

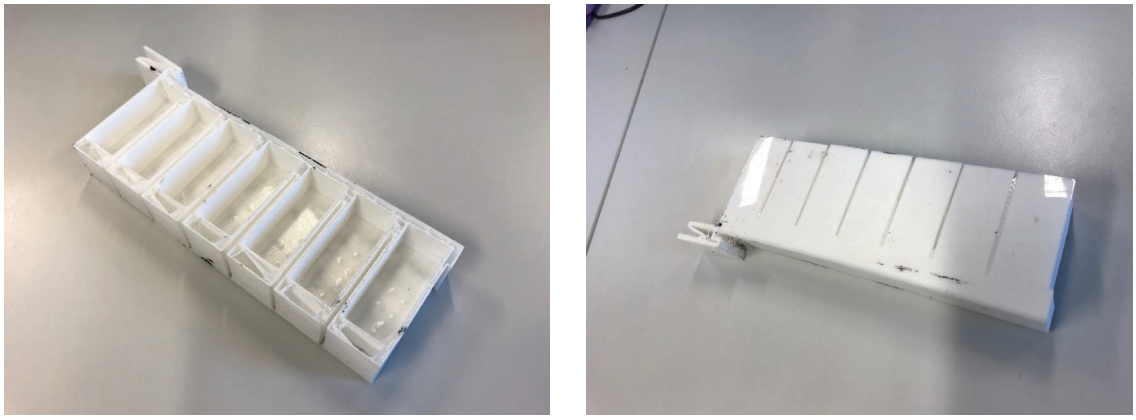

Figure 4: 3D printed SPA section

Source: Own image

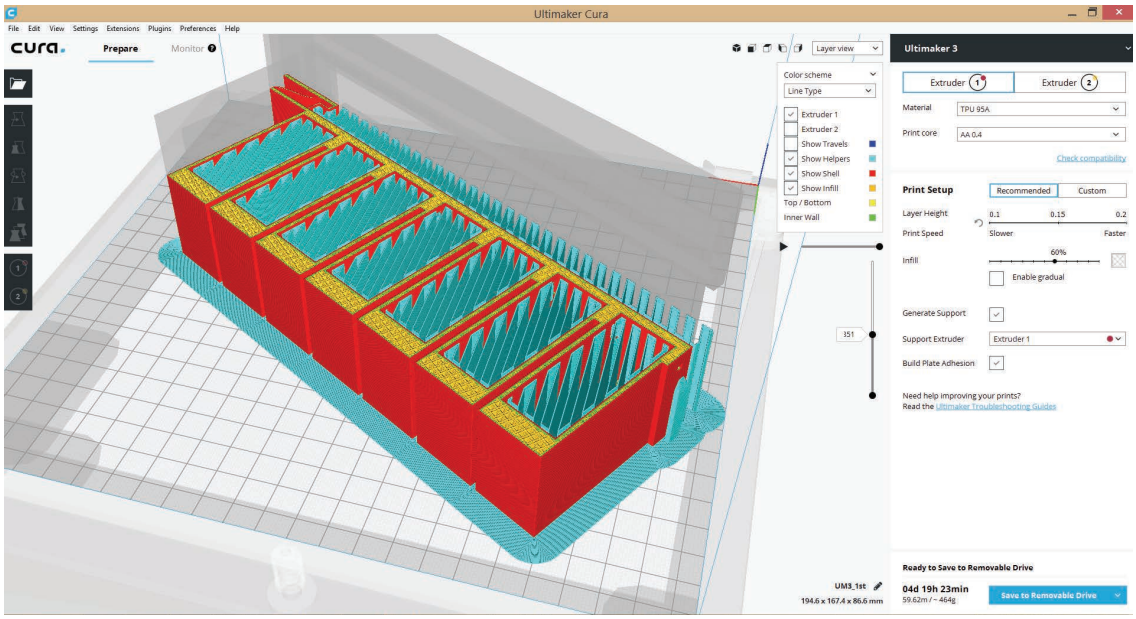

Figure 5: Cura simulation

Source: Own image

In the figure, we can find the difference between these two configurations. On the top, air cavity thickness is larger than the model on the bottom. The segment number increases when air cavity thickness decreases.

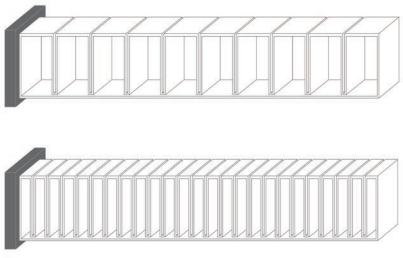

Figure 6: SPA confugurations

Source: Own image

Considering the connection of 3D printed SPA and thin glass will be difficult. Also after inflating thin glass panel cannot be formed continuously by SPA. Delamination will happen between SPA and thin glass panel after multiple bending behaviors. In the figure below, when the thin glass does not bend the same curvature like SPA, delamination between the two layers will happen. (**Figure 7-8**)

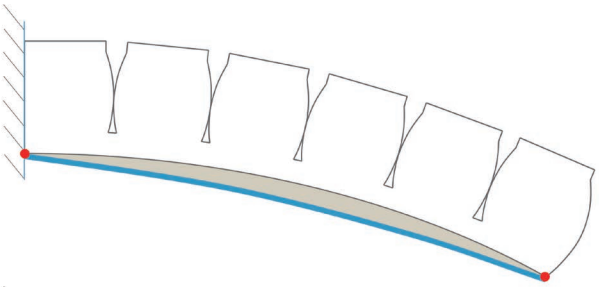

Figure 7: SPA edge fixed
Source: Own image

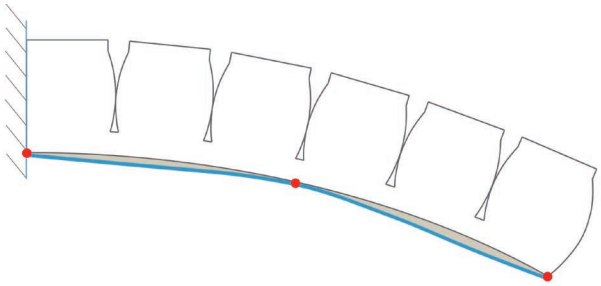

Figure 8: SPA more fixed location
Source: Own image

To avoid the delamination, strong connection between two layers is very important. At first, I use the plastic panel to simulate thin glass panels and drill holes on it. The reason to make a draft mock-up is to find more detail possibilities and learn from the model. As the result, I can analyze how it works or why it does not work.

In the draft mock-up, I use bike tire to simulate SPA inflating. I fold the bike tire and screw the tire to the plastic panel by two screws in a row and between two screws is the gap for air going through. The hight of bike tire I left is 5cm and the width is 4cm. The contacting area is 50mm*40mm, equals to 2000mm2. Comparing to the assumption from the previous calculation which is 33mm*68mm, equals to 2244mm2, the contacting areas are very close. The segments number contacting with each other is 36 in one row. The size of the window is 400mm*450mm. (**Figure 9**)

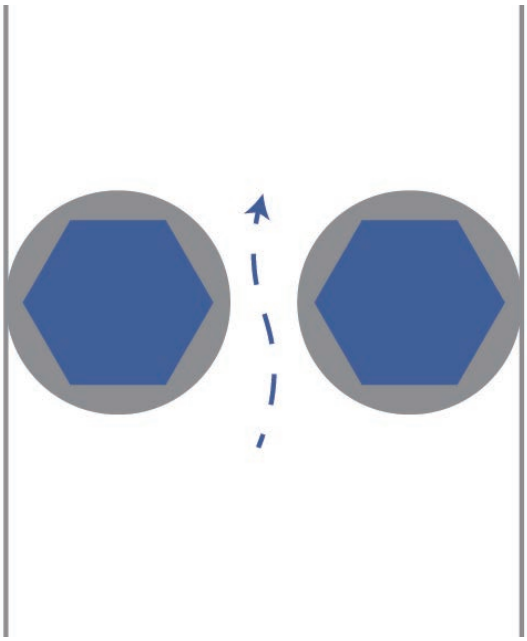

Figure 9: Fixed points
Source: Own image

After assembling the bike tire and screws on one layer of plastic panel, insulating this window will be the next step. As we discussed before, I use silicone adhesive and Super Spacer TriSeal Premium Plus to insulate this window. To make sure the bending moment from bike tire on the window can be more effective, I put the super spacer between two rows of screws and in the middle of the bike tire. As the result, the bending moment from the bike tire will act on the plastic panels- silicone glue-super spacer- silicone glue- plastic panel composite. (**Figure 10**)

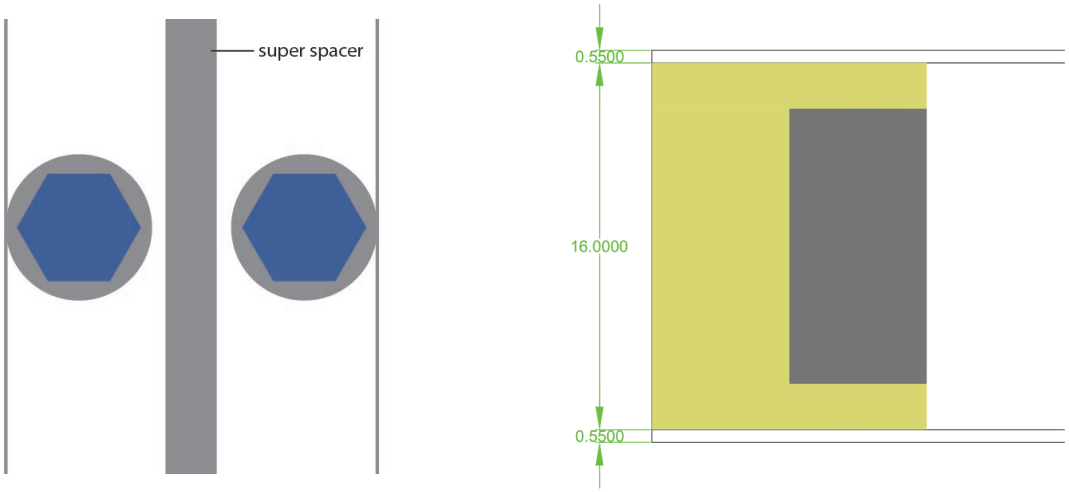

Figure 10: Silicone and super spacer location
Source: Own image

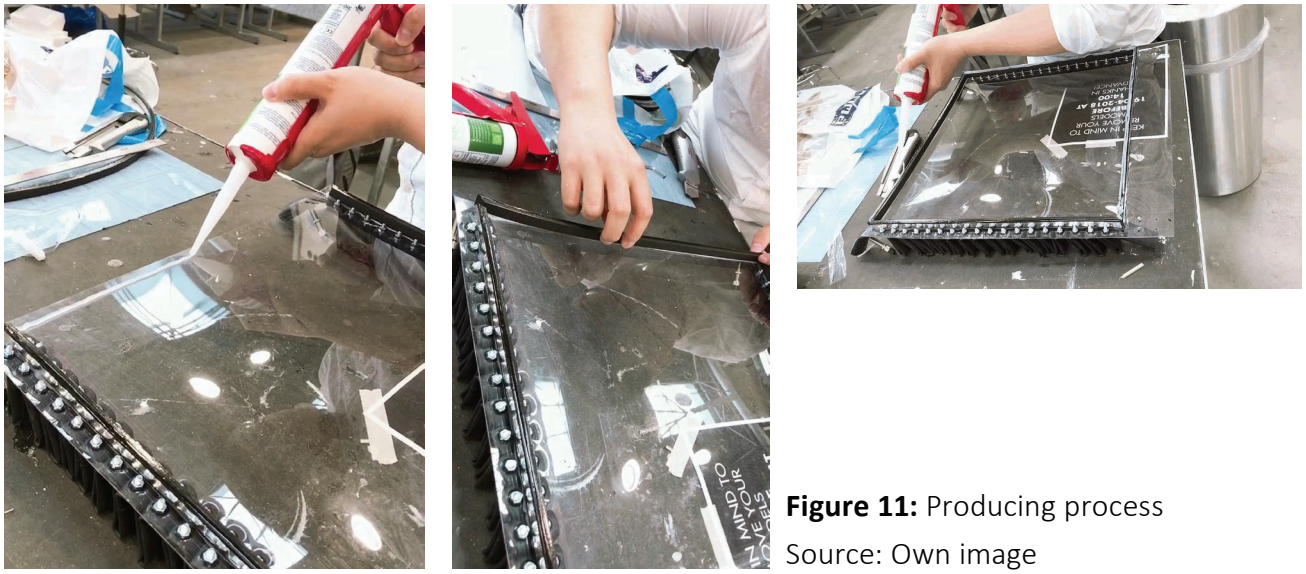

Figure 11: Producing process
Source: Own image

To seal the whole window, I used silicone glue filling the window edge to protect the super spacer and make it watertight and airtight. Also, the silicone material is soft to generate shear movements. The reason I use silicone is that when bending the window, the bottom layer will extend longer than the upper layer. (**Figure 12**)

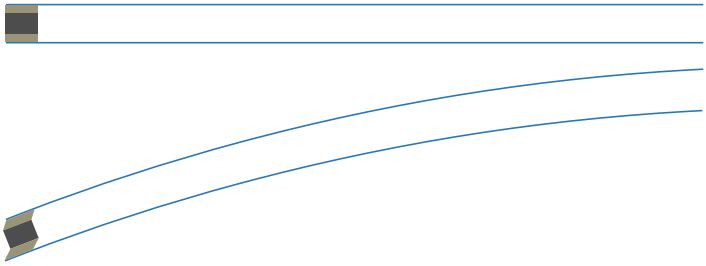

Figure 12: Bending behavior in silicone adhesive
Source: Own image

7. FURTHER DESIGN

In this chapter, this project will be designed further based on the experiment chapter. From the last chapter, I find some advantages of using bike tire to simulate soft pneumatic actuator bending behavior. First of all, butyl rubber can resist large air pressure due to its high tensile strength. Also, when air pressure increase, butyl material can stretch more than TPU which increases contacting area between adjacent air chambers. Without large stretching behavior, adjacent air chambers are difficult to contact each other and generate large bending moment. Secondly, because air chambers are separately connected with thin glass, the whole beam becomes robust. The more connections are made, the smoother curvature it will provide. Last but not least, when leakage happens in the actuator, there is no way to fix it in the draft mock-up. So the better solution should separate each air chamber and modularize actuator.

7.1. Actuator morphology optimization:

In this paragraph, based on the conclusion of the last chapter, actuator morphology has to be optimized. At first, air chambers have to be separated (**Figure 1**). There are two reasons, one is that the joint between air chambers has rigidity. Part of the bending moment is going to be wasted on bending the joint. If the joint is very soft and flexible, it becomes threshold of air pressure, which means even air chamber can resist large air pressure, failure will happen in joint part. The other reason is about replacing segments. Maintenance is a challenge in this product. If leakage happens on actuators, replace the whole one will not be cost-effective. However, if segments are separated, just changing one broken air chamber will be more effective.

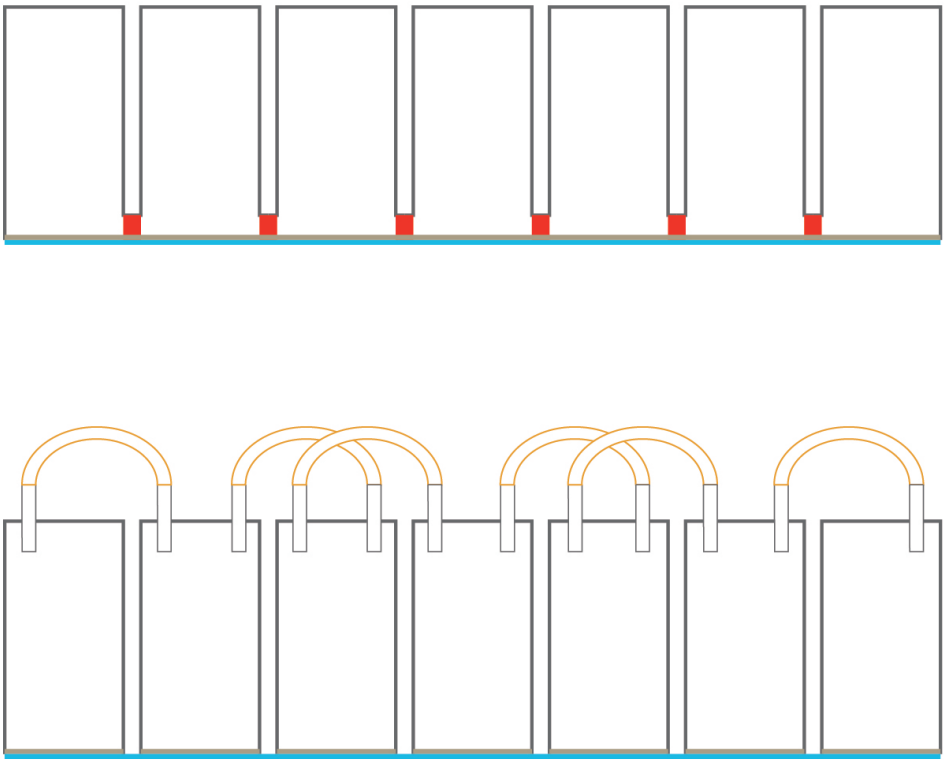

Figure 1:
Actuator morphology optimization
Source: Own image

Secondly, the connection method has to be discussed. In the market, there are two different joints, one is 6mm diameter straight metal joint (**Figure 2**), the other one is 6mm diameter Y shape joint (**Figure 3**). To connect these joints, 6mm inner diameter soft pipe (**Figure 4**) can be used.

Figure 2:
Straight metal joint
Source: Own image

Figure 3:
Y shape joint
Source: www.ythaifengsuli-ao.1688.com

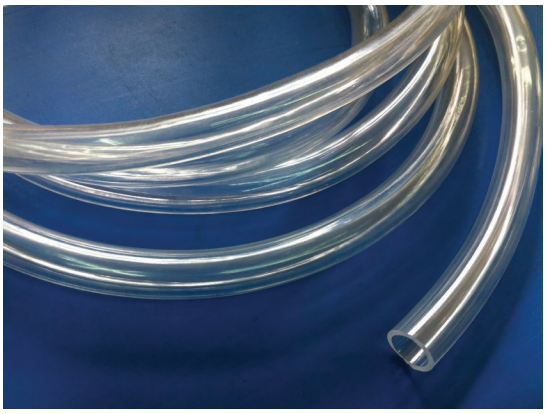

Figure 4:
Soft pipe
Source: Own image

Design A (**Figure 5**) used straight metal joint (**Figure 6**) and design B (**Figure 7**) uses Y shape joint. The thickness of rubber cube is different. The contacting wall thickness is 1mm and the other walls thickness are all 6mm. Because the other walls do not need to deform much, but contacting walls need to deform much more.

Design A

Figure 5:
Straight metal joint design
Source: Own image

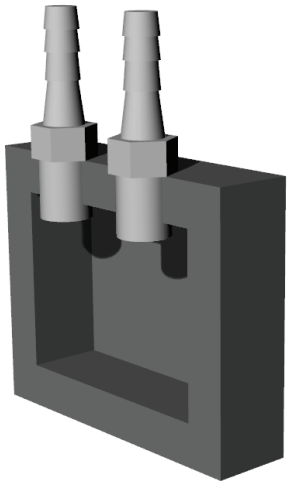

Figure 6:
Design A section
Source: Own image

Instead of using two joints, design B (**Figure 7**) uses Y shape joints which can be found on market. So the rubber block just needs one hole to plug in (**Figure 8**), this will reduce unnecessary trouble in making the mold. Also, one hole decreases the failure possibilities compared to two holes.

Design B

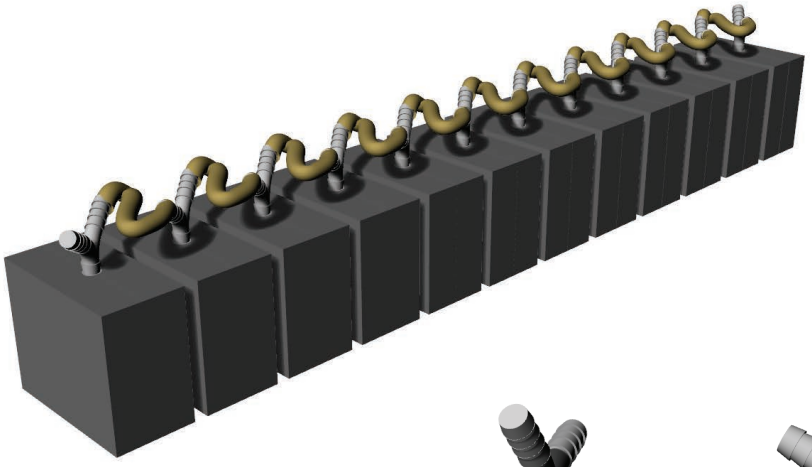

Figure 7:
Y shape joint design
Source: Own image

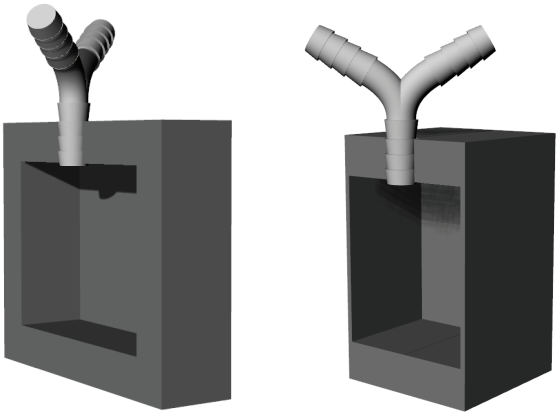

Figure 8:
Design B section
Source: Own image

Thirdly, the inner air chamber is the most important part. The size and the geometry influence the output result. The height of the air chamber needs to be small, because of the horizontal movement will increase shear force between the segments and with thin glass. (**Figure 9**) So if decrease the segments height, this actuator will be more robust.

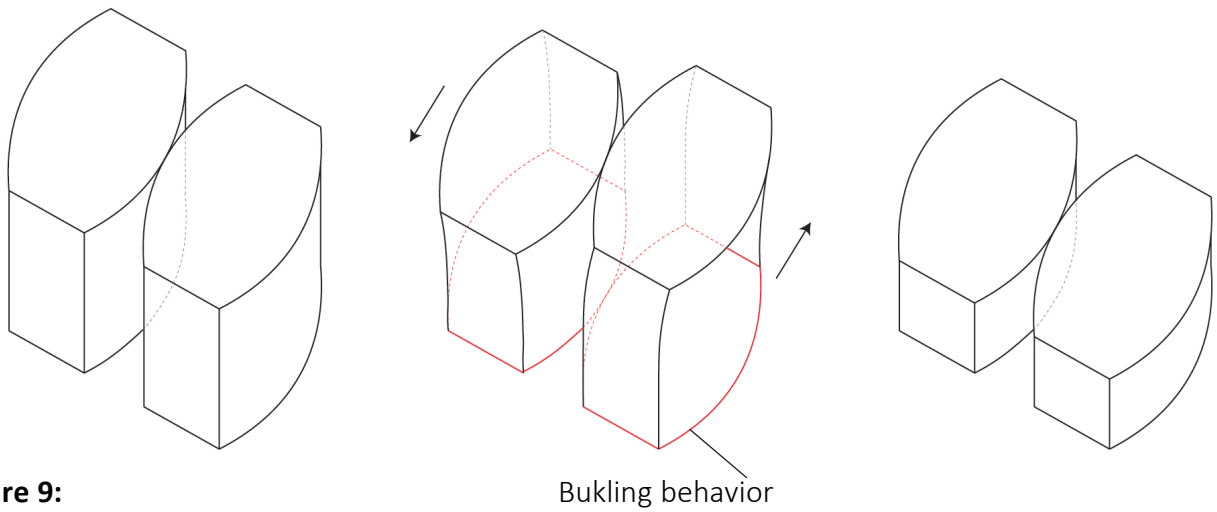

Figure 9:
Shear movement of segments
Source: Own image

So the length of the segment changes from 60mm to 80mm, (**Figure 10-13**) the height changes from 60mm to 45mm and the width changes from 30mm to 20mm because of increasing segments number. The other change has to be mentioned is that inner cavity corner changes from 90-degree corner to round a corner, the reason is to decrease stress concentration in a corner.

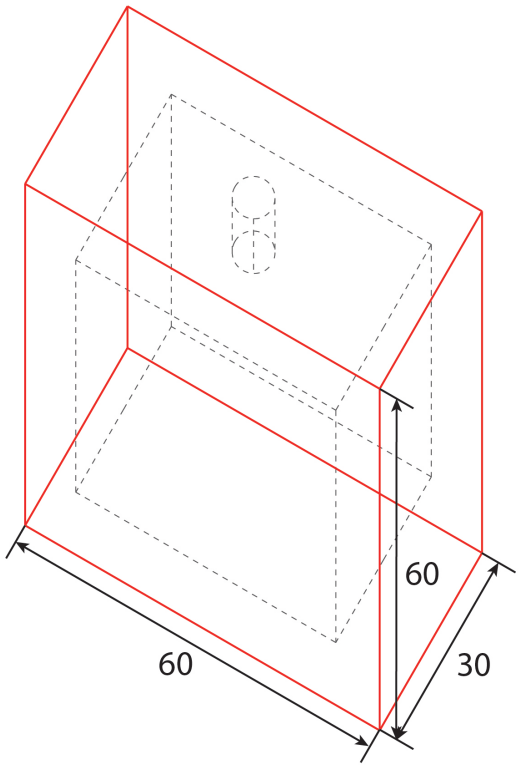

Figure 10:
Previous design
Source: Own image

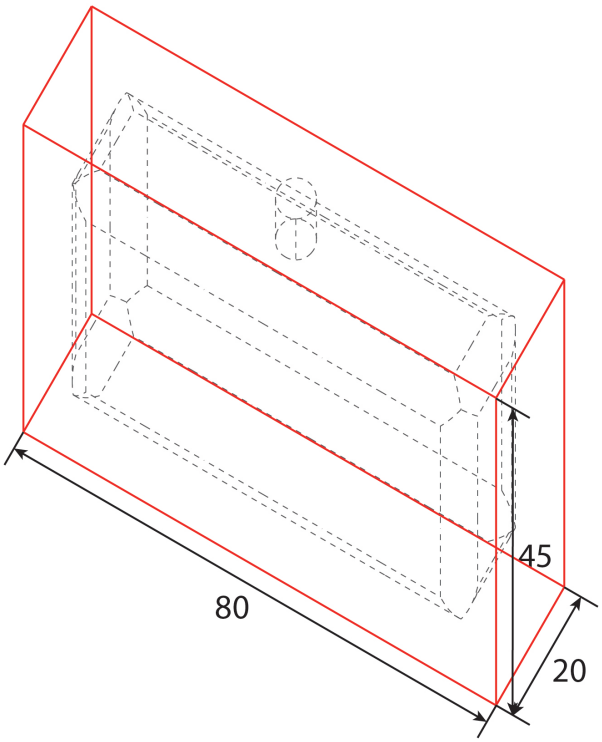

Figure 11:
Optimized rubber block
Source: Own image

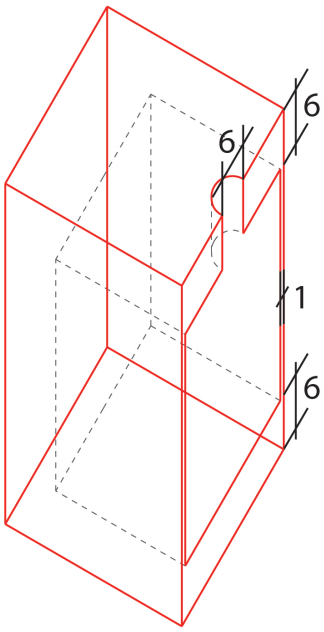

Figure 12:
Section of previous design
Source: Own image

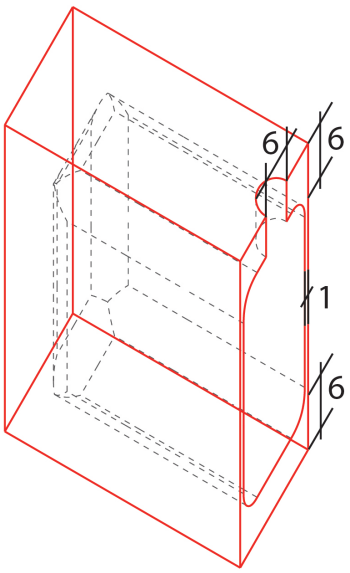

Figure 13:
Section of optimized rubber block
Source: Own image

7.2. Window design configurations:

In this section, to answer the third sub-question, I make a few detailed designs of exoskeletwindow. After illustrating the design configurations, one of them will be designed further. The selection is based on durability, operability and aesthetic.

Detailing design A

The concept of design A is to make a flexible window edge protection. Because of the bending behavior, the right and left side edge has to be bendable. Based on equation of moment of inertia, $bh^3/12$, the less h is, the less stiffness it will be. So, I designed a thin window edge protection and a curved section. The curved section shape means to decrease monents of inertia.

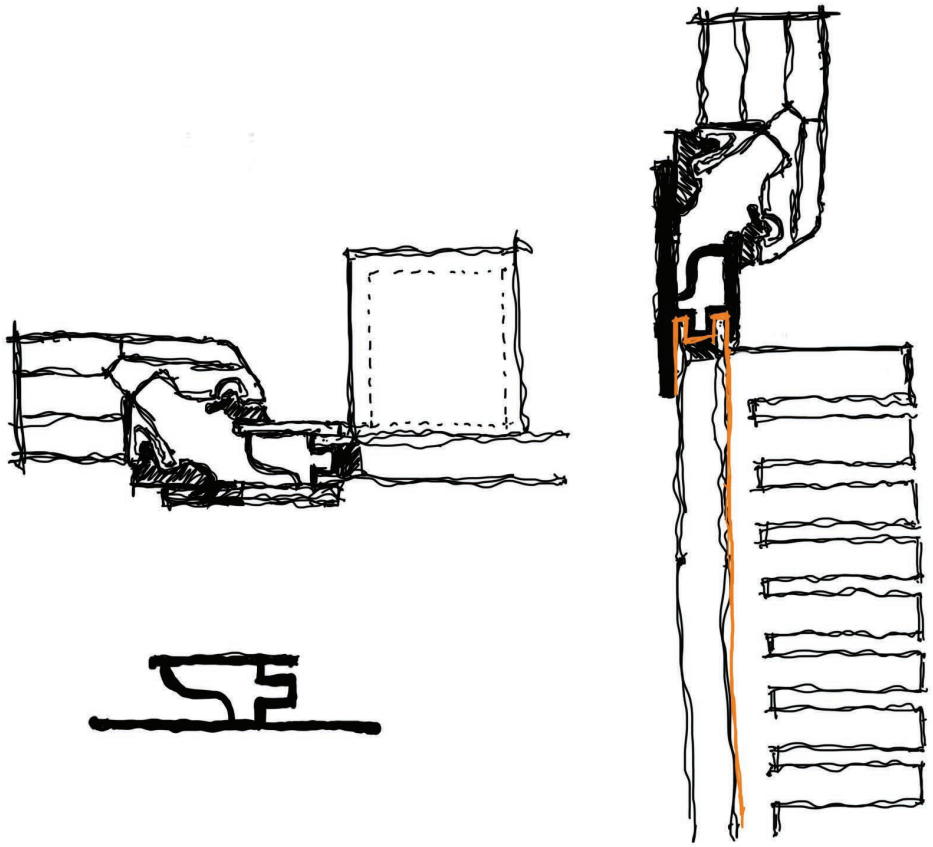

Figure 14:
Section of flexible window protection
Source: Own image

In this deisgn, wooden window frame is used. Because the window opening method is different, and window bottom edge is clamped but the other three edges are just supported. So it make detailing deisgn very difficult on window frame corner joint.(**Figure 15-17**)

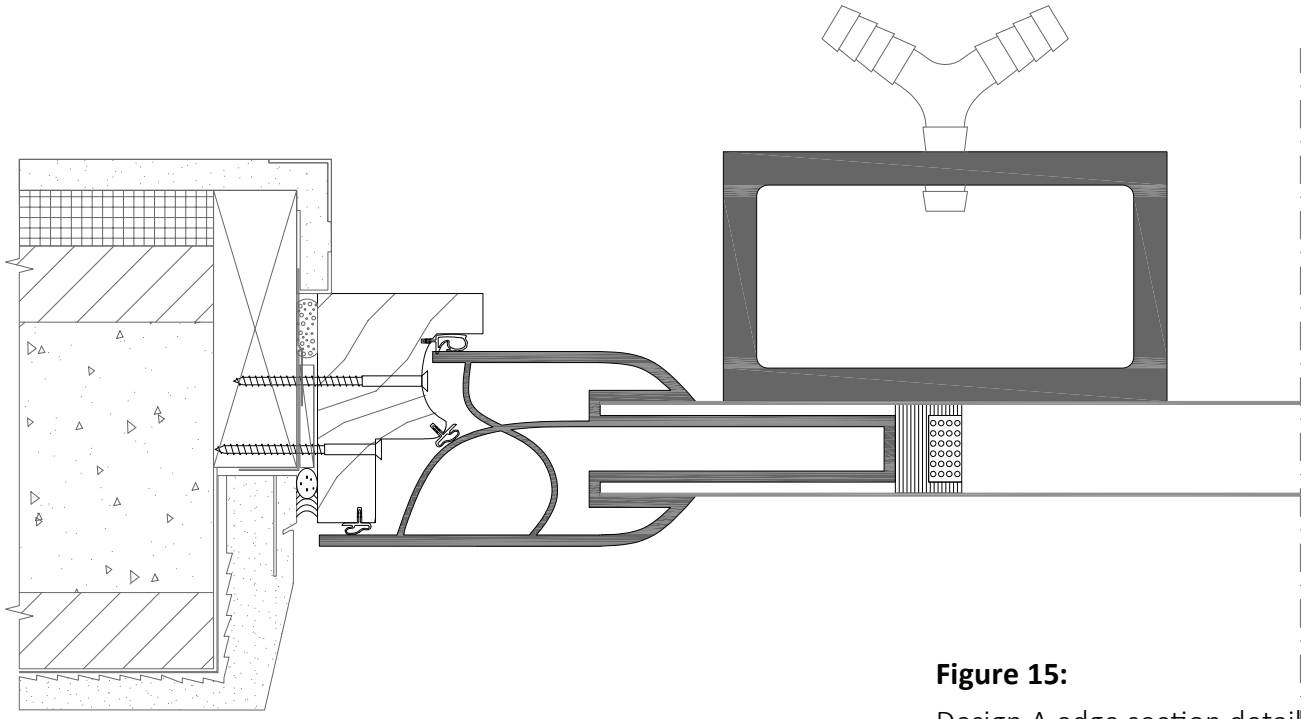

Figure 15:
Design A edge section detail
Source: Own image

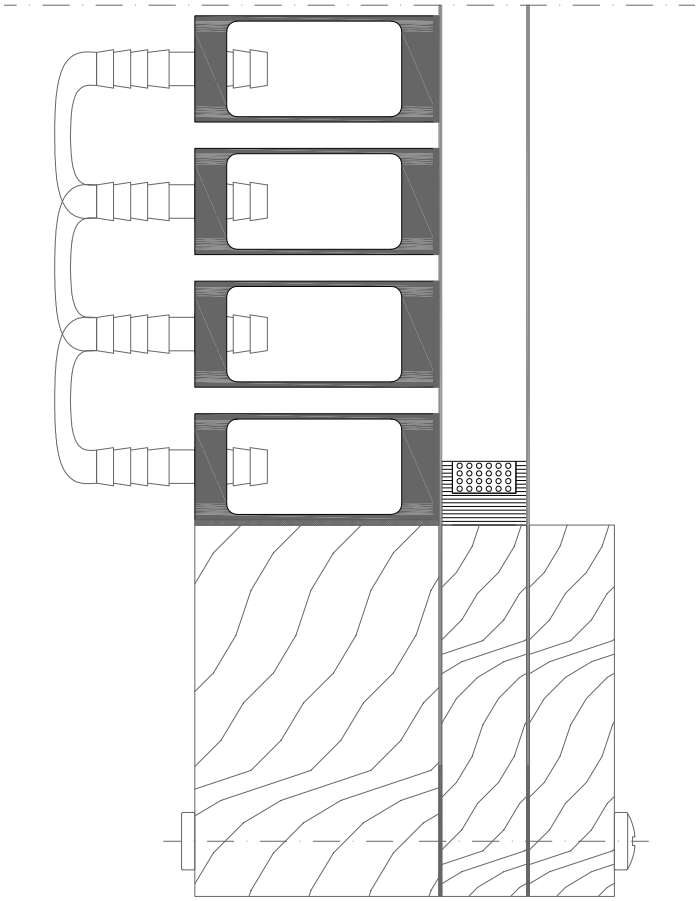

Figure 16:
Design A bottom section detail
Source: Own image

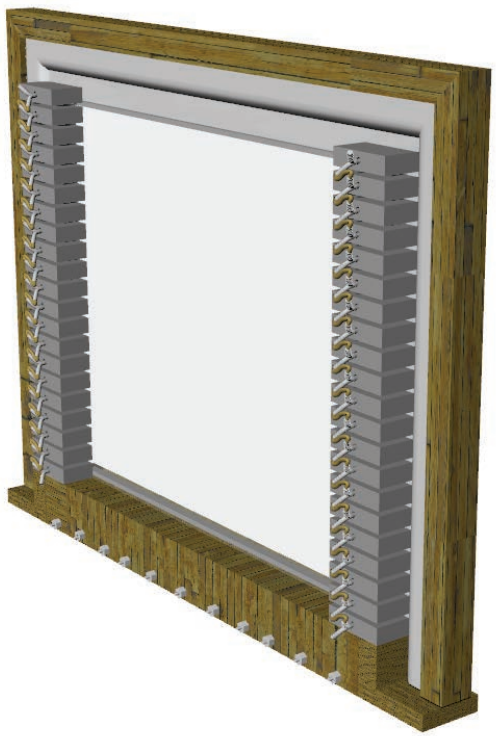

Figure 17:
Design A rendering
Source: Own image

Detailing design B

Design B concept is about using wooden window frame to hide and protect actuator. In this design, I use three pieces of wooden plates to build a hollowed box, and cover the window actuators.

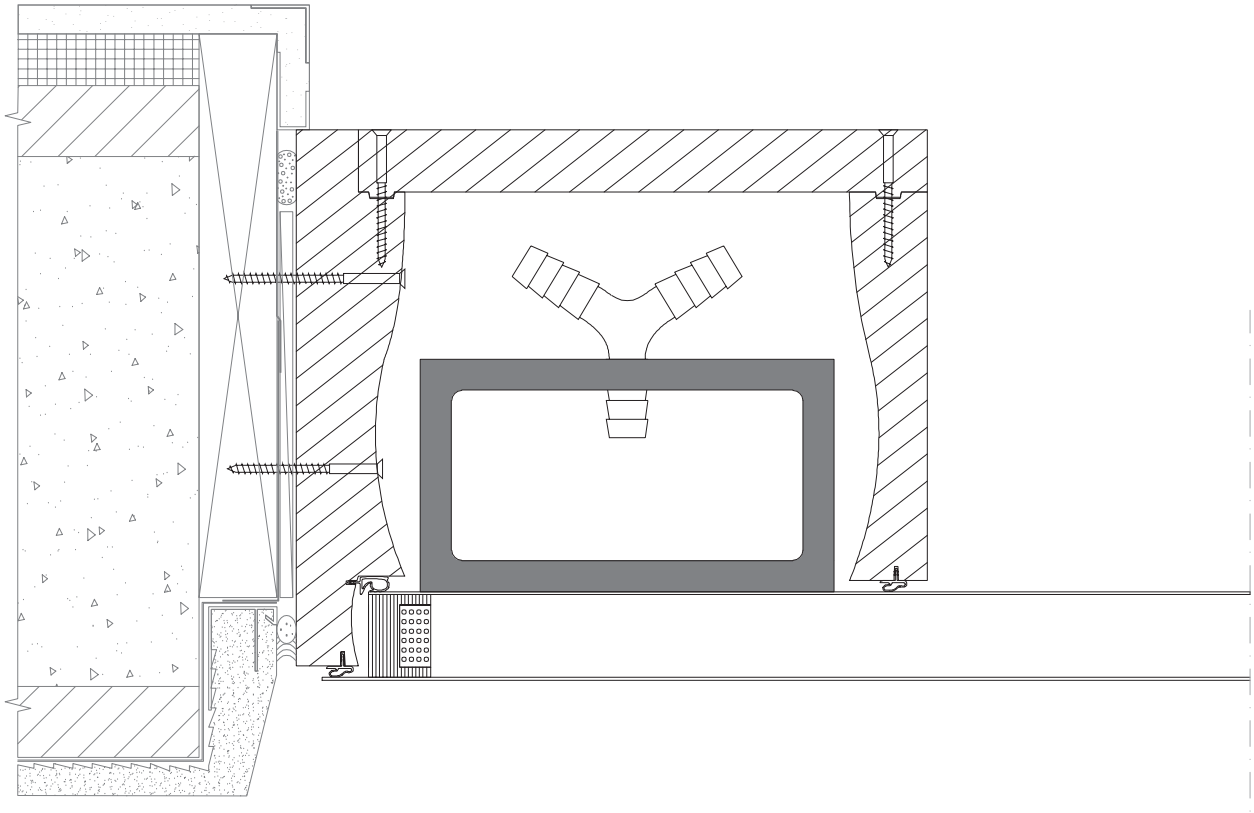

Figure 18:
Design B edge section detail
Source: Own image

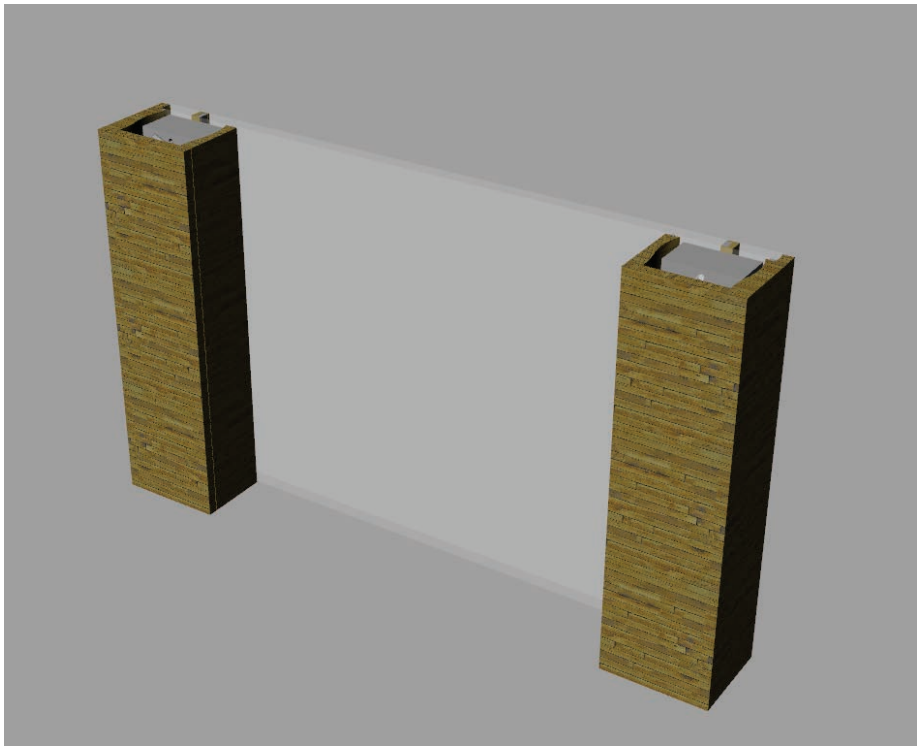

Figure 19:
Design B rendering
Source: Own image

Detailing design C

Design C concept comes from RT 82 HI+ aluminum-frame window, which has good thermal insulation property, Uf 0.79 W/m²K. There are some challenges using aluminum window frame. First is bottom edge clamping. Because of the flexible super spacer and silicone adhesive, clamping the whole panel seems difficut. In **Figure 20,** super spacer will deform when pressure on clamping structure increase. Also, when clamping structure generate shear movement **Figure 21**, silicone adhesive and super spacer will generate shear deformation. So, I use aluminum structure to clamp thin glass panel seperately **Figure 22** on the bottom, when window has to open, two clamping profile can be removed. Based on this concept, I made the detailing design C.

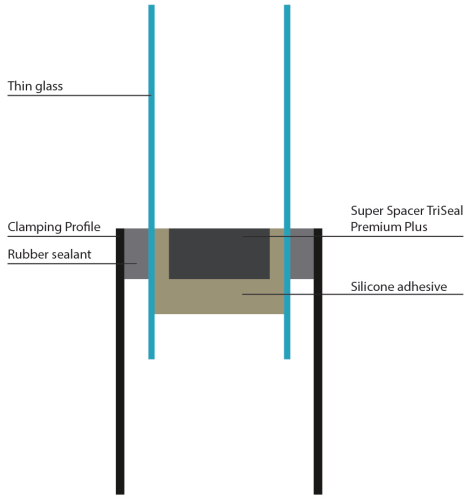

Figure 19:
Design C bottom clamping
Source: Own image

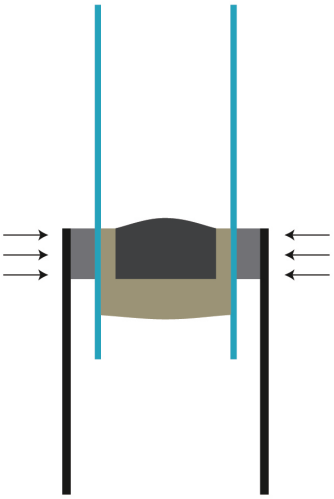

Figure 20:
Design C bottom squeezing
Source: Own image

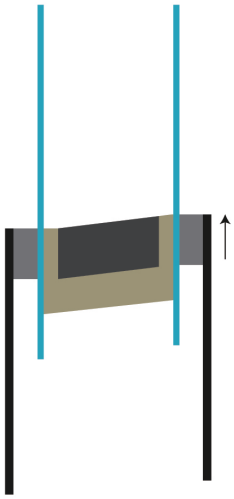

Figure 21:
Design C bottom shear
Source: Own image

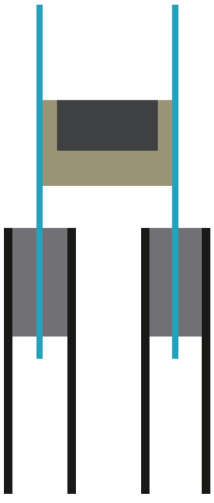

Figure 22:
Design C bottom seperate clamping
Source: Own image

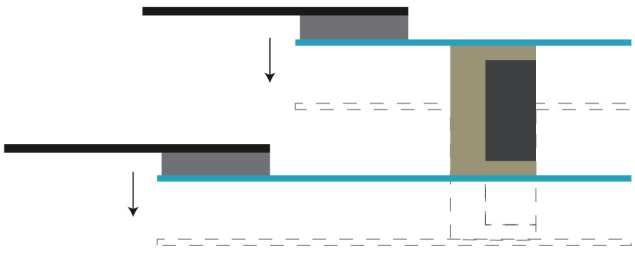

Figure 23:
Design C edge supporting
Source: Own image

Detailing design C

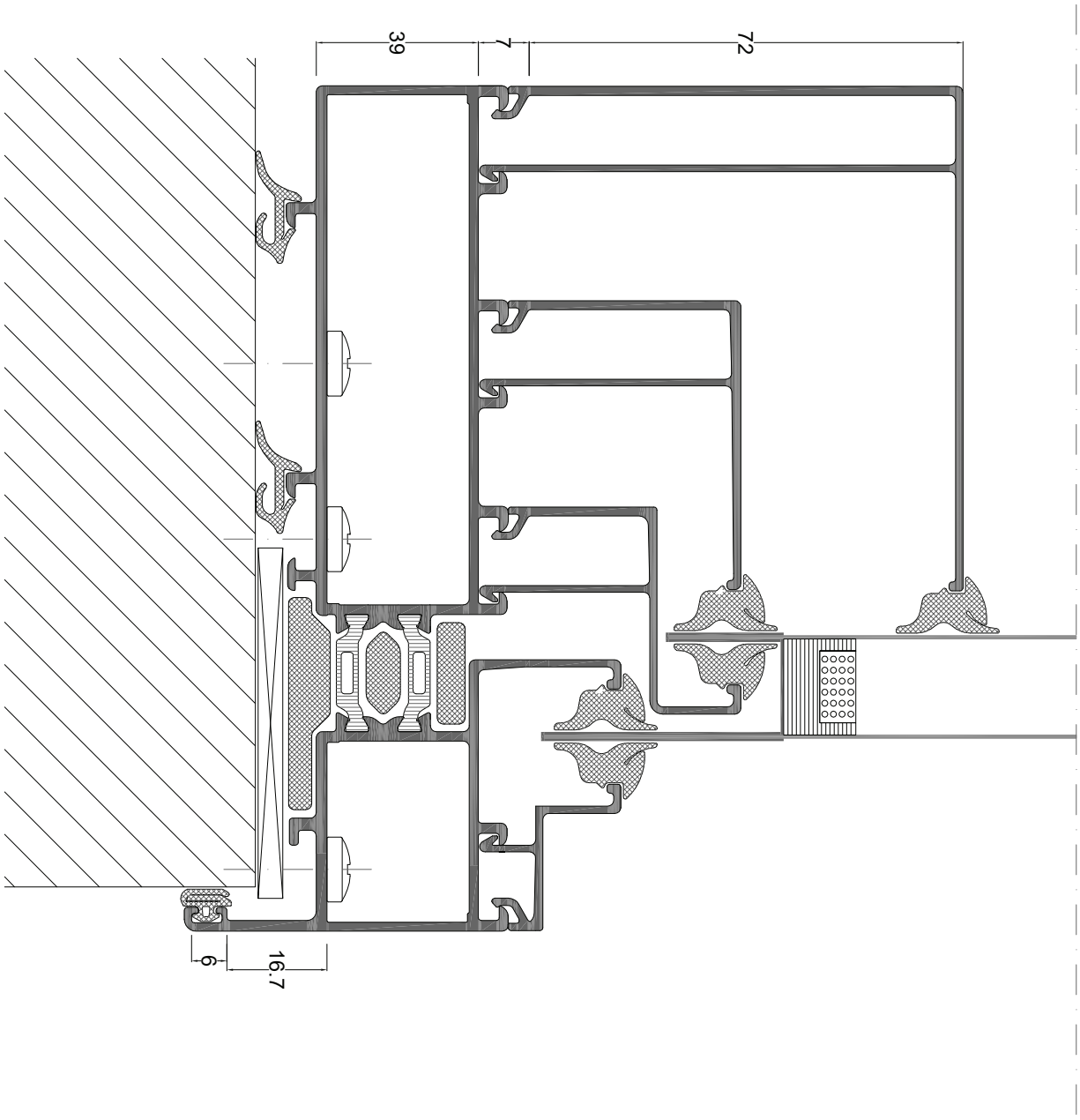

Figure 24:
Design C bottom clamping details
Source: Own image

Detailing design C

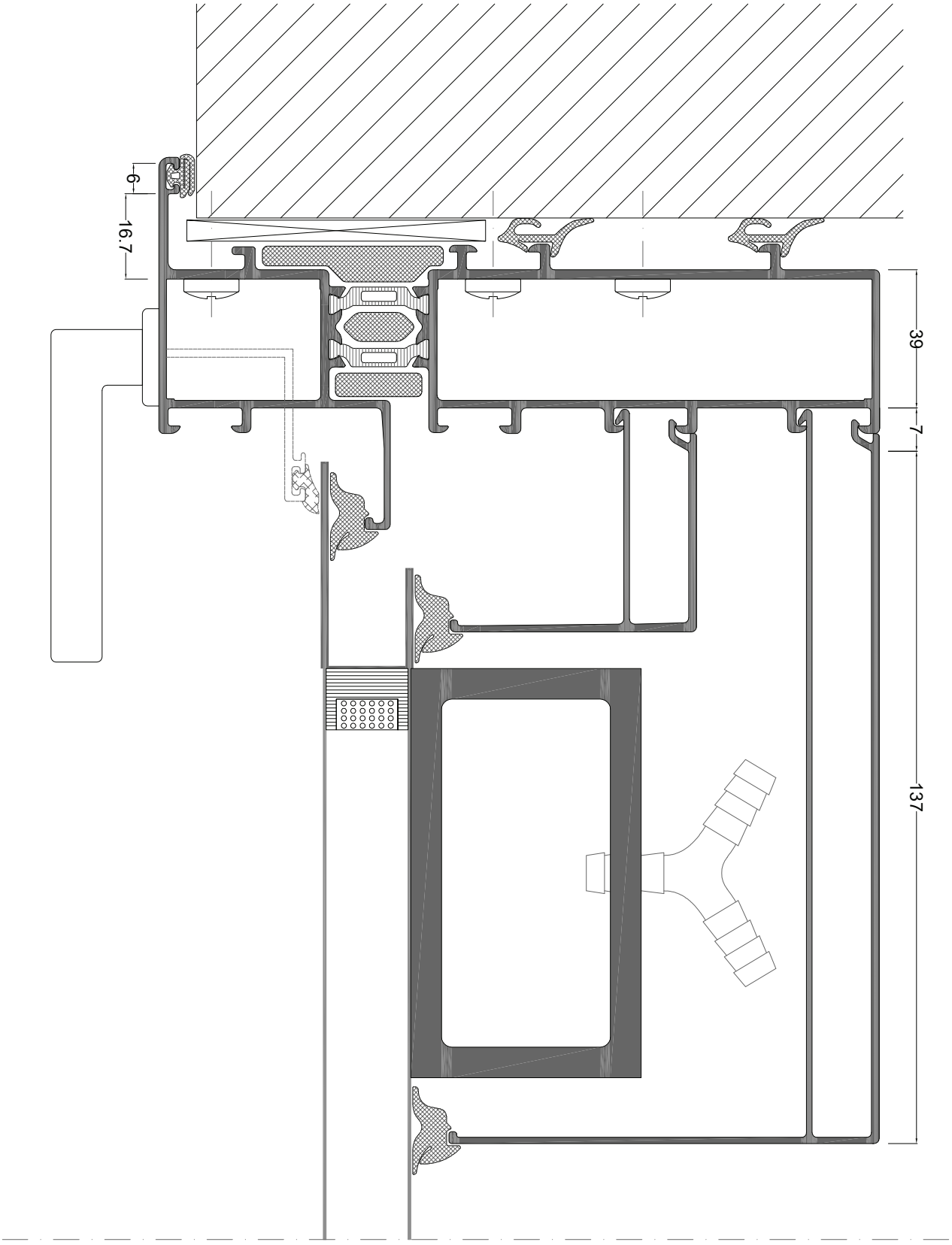

Figure 25:
Design C edge support details
Source: Own image

Detailing design C

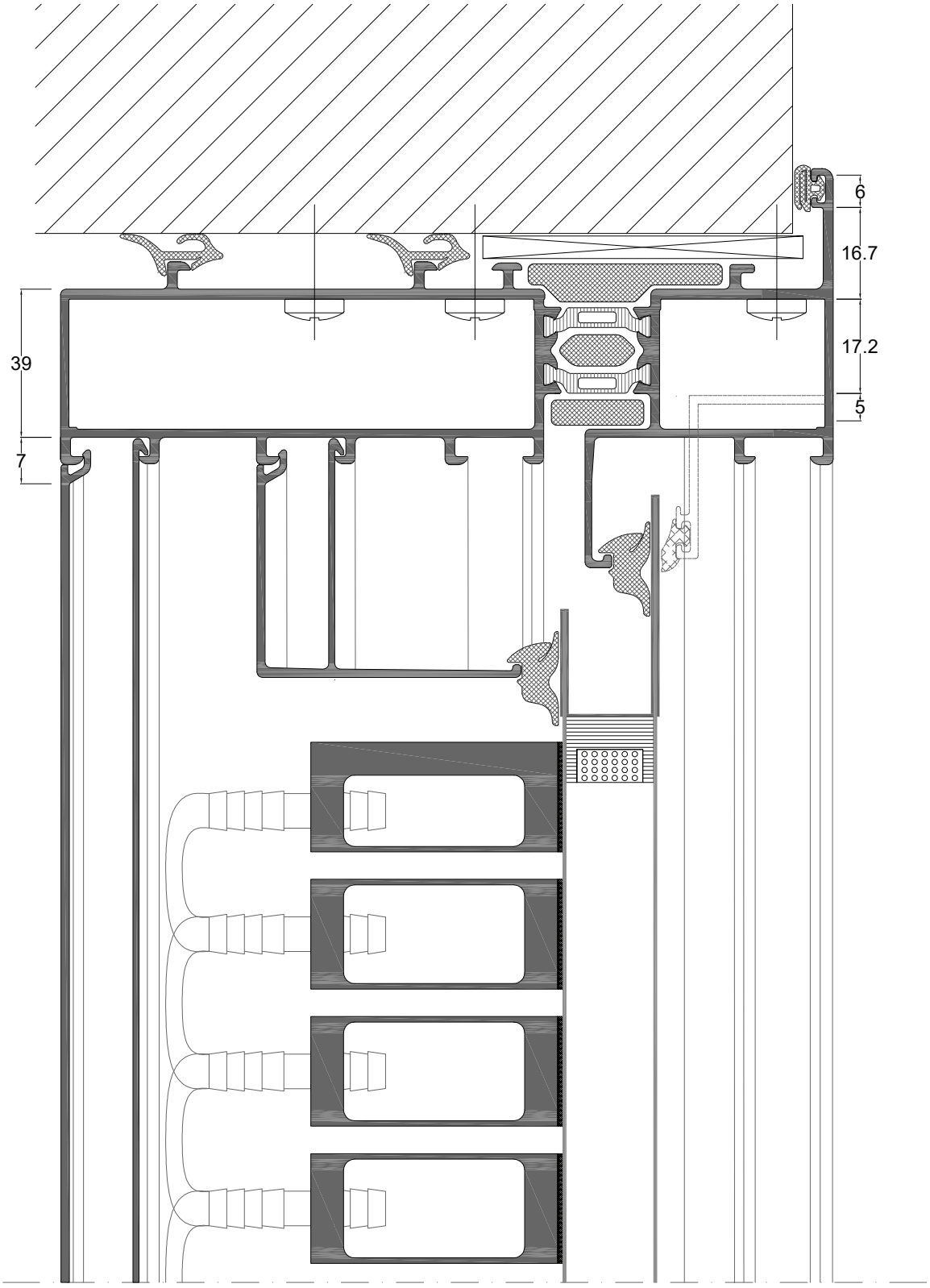

Figure 26:
Design C top edge support details
Source: Own image

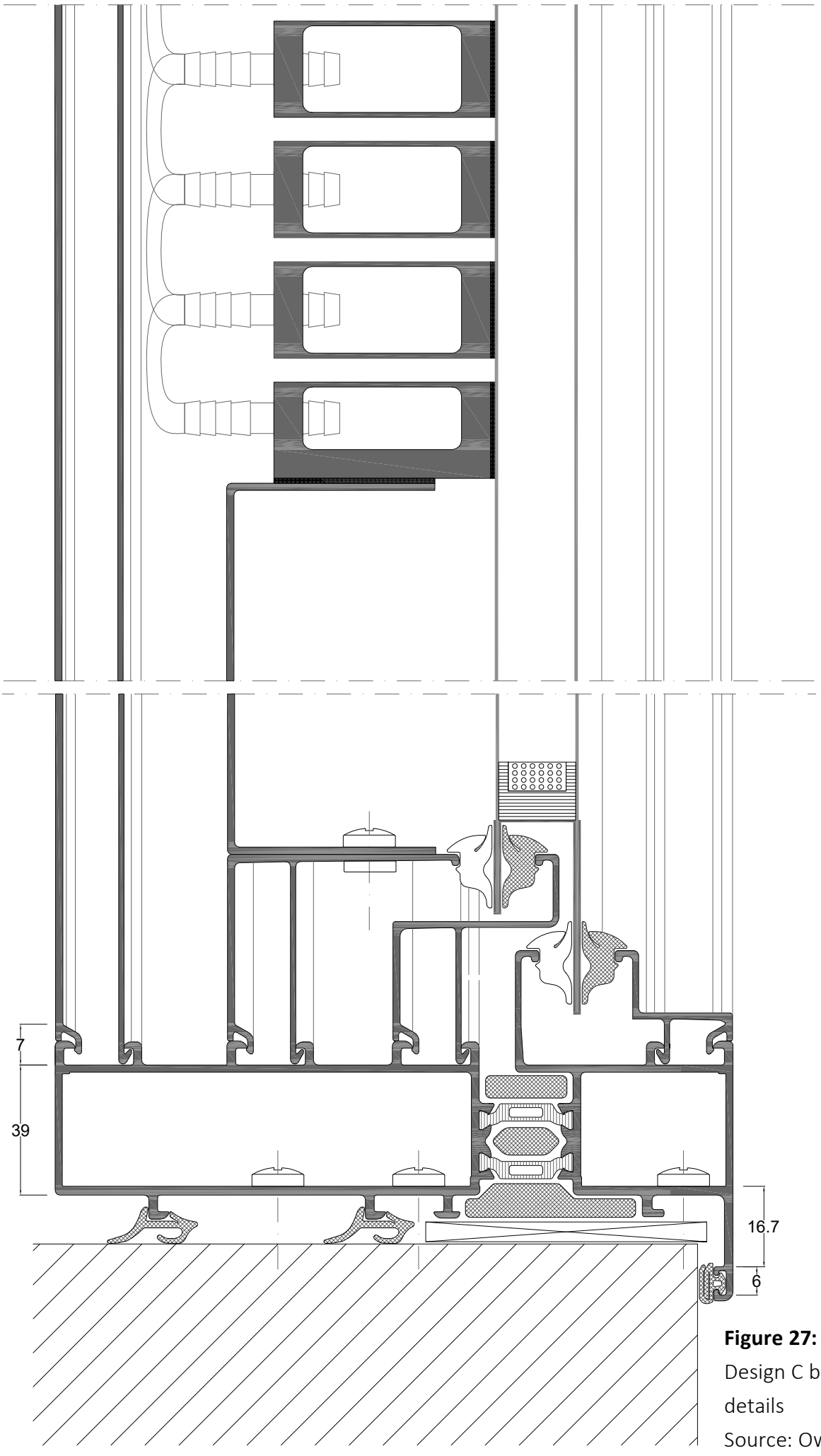

Figure 27:
Design C bottom edge support details
Source: Own image

7.3. Benchmark exoskeletwindow:

Exoskeletwindow has a lot of advantages compared to the other window product. There is an extensive range of configurations incorporated with thin glass and soft pneumatic actuator. Based on window opening directions and actuated edges, here is a list of configurations when window curved in single curvature way.(**Figure 28-31**)

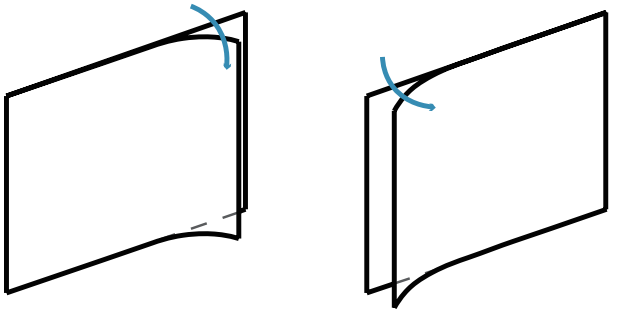

Figure 28:
Single side edge opening window
Source: Own image

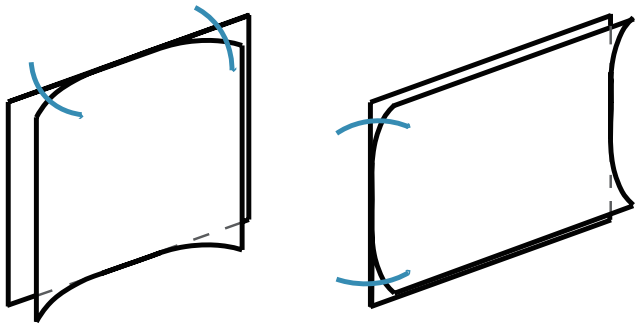

Figure 29:
Double top and bottom edge opening window
Source: Own image

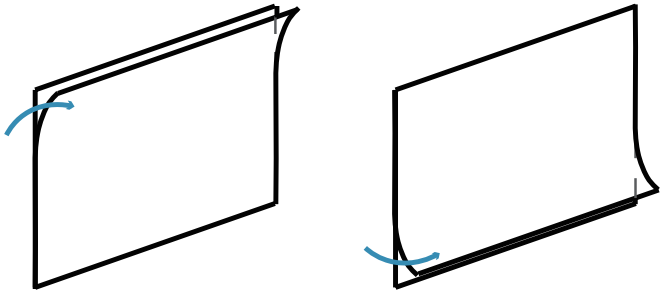

Figure 30:
Single top and bottom edge opening window
Source: Own image

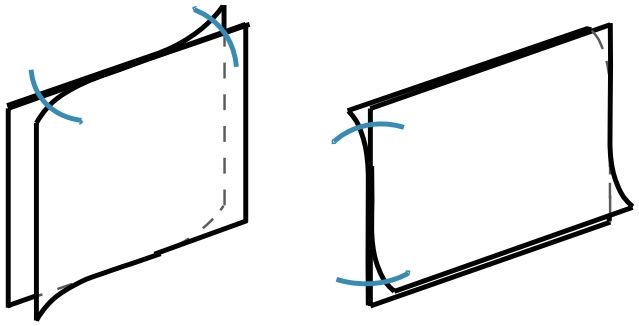

Figure 31:
Double top and bottom edge opening window
Source: Own image

Depend on different orientation and different weather data, exoskeletwindow can be assembled and designed in different ways. The size can be customized, even the maximum opening size can be chosen.

7.3.1. Product features

Air flow rate changing ratio

From the previous explanation, exoskeletwindow owns smoother and more continuous air flow rate changing ratio than the other windows. With this feature, the window can be smoothly open into certain curvature to fit inside and outside environment. Also, by using sensors inside and outside, the window can automatically respond to the environment in order to provide a comfortable indoor environment.

Adaptive hinge system

The hinge system is pneumatically controlled to adapt to the environment. In the different period of a day, wind velocity and temperature will change outside, also, when a room is full of people, CO2 density will increase. At this time, hinge system will start to activate window panel for ventilation.

Low maintenance compared to kinetic facade

Normally the kinetic facade needs large numbers of motors, sensors, and drives to move. Also, electrical equipment cost a lot. Furthermore, this motors and metal elements have the limited time of use, replacing them is not time efficient or cost efficient. However, exoskeleton window has less maintenance cost because of rubber block and pipes are cheap.

Easy to control and measured

The actuator and window opening is controlled by air pressure and amount. The relationship between air pressure and bending radius is fixed. Based on the equation, this system is very easy to be controlled and measured. By measuring inside and outside temperature, CO2 density, precipitation, indoor humidity, wind direction and wind speed, the soft pneumatic actuator can open the window into different positions to achieve the ideal indoor environment.

Meet different architecture function and aesthetic

Nowadays modern architecture is more and more popular in the world. Not only the building geometry keeps innovating, the function of buildings also become more and more integrated and complex. Exoskeletwindow has different size and different geometries, the most amazing feature is that the windows can keep changing its curvature, which makes it possible to meet different functions and aesthetic.

7.4. Exoskeletwindow producing and installing

In this part, I will discuss the installing process. This process need to be assembled on the construction site. Firstly, the edge frame need to be assembled (**Figure 32-36**) and then the assembled profile will be srewed on the wall (**Figure 37**). Installing top edge is the next step. (**Figure 38**)

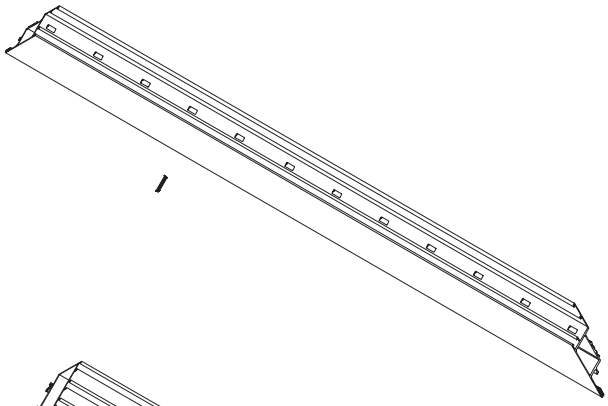

Figure 32:
Aluminum profile with locking holes
Source: Own image

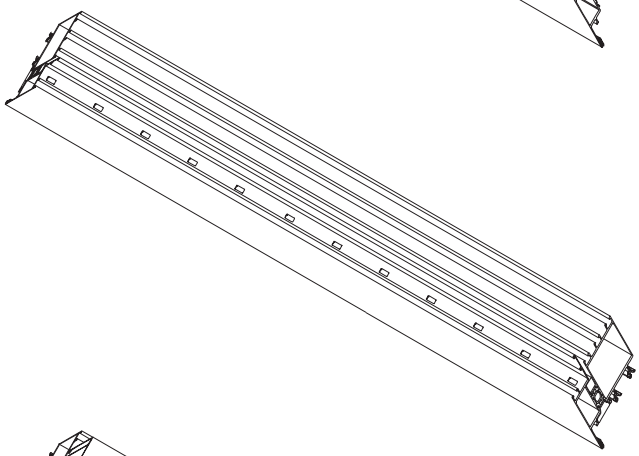

Figure 33:
Aluminum profile assembling
Source: Own image

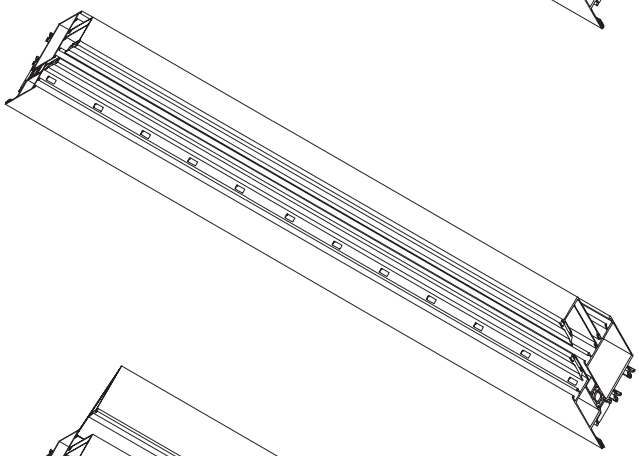

Figure 34:
Aluminum profile assembling
Source: Own image

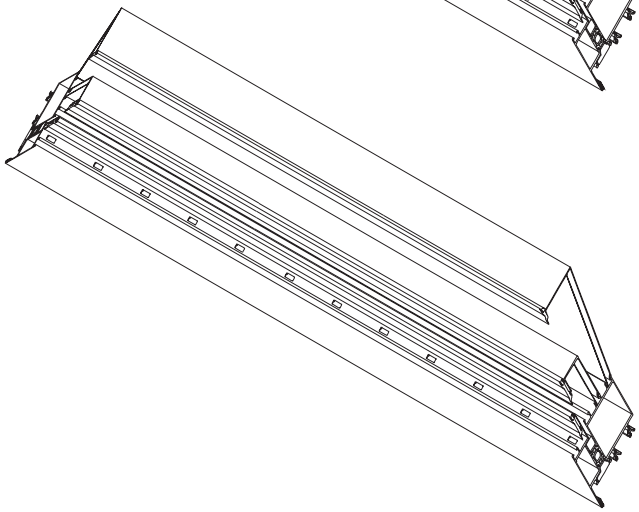

Figure 35:
Aluminum profile assembling
Source: Own image

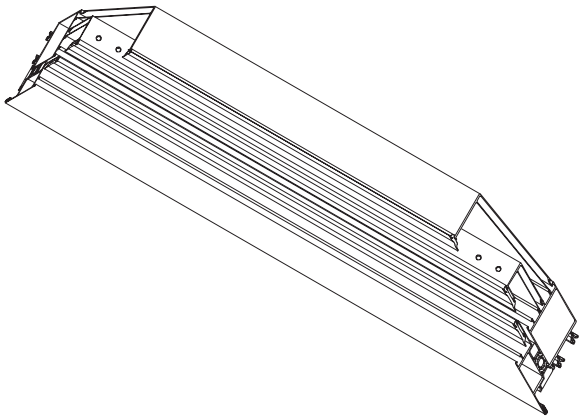

Figure 36:
Aluminum profile assembling
Source: Own image

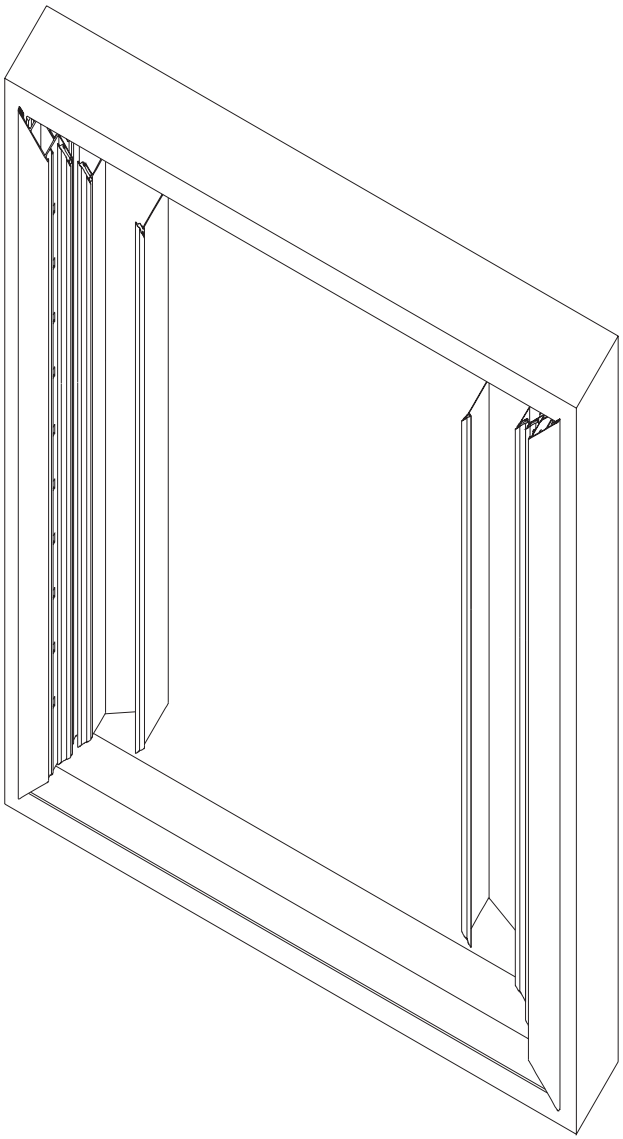

Figure 37:
Aluminum profile side edge installing
Source: Own image

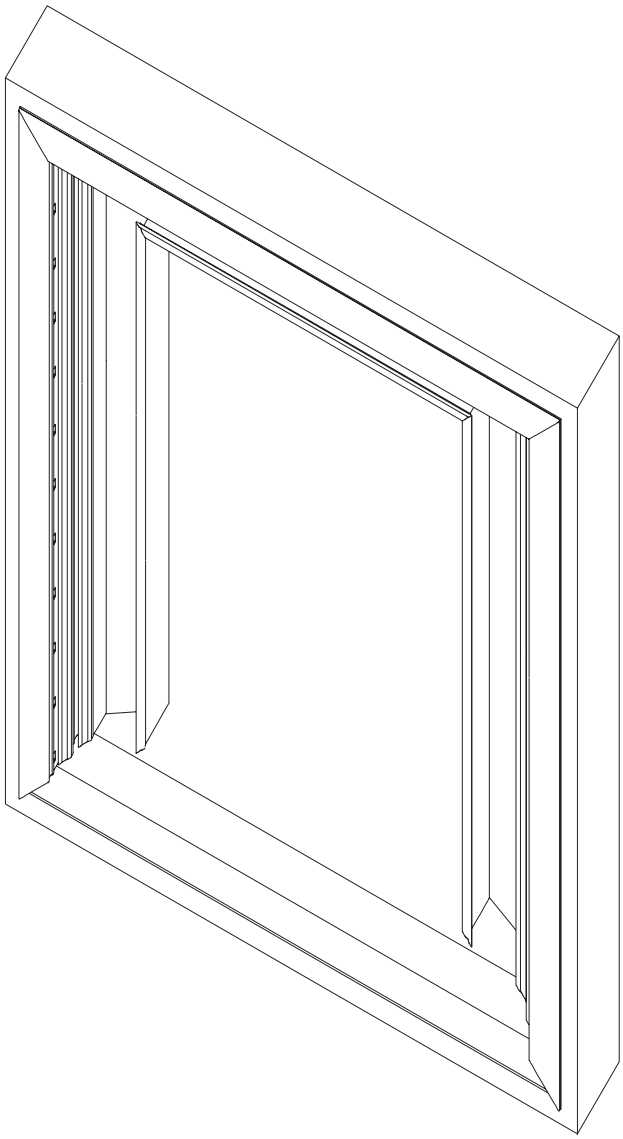

Figure 38:
Aluminum profile top edge installing
Source: Own image

This step is to install the clamping part. Three profiles need to be installed first(**Figure 39 and Figure 40**) and then double glazing unit has to be put onto the profile. At last two more profiles need to be sliding into the gap between two thin glass layers to clamp both panel. (**Figure 41 and Figure 42**)

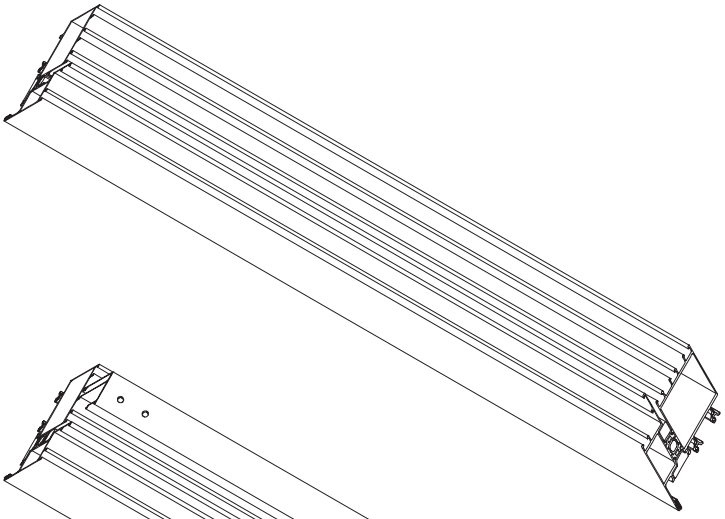

Figure 39:
Aluminum profile on bottom edge
Source: Own image

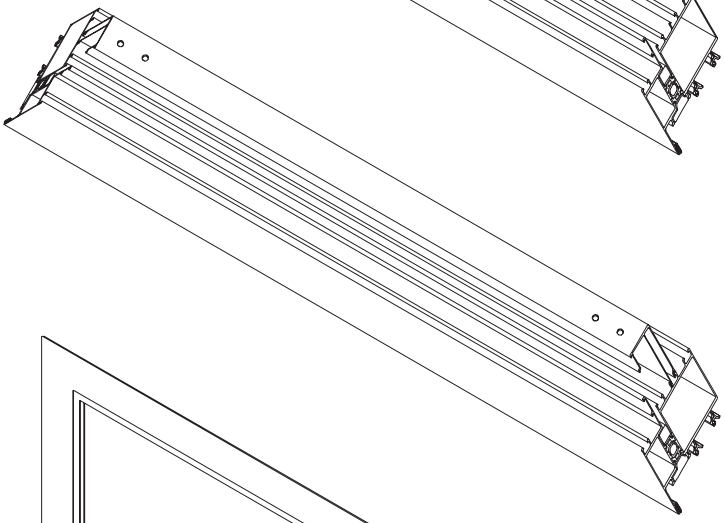

Figure 40:
Aluminum profile on bottom edge
Source: Own image

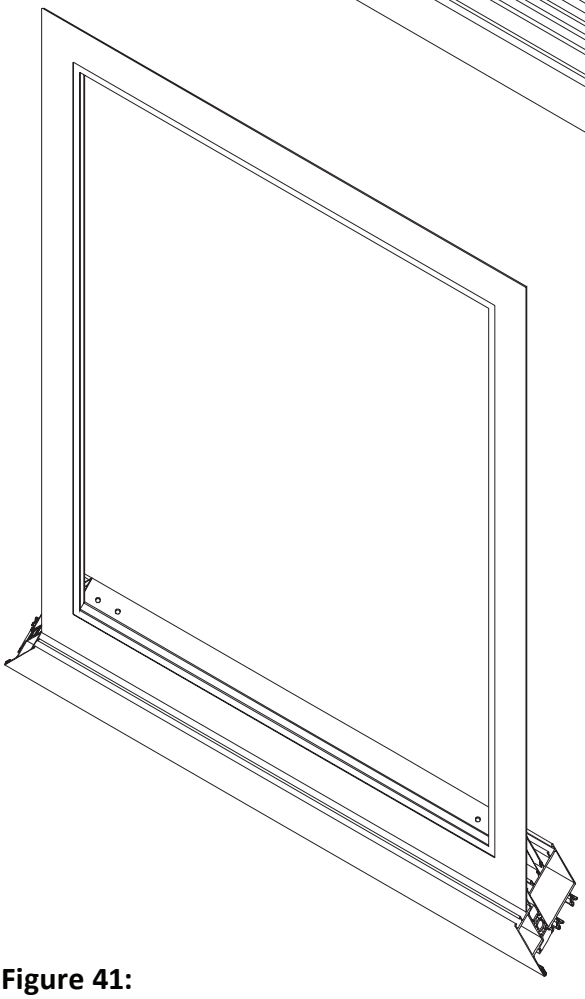

Figure 41:
Aluminum profile clamping on bottom edge
Source: Own image

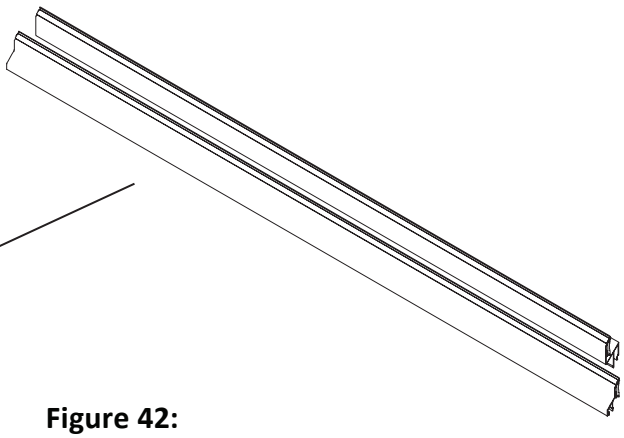

Figure 42:
Clamping profile on bottom edge
Source: Own image

In this step, **Figure 43-46**, double glazing unit has to be made. Both thin glass panels need to be painted on the edges and assembled with super spacer and silicone adhesive.

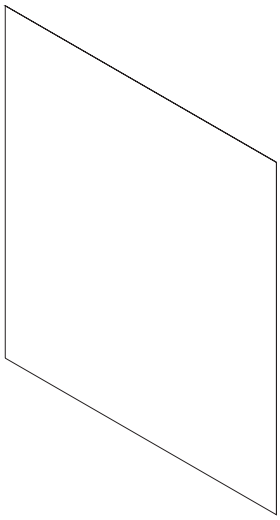

Figure 43:
Thin glass panel
Source: Own image

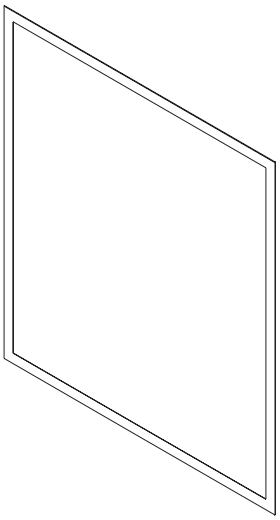

Figure 44:
Thin glass panel with edge painting
Source: Own image

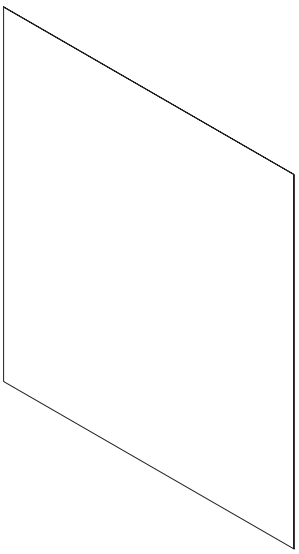

Figure 45:
Thin glass panel
Source: Own image

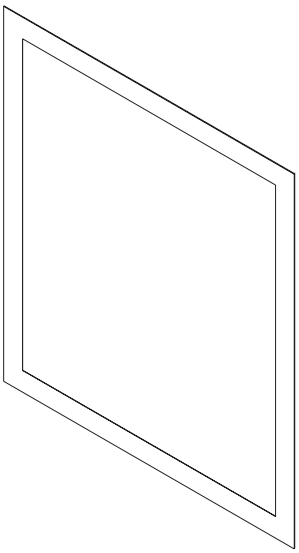

Figure 46:
Thin glass panel with edge painting
Source: Own image

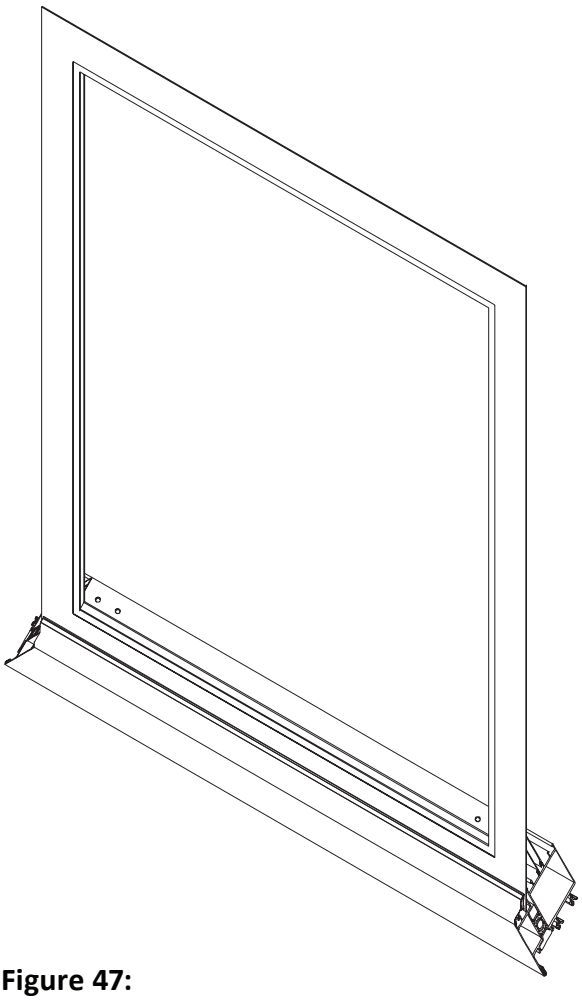

Figure 47:
Double glazing panel clamping system
Source: Own image

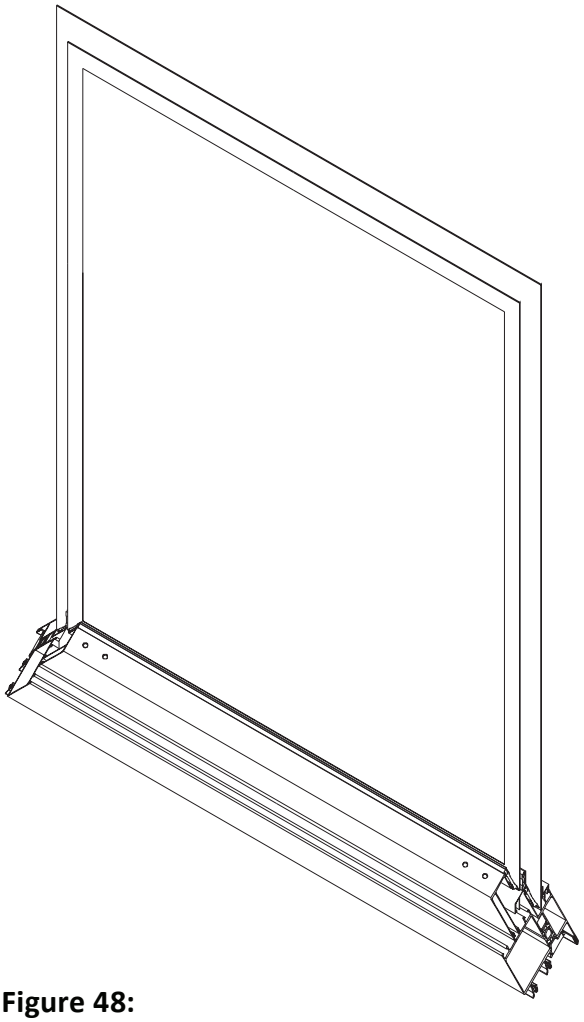

Figure 48:
Double glazing panel clamping system
Source: Own image

This step is to install SPA and assemble it with window frame. First of all, the support need to be fix on existing profile (**Figure 49**). And then SPA segments need to be glued on thin glass and the last one on the bottom has to be connected with the support. (**Figure 50**) After all steps are done, the last step is to put clamping window unit into window frame and screw it in the corner.(**Figure 51**)

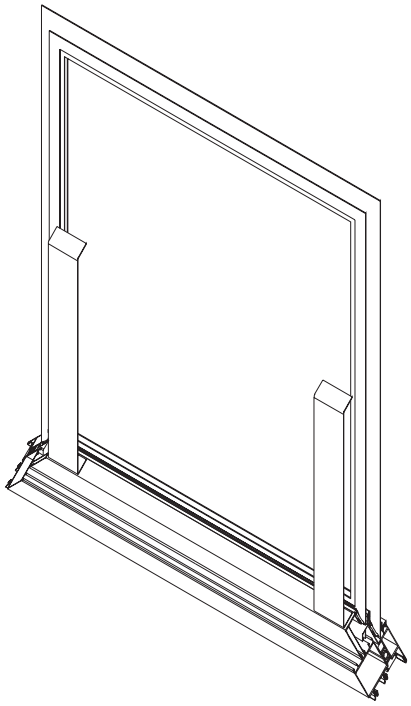

Figure 49:
SPA support installing
Source: Own image

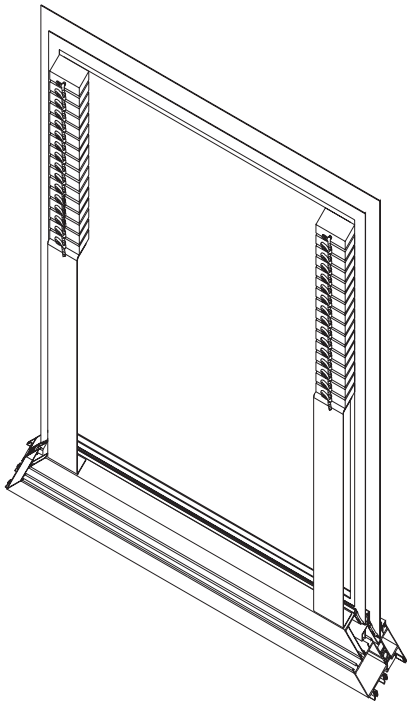

Figure 50:
SPA installing
Source: Own image

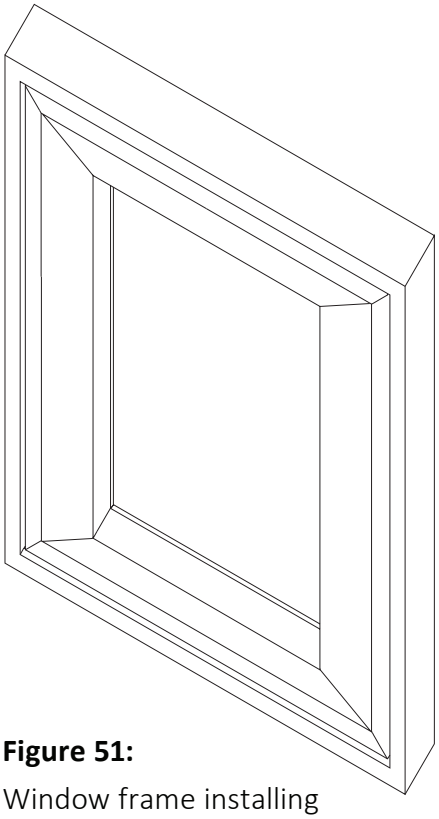

Figure 51:
Window frame installing
Source: Own image

Figure 52:
Window opening rendering inside view
Source: Own image

Figure 53:
Window opening rendering outside view
Source: Own image

7.5. Window opening and locking system

Window can be locked on two sides by extending locking supports from window frame holes. When window needs to open, locking supports will be pulled back and actuator will be inflating. When window needs to close, actuator will be deflating and the locking system will extend to hold the window from wind load.(**Figure 54**)

Figure 54:
Window locking status
Source: Own image

8. CASE STUDY

8.1. Case study A:

In the case study, the selected facade to analyze is the located on the Southwest side of the Technology, Policy and Management Building at TU Delft in the Netherlands. (**Figure 1** and **Figure 2**)This building was finished in 1999 and it contains offices, lecture rooms, a cafeteria and a small library. The complex has a "U" shape and a Surface of 13,290m2 approximately. The construction of the building was based on prefabricated elements that were made in a factory and then assembled in place.

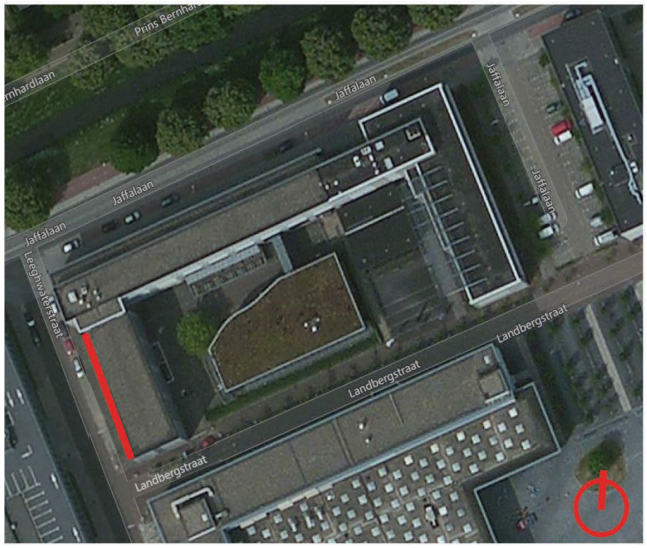

Figure 1:
Google map view
Source: Google map

Figure 2:
Building facade
Source: Google map

The case study is an office room with two openable window and two fixed window. (**Figure 3**) The openable window edge hung window with 900mm width times 1600mm hight frame.

Figure 3:
Inside view of office
Source: Own image

Figure 4:
Window hinge system
Source: Own image

The original window frame is made of wood. In this chapter, I will use RT 82 HI+ aluminum-frame window from KAWNEER, IDEAL 5000 uPVC-frame window from AIKON and EXOSKELETWINDOW from myself to replace the existing window and to make a comparison. (**Figure 5-7**)

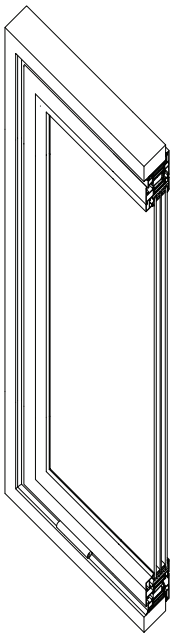

Figure 5:
RT 82 HI+
Source: Own image

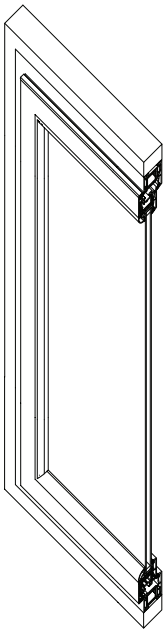

Figure 6:
IDEAL 5000
Source: Own image

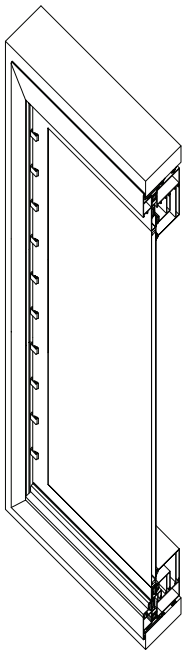

Figure 7:
Exoskeletwindow
Source: Own image

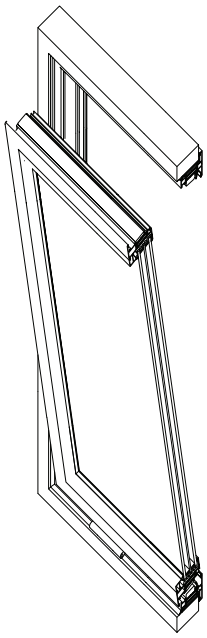

Figure 8:
RT 82 HI+
Source: Own image

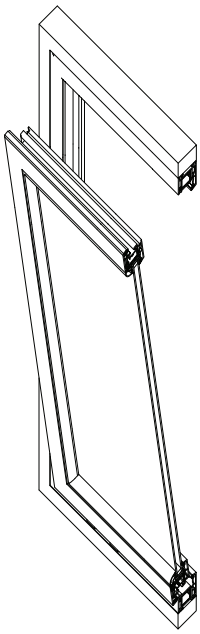

Figure 9:
IDEAL 5000
Source: Own image

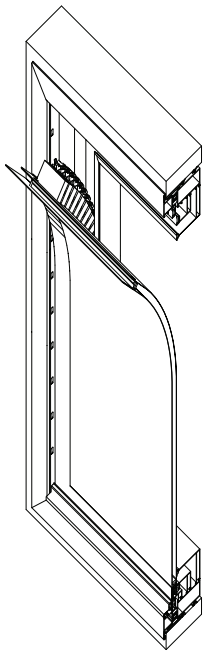

Figure 10:
Exoskeletwindow
Source: Own image

The window hole on the wall is 1000mm*1200mm. To make the window possible to compare with, all types of windows are fixed on the bottom and can be turned inside for ventilation. Instead of turning the whole panel inwards, exoskeletwindow just has to open the upper part, which can get the same amount of fresh air as the other two types.(**Figure 8-9**)

The other advantage is lightweight window panel, compared to the other two windows, thin glass window is very light, the thickness is 0.55mm each piece. The other reason is that exoskeletwindow frame is fixed on the wall and thin glass panel edges don´t need the extra frame, which decreases the weight of the whole panel.

There are also some disadvantages of exoskeletwindow. Because of the actuator size, the width of the window frame is big, which means wide window frame will decrease glass to window panel ratio. In the comparison below, the width of RT 82 HI+ aluminum-frame window is 90mm, the width of IDEAL 5000 uPVC-frame window is 122mm and the width of exoskeletwindow is 180mm. In the discussion chapter, how to decrease the window frame size will be discussed. (**Figure 11-13**)

The other disadvantage is worse thermal insulation than the other two windows. The reason is thermal insulation of thin glass is worse than normal glass.

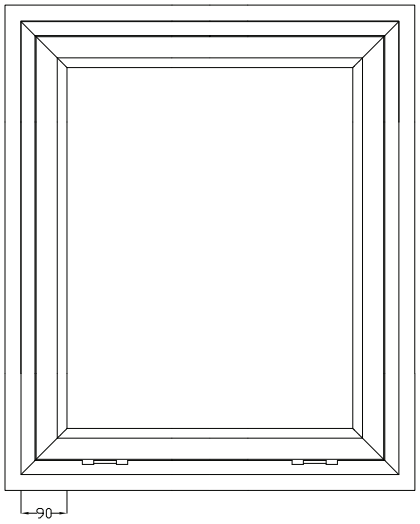

Figure 11:
RT 82 HI+
Source: Own image

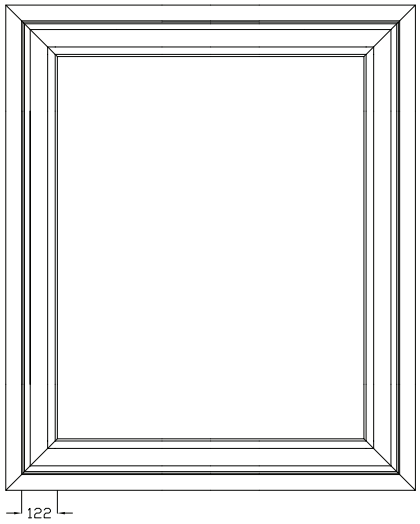

Figure 12:
IDEAL 5000
Source: Own image

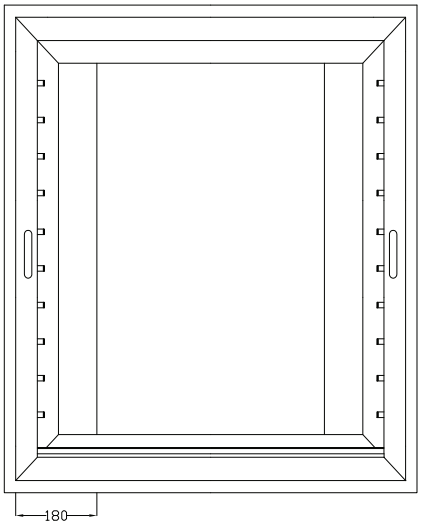

Figure 13:
Exoskeletwindow
Source: Own image

8.2. Case study B:

In the case study B(**Figure 13-17**) (Wateringse veld College), the function of this building is school. This is a real project which needs to be renovated in the greenhouse part. The architect wants to keep the industrial structure and replace the single glazing faced by double glazing facade to increase thermal insulation. However, the architect wants to decrease the glass weight also need good insulation. My suggestion of this project is to use thin glass double glazing unit insulating with argon. To ventilate the atrium, the curved window can be used to improve the indoor climate.

Figure 13-17:
Google map view
Source: Google map

8.3. Case study C:

In this case study, I will discuss how to use this system in the second facade. The advantage of this system is continuously geometry changing. Inspired by other sun shading system, I integrated this system with sun shading system. (**Figure 18-19**). By changing the curvature of each plate, the daylight will come into the room. The shape of the plate can be developed. Also, the surface of the plate can integrate with solar cell system to generate electricity.

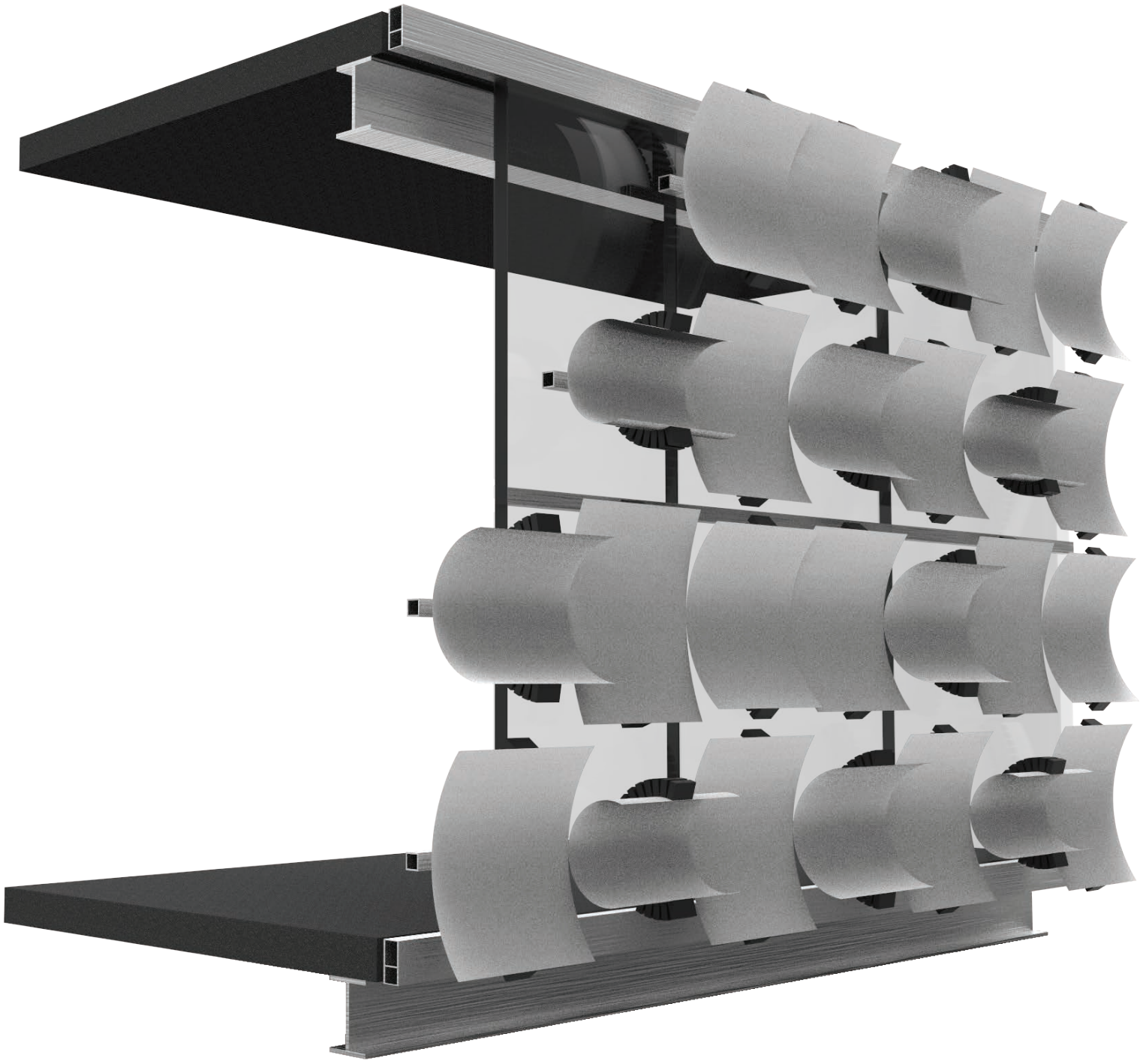

Figure 18:
Outside view of sun shading system
Source: Own image

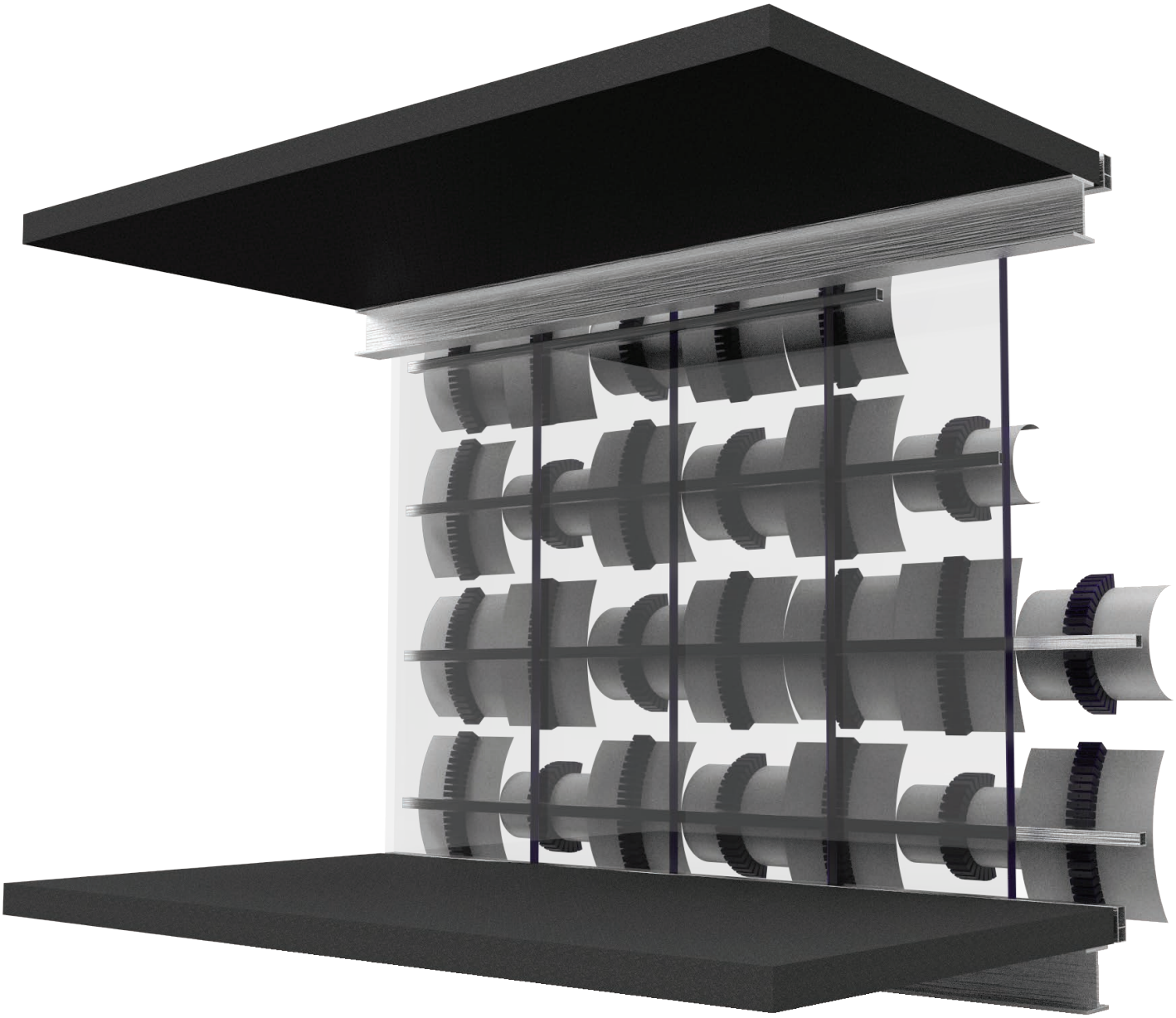

Figure 19:
Inside view of sun shading system
Source: Own image

8.4. Case study D:

In the case study D, pneumatic actuators are placed in the middle to bend the window top. The reason for this design is to minimize the size of the window frame. So the width of the window frame is smaller than the previous design and enlarge the view from inside.(**Figure 20-23**)

Figure 20:
Outside view of window system
Source: Own image

Figure 21:
Inside view of window system
Source: Own image

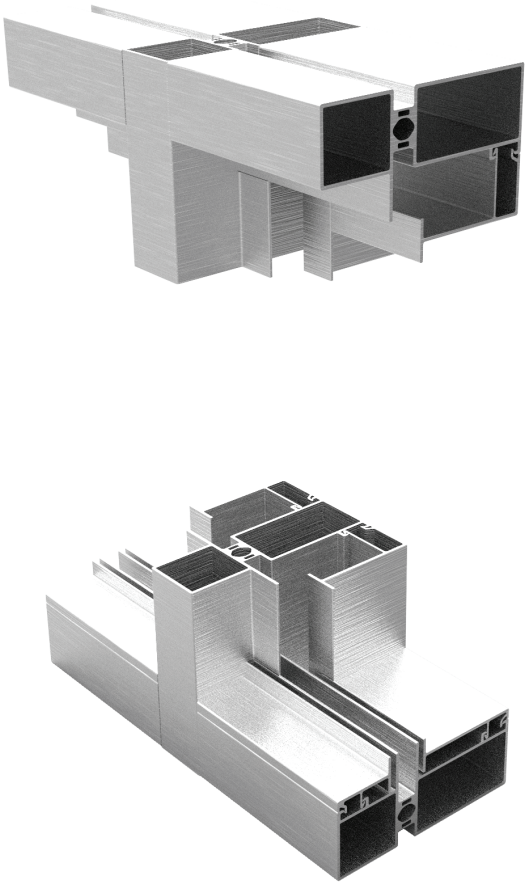

Figure 22:
Window frame details
Source: Own image

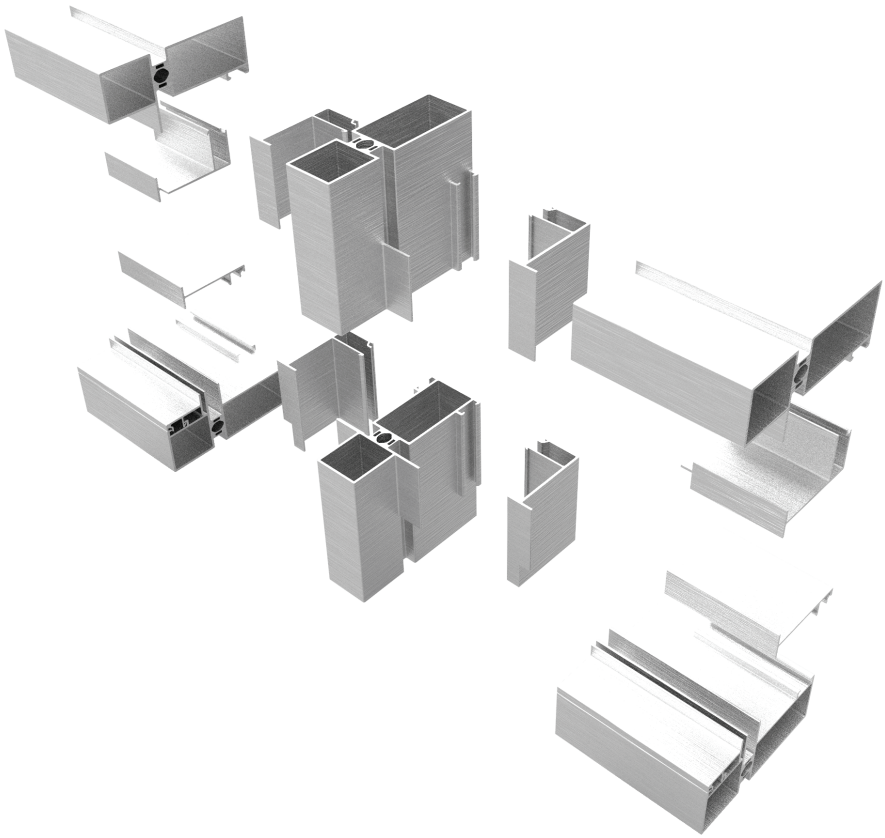

Figure 23:
Window frame Joint
Source: Own image

9. SIMULATION

In this chapter, I use Abaqus CAE to simulate bending behavior. The reason for simulation is to validate hand calculation. Here is the methodology of simulation. At first, three models need to be set up. We can see from the figures below, SPA without bottom connection (**Figure 1**), SPA with bottom connection(**Figure 2**) and SPA without contacting segments (**Figure 3**). The meaning of simulate SPA without contacting elements is calculating stretching bending behavior and compare with contacting bending behavior to prove my previous theory. The previous theory is contacting bending moment is much larger than stretching bending moment, which means contacting will help to bend thin glass more than stretching. Meanwhile, SPA with connection on the bottom will overcome resistance from rubber connection, this will also counteract contacting bending moment. In these three simulations, the deformation on the top edge of first design is the largest.

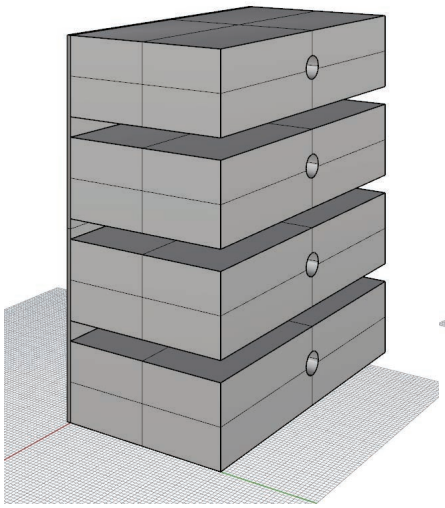

Figure 1:
Seperate segments
Source: Own image

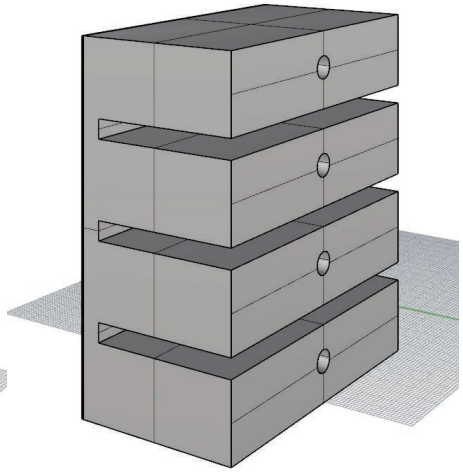

Figure 2:
Connected segments
Source: Own image

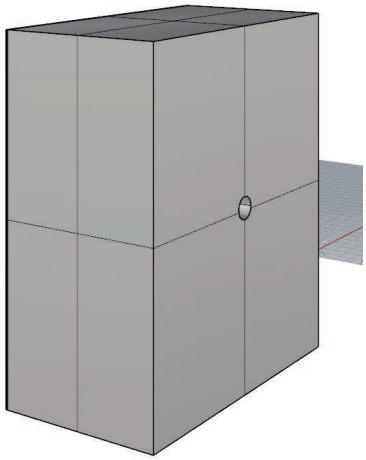

Figure 3:
Whole segment
Source: Own image

To prove this assumption, I run the three simulations in Abaqus CAE and calculate the maximum deformation on Y direction. To simplify the simulation, I calculate the equivalent of the object. Here is the calculation process about $EI_{effective}$. In the equivalent process, the goal is to transfer insulation window into single layer glass plate. So, equivalent young's modulus and thickness need to be calculated. (**Figure 4**)

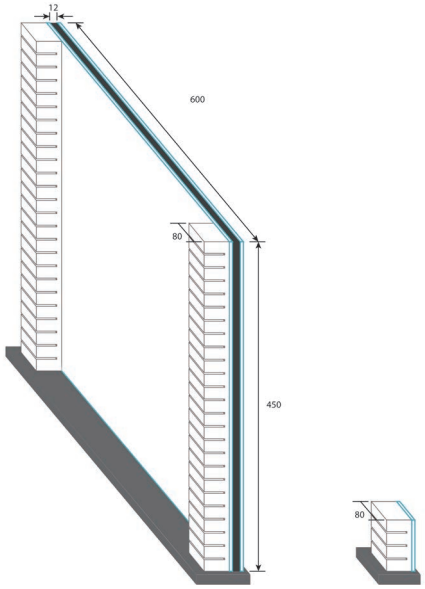

$$2E_{thin\ glass} * I_{thin\ glass} + E_{spacer} * I_{spacer} = E_{equivalent} * I_{equivalent}$$

If we set glass thickness is 1.1mm, in this formular we can get $E_{equivalent}$=84556MPa

Figure 4:
Equivalent model
Source: Own image

In the simulation, I use 1.1mm thickness glass material on the bottom and natural rubber SPA on the top. The air pressure is 2 bars only. In the simulation below, we can find the bending behavior and deformation on Y-Axis. (**Figure 5**)

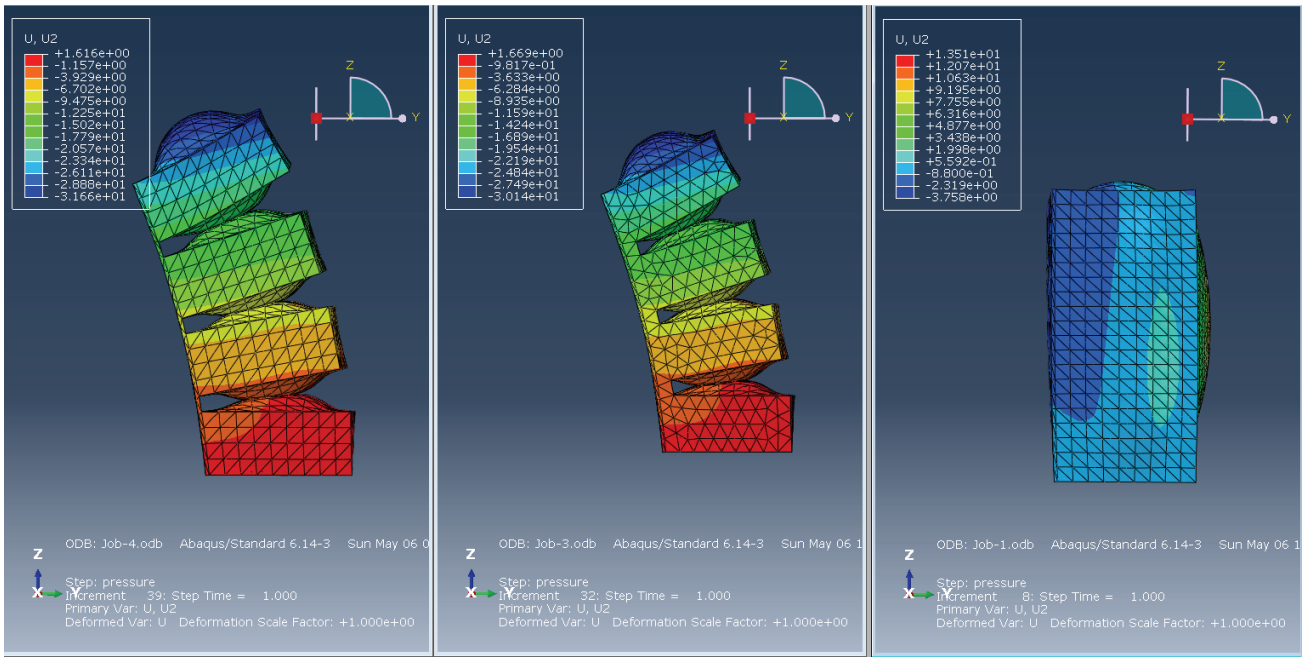

Figure 5:

Abaqus simulation under 2 bars

Source: Own image

In the simulation below, we can find the maximum deformation on the first design is -23.27mm, comparing to the second design, the maximum deformation on Y-axis is -22.14mm, which is smaller. The top edge of the third design is -1.348mm. From this result, it is very clear that without connection between the air chamber will make the bending behavior easier. (**Figure 6**)

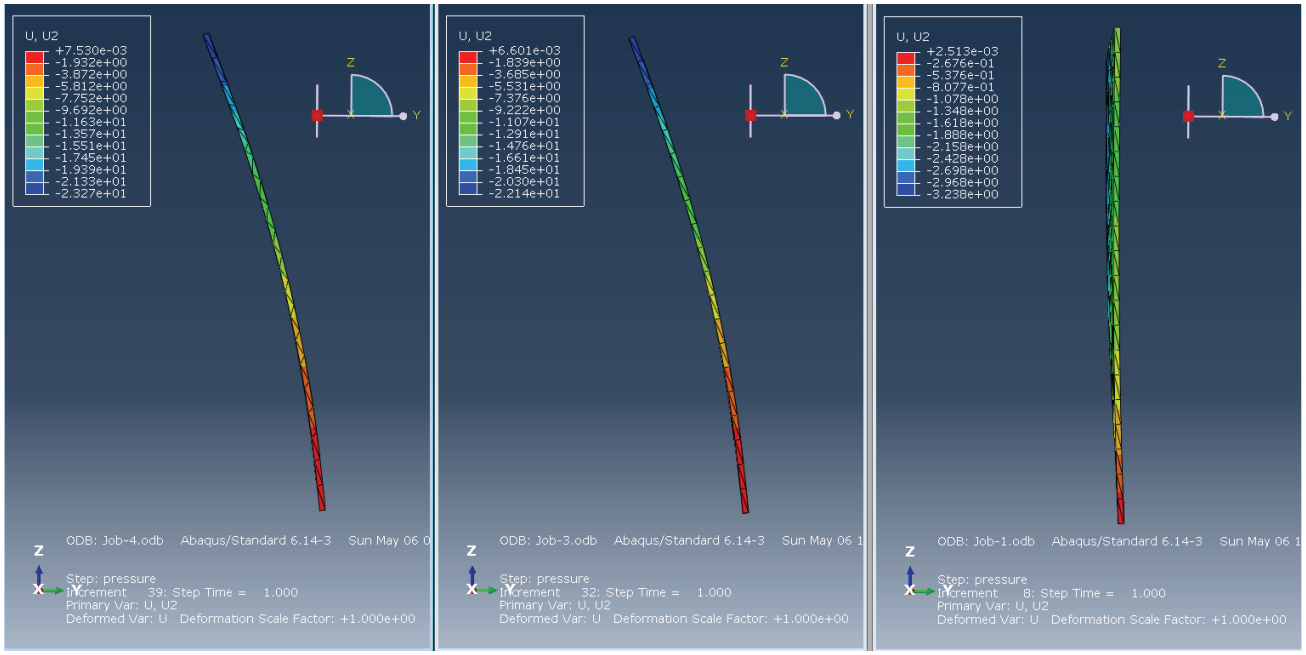

Figure 6:

Thin glass bending behavior in Abaqus

Source: Own image

Secondly, the important outcome of this simulation is stress on the thin glass. (**Figure 7**)From the information in previous research, the maximum stress on the thin glass surface is 260MPa. In this simulation, the goal is to control maximum stress under 260MPa and find a relationship between air pressure and tensile stress. From the result I show below, the maximum stress on glass plate surface is 163MPa. The results of first design and the second design are almost the same.

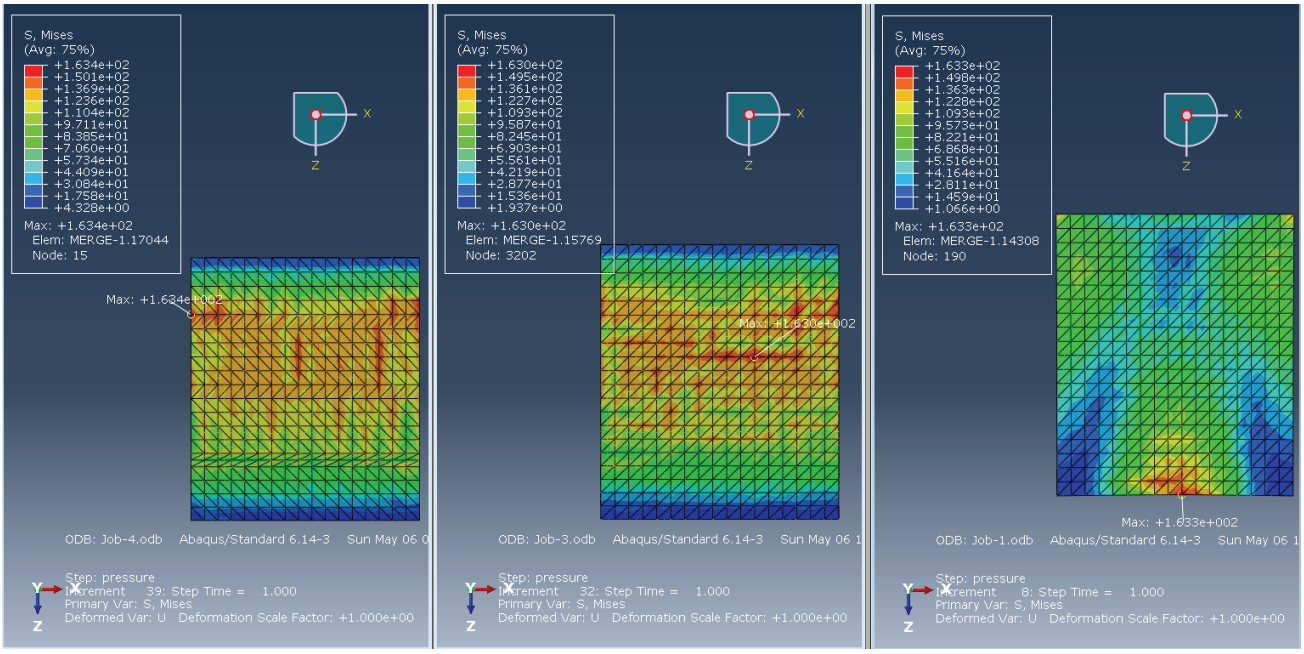

Figure 7:

Stress on thin glass simulation

Source: Own image

Validation

Because of the air chamber is contacting with each other, the air pressure will be higher than 2 bars. In the hand calculation, the air pressure can be approximately 2.8 bars and the contacting coefficient can be 0.75. The stress result on the glass plate surface is 163.76MPa, which is almost the same as the simulation result. This means the Abaqus model can be validated. (**Figure 8**)

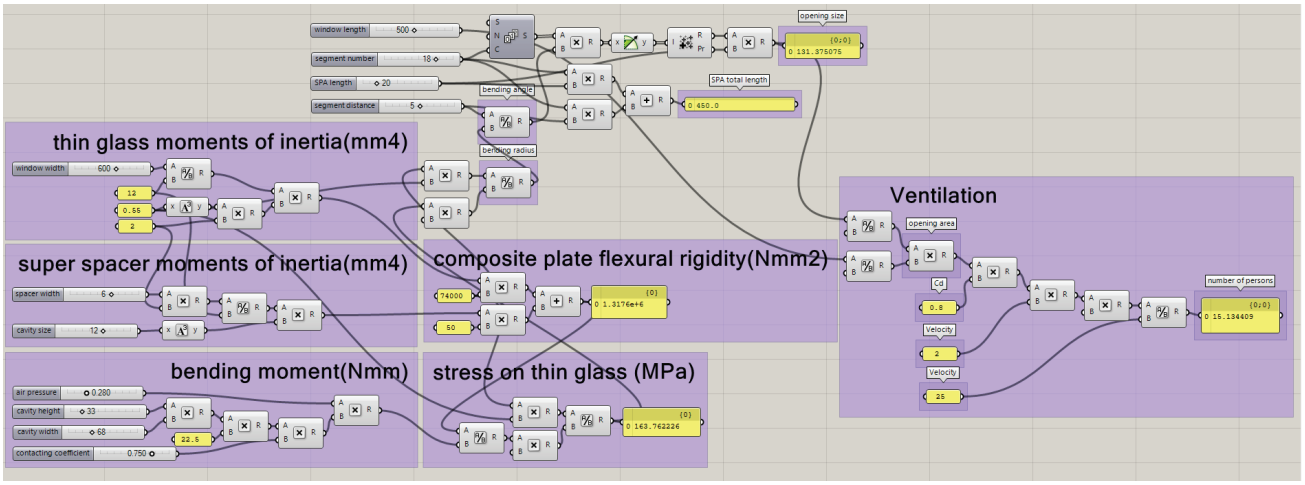

Figure 8:

Hand calculation in grasshopper

Source: Own image

Last but not least, Abaqus can also simulate in different marerials. In the simualtion below, the same geometry is used, but the materials are nature rubber and elastosil M4601 respectively.(**Figure 9-11**)

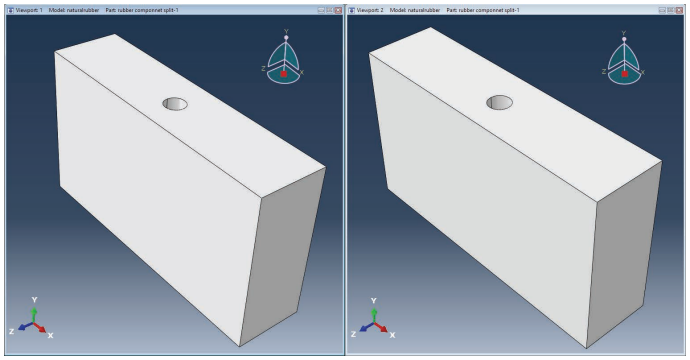

Figure 9:
Same geometry with different materials
Source: Own image

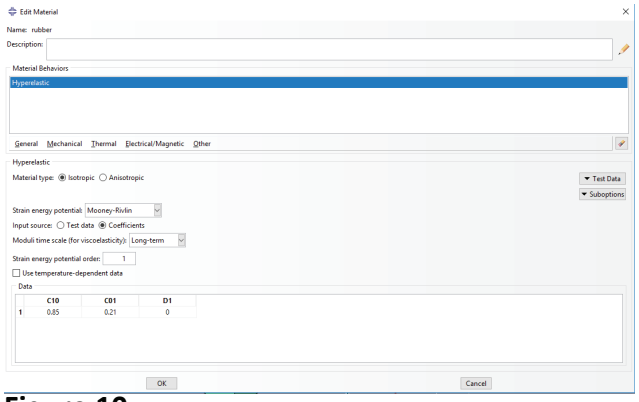

Figure 10:
Natural rubber setting
Source: Own image

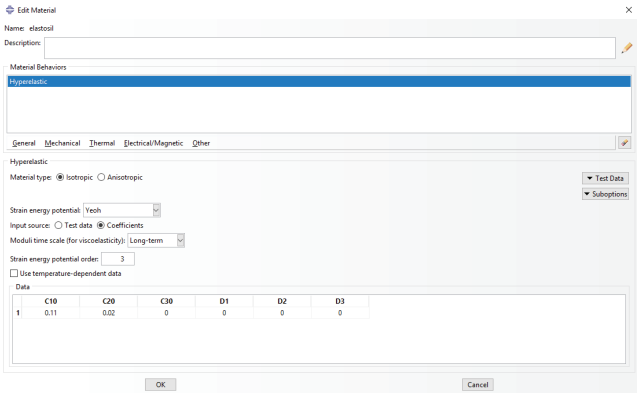

Figure 11:
elastosil M4601 setting
Source: Own image

In the simulation result, under 1 bar air pressure, nature rubber block expand much less than the elastic block. The deformation on Z-axis is 8.07mm and 41.1mm respectively. Also, on the top layer surface, rubber block almost doesn't deform, however, elastic block deforms a lot which will cause cohesive failure between SPA and the thin glass plate.

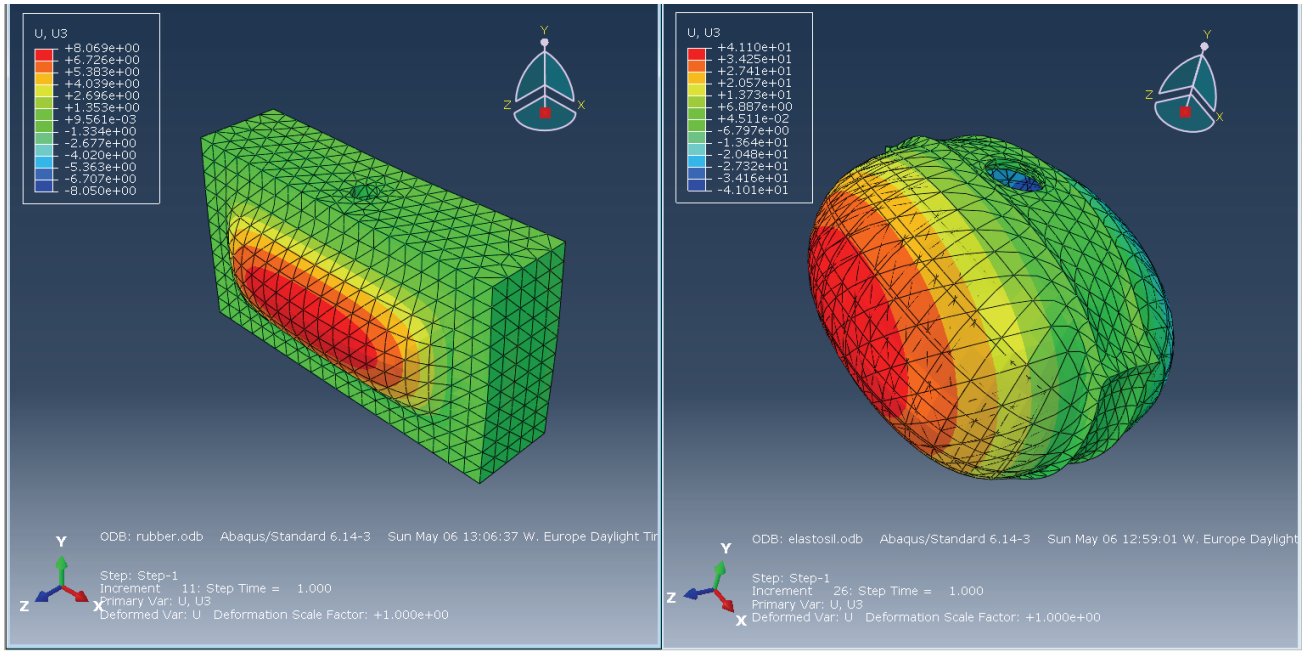

Figure 12:
Segments inflating deformation
Source: Own image

From the previous research, the maximum tensile strength of natural rubber is 28MPa, but elastosil just has 6.5MPa. From the simulation result below, maximum tensile stress happens on natural rubber is just 1.54 MPa, however, maximum tensile stress on the elastic block is 20MPa. This also means elastosil block cannot stand 1 bar air pressure. (**Figure 13**)

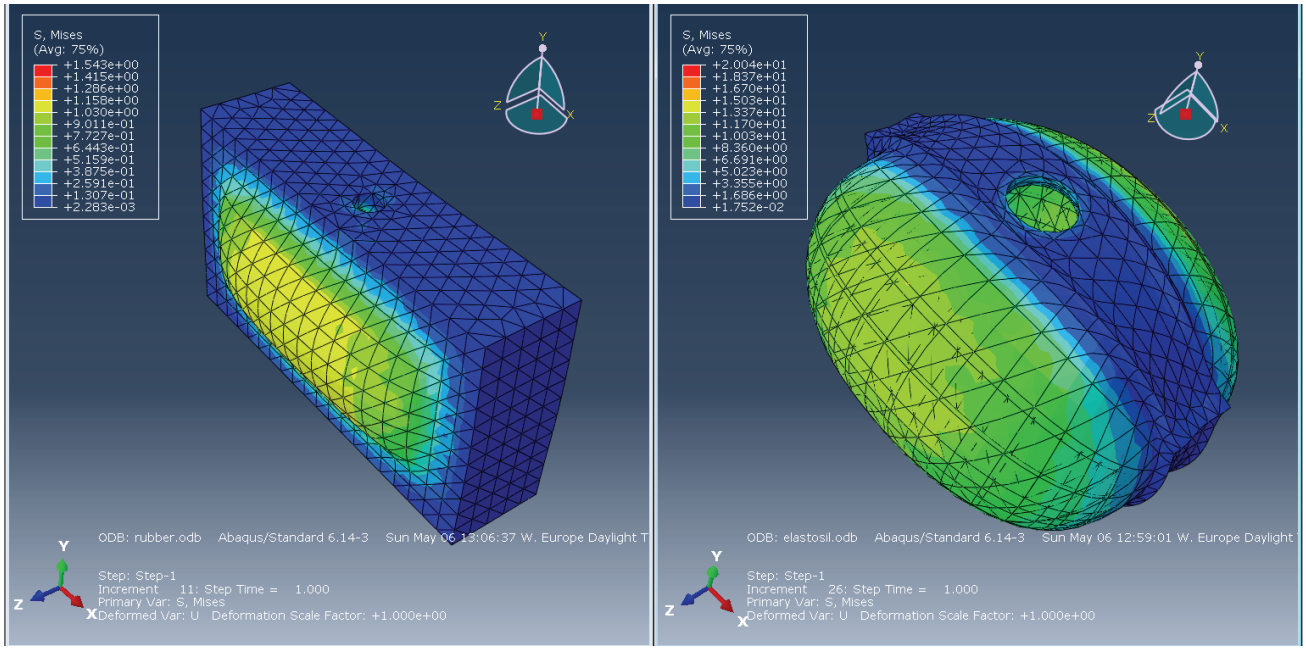

Figure 13:
Segmens inflating stress simulation
Source: Own image

Instead of using equivalent formula, I made the composite simulation in Abaqus. The reason of this simulation is to find the stress concentration in IG unit and bending edge deformation. To build the Abaqus model, IG unit should be set as a sandwich composite, silicone cohesive-super spacer- silicone cohesive. To simplify the simulation process, I use silicone material as IG unit instead of using complex sandwich composite. (**Figure 14**)

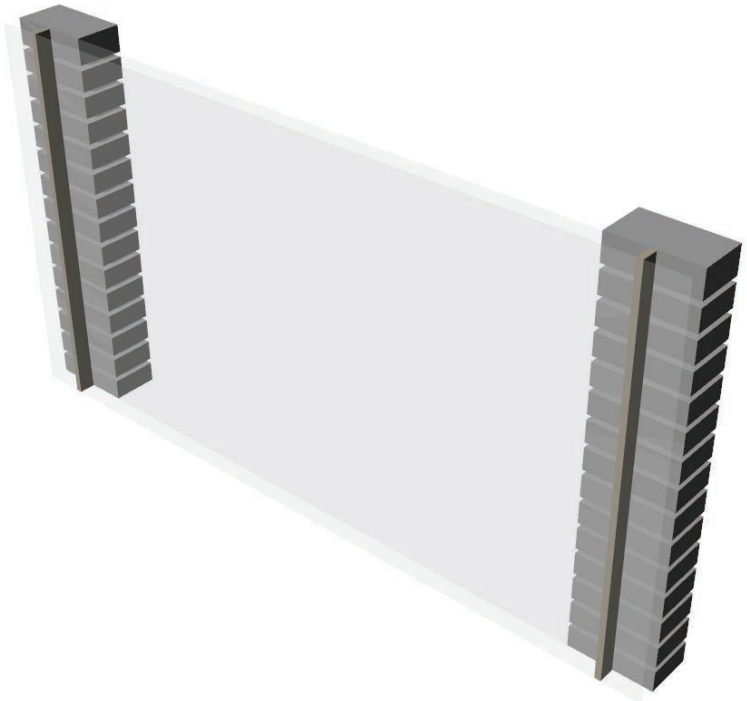

Figure 14:
Composite simulation
Source: Own image

The air pressure in chambers is 1 bar. The length of the window is 700mm. There are 15 segments on each side. When inflating, The maximum deformation on Y-axis is 21mm, which happens on the top edge. By increasing air pressure, there will be more deformation. (**Figure 15**)

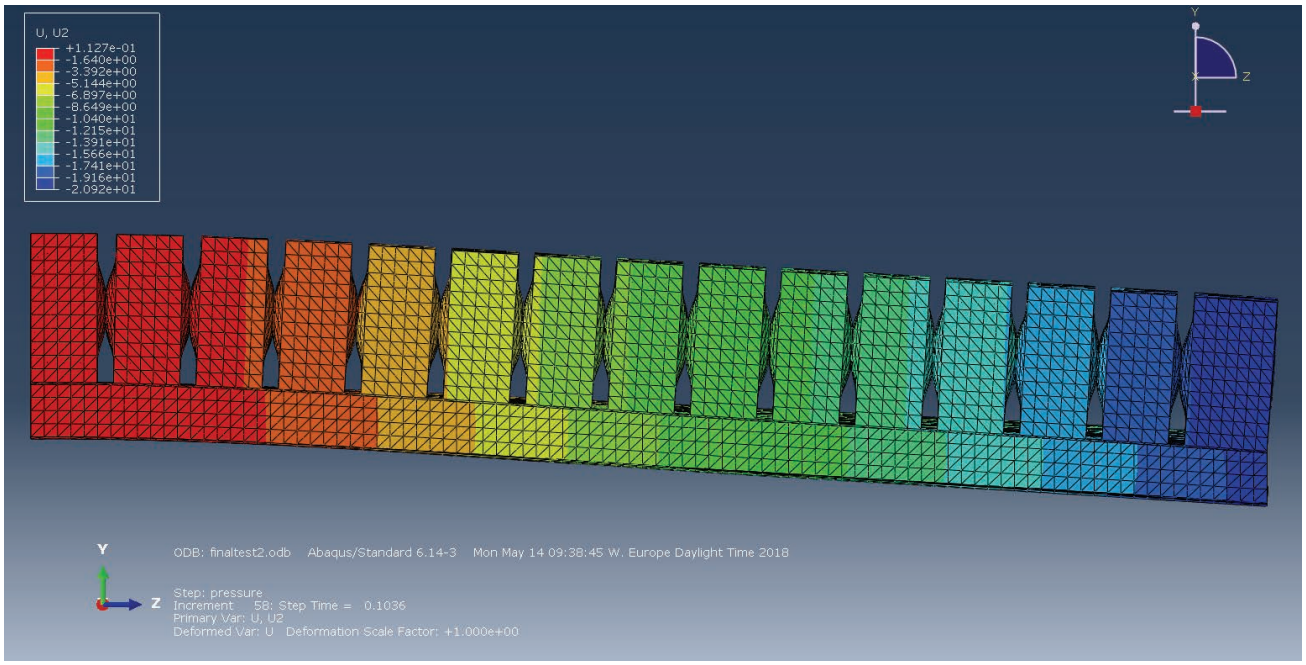

Figure 15:
Composite simulation
Source: Own image

To validate the result, I use hand calculation. The air pressure should be more than 1 bar because of segments squeezing. I set 1.2 bars in air pressure, and the contacting coefficient is almost 50%. From the grasshopper calculation, the outcome of opening size is 19.6mm, which is close to simulation result. (**Figure 16**)

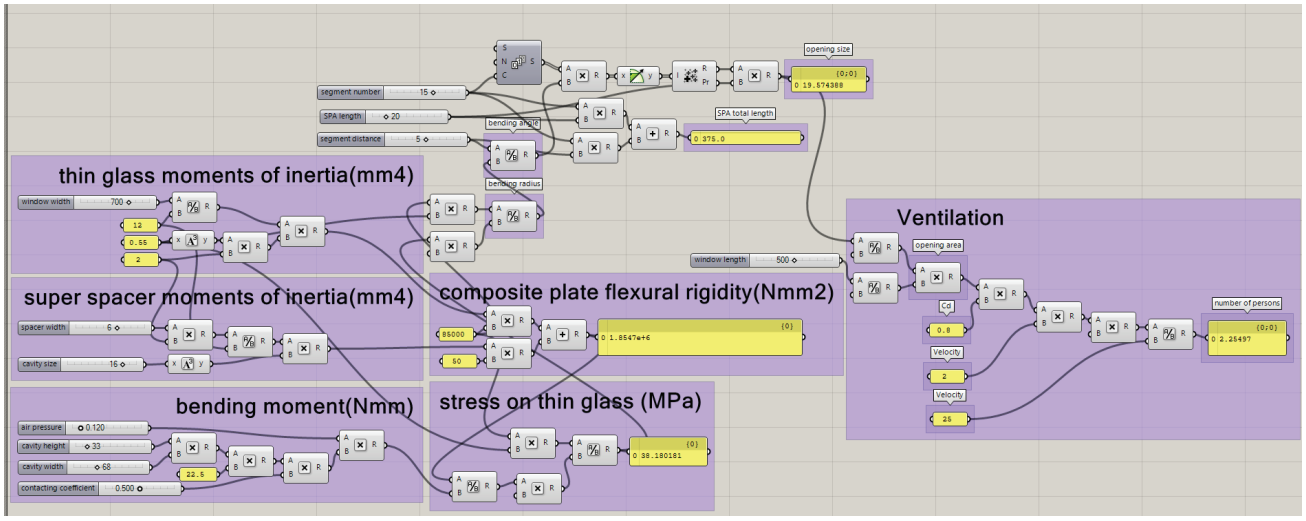

Figure 16:
Hand calculation validation
Source: Own image

To validate the result, I use hand calculation. The air pressure should be more than 1 bar because of segments squeezing. I set 1.2 bars in air pressure, and the contacting coefficient is almost 50%. From the grasshopper calculation, the outcome of opening size is 19.6mm, which is close to simulation result.

The maximum tensile stress of rubber segment is 0.88MPa on contacting area.
In this simulation, I find the maximum tensile stress happens near the inside corner of segments. This proves the speculation before, which is maximum shear stress happens on the inner corner. This is the reason inner corner is rounded instead of 90 degrees straight.(**Figure 17**)

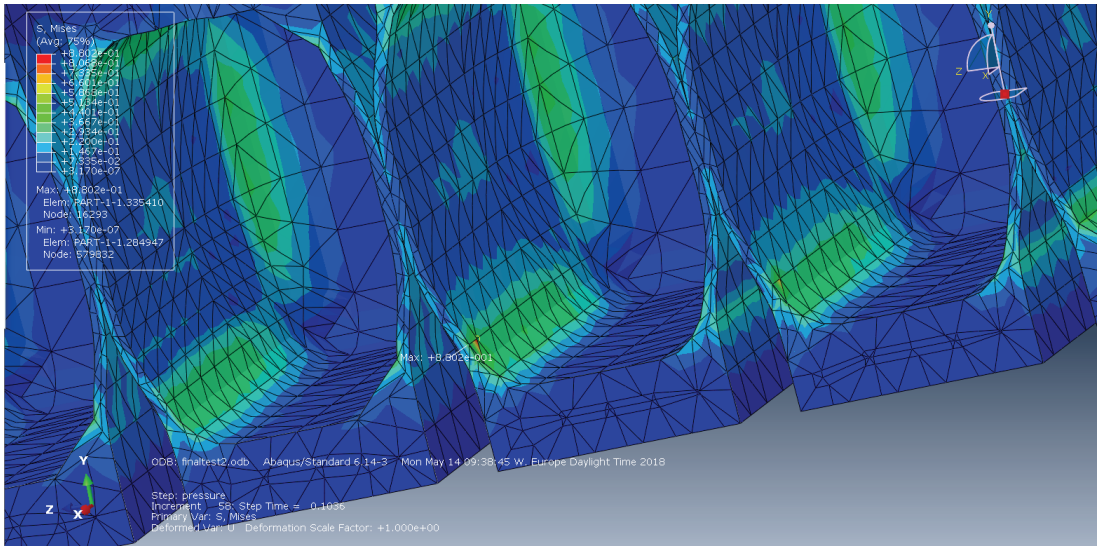

Figure 17:
Tensile stress inside segments
Source: Own image

From the previous chapter, I discussed comfort and aerodynamic theory which is the reason exo-skeleton is developed. In this chapter, I will discuss how it improves room comfort. The three main aspects to improve percentage dissatisfied due to draft are air temperature, mean air velocity, and turbulence intensity. In this standard room, the window is the only way to generate airflow, so the inlet airflow rate and inlet airflow turbulence intensity will affect the result. When the air velocity increases in the room, people will feel cooler because air takes away the heat from people's body. In different mean radiant temperatures and different airspeed situations, how much cooling is possible, ASHRAE 55 standard gives guidelines for this answer. When the air temperature is 5°c lower than radiant temperature, every 3°c temperature increasing will need 0.8m/s air velocity increasing to keep the balance of comfortable feeling. However, when the inlet air temperature is 5°c higher than radiant temperature, every 3°c temperature rasing needs 1.6m/s speed increase, which is much higher than acceptable wind condition for office. (**Figure 18-19**)

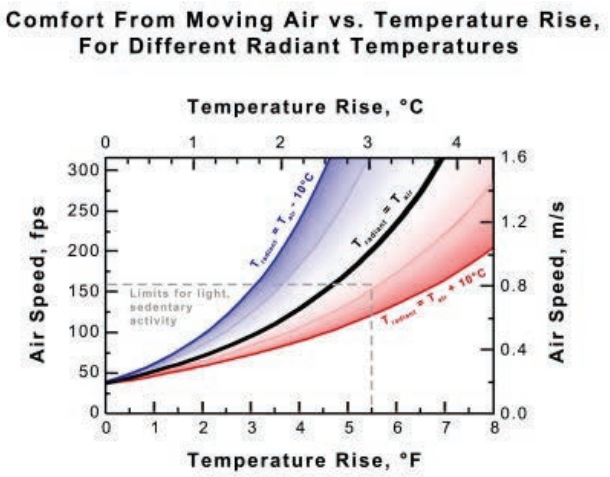

Figure 18:
Comfort from moving air vs temperature rise
Source: Own image

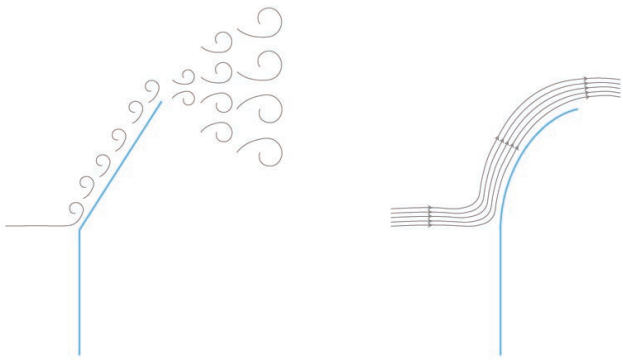

Figure 19:
Wind on straight surface and curved surface
Source: Own image

When the temperature increase inside, higher airflow rate is needed to cool down people in the room. But how much window opening is needed for ventilation is difficult to control. Also, airflow changing ratio on straight window panel is much higher than the curved window, this means that when a small amount of airflow rate changing can be achieved by window curvature changing. In other words, by changing window curvature can continually changing inlet air flow rate more smoothly than straight window panel. The other benefit of using curved window is when the wind hit on the curved surface, it will generate laminar air flow instead of turbulent air flow. (**Figure 20**)

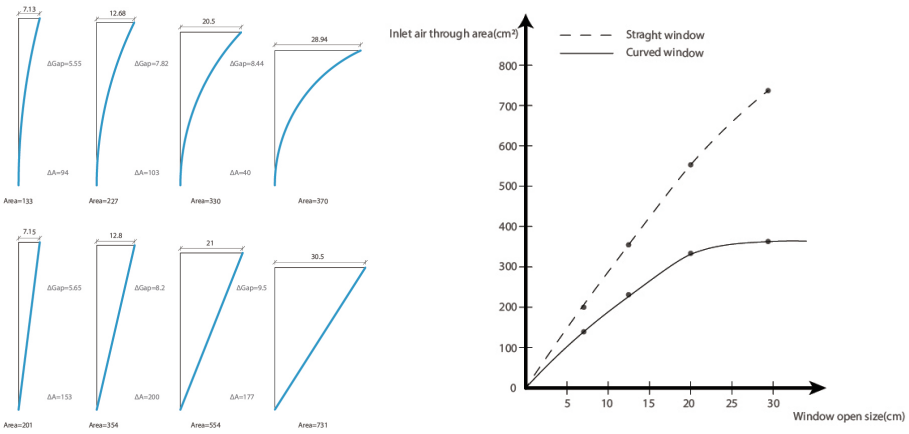

Figure 20:
inlet air flow rate changing ratio
Source: Own image

Here are some ventilative cooling configurations. The first section below shows how to use ventilation to exhaust heat out for cooling indoor environment. The second section shows how fresh air outside circulates in the room and bring warm air out. The third section illustrates single side ventilation. (**Figure 21**)

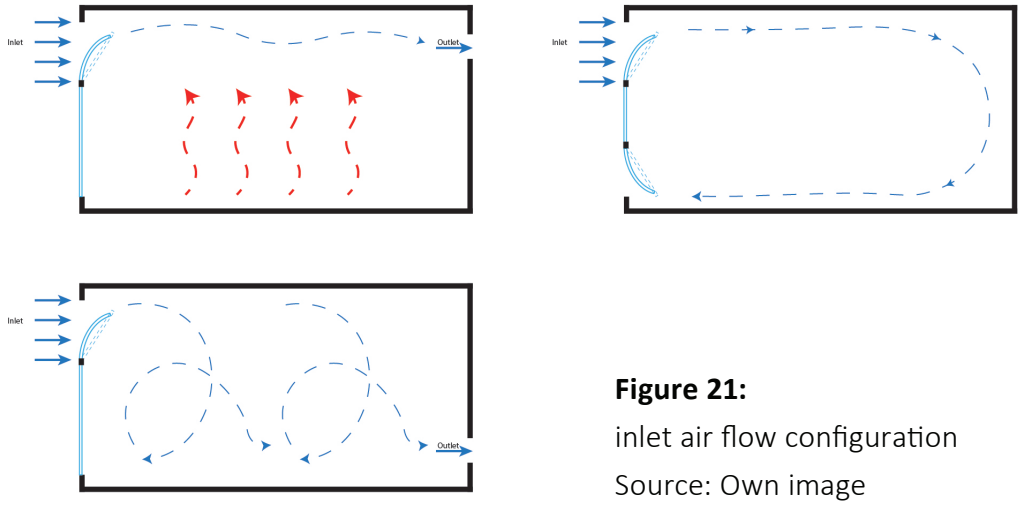

Figure 21:
inlet air flow configuration
Source: Own image

The curved window can also replace wing wall system. By changing the curvature, windows can introduce fresh air into the room adaptively to outside environment. (**Figure 22**)

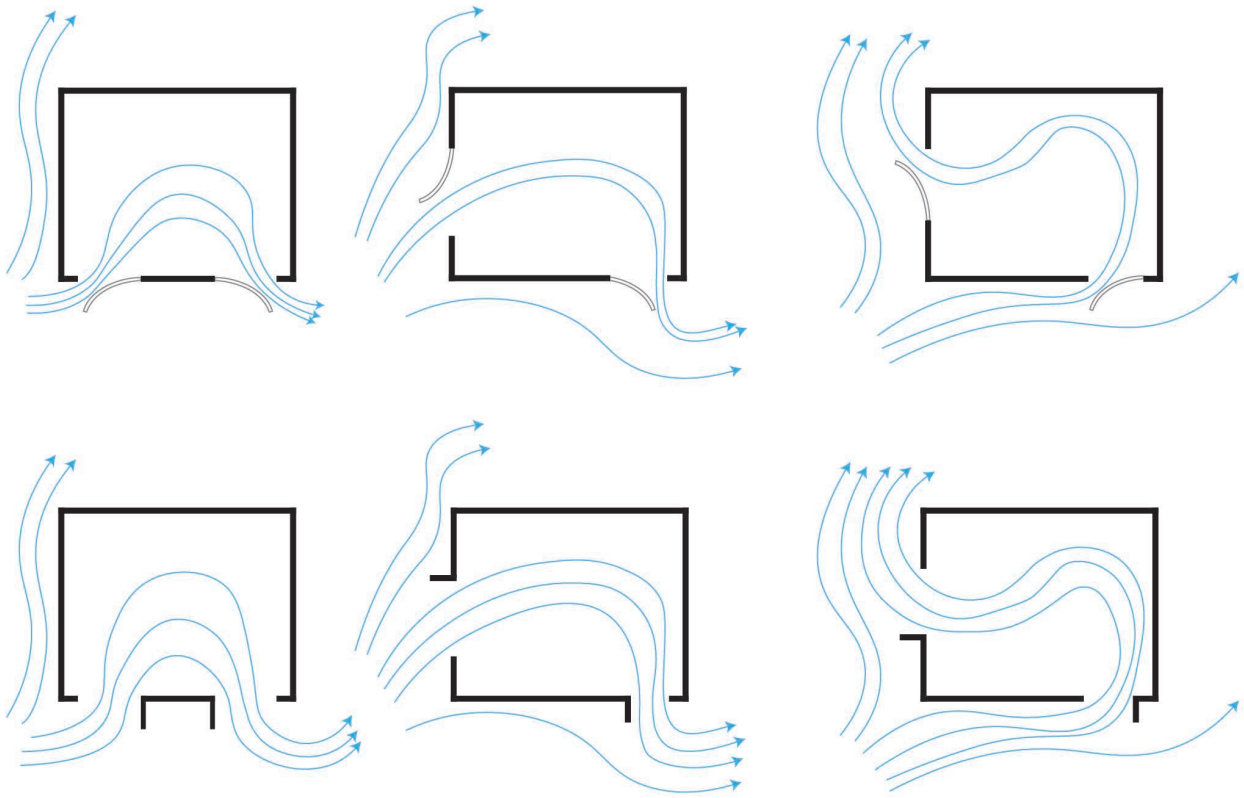

Figure 22:
Wing wall system
Source: Own image

In the market, there are different types of window. Based on the ventilation function, I made a list below. The differences between windows are their opening mechanism. The main benefit of these windows is the potential of high ventilation capacity as well as exoskeletwindow. (**Figure 23**)

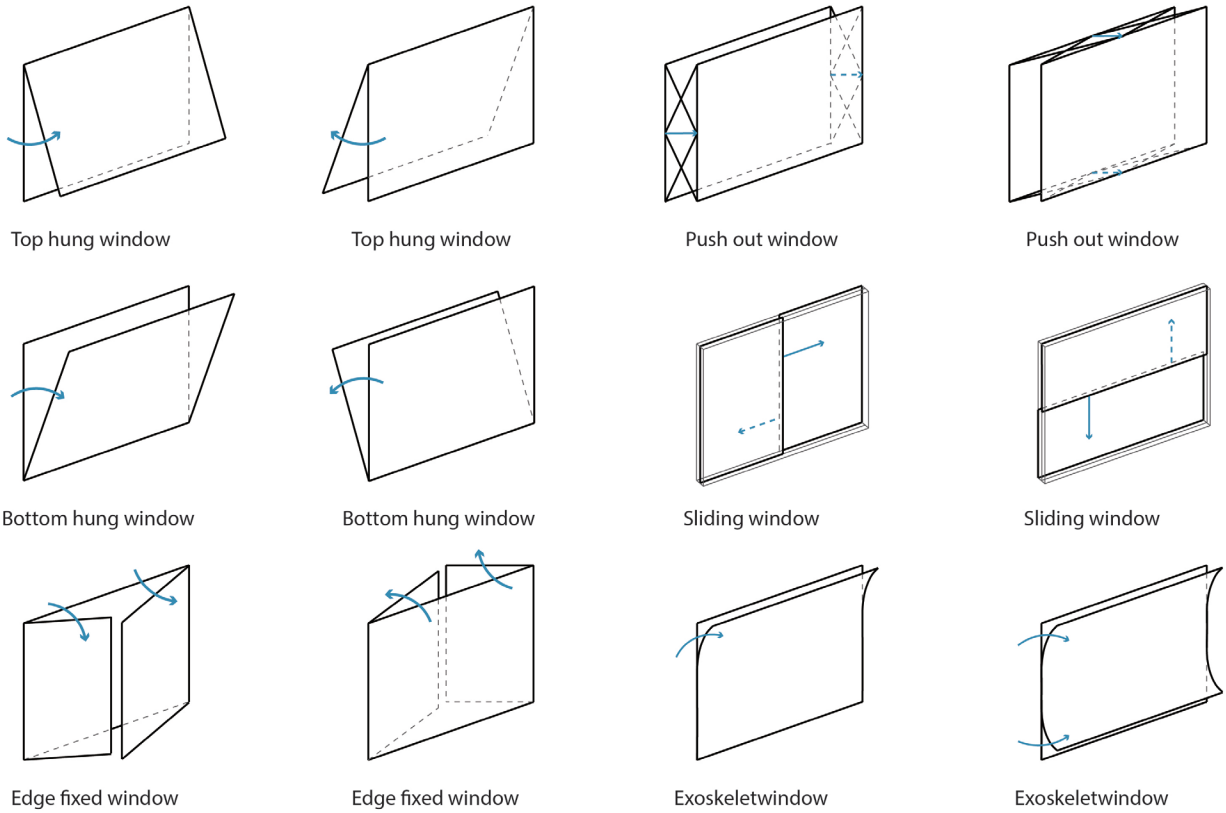

Figure 23:
Existing window types
Source: Own image

To simplify the simulation process, I build a standard model with 2.4M width, 3M hight, and 6M deep. The window is located on one side and the opening is on the opposite wall side. Input air direction is perpendicular on outside wall surface, and the temperature inside and outside is both 18oc. The reason to keep the temperature the same is to make sure the pressure difference due to temperature is zero. (**Figure 24**)

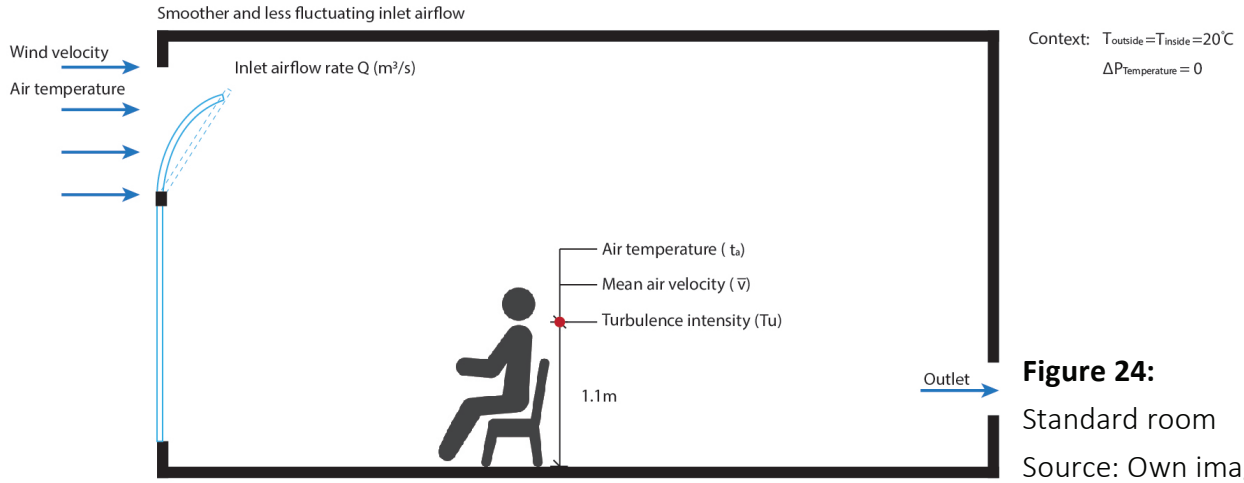

Figure 24:
Standard room
Source: Own image

In the two simulations below, I compare the air velocity, predicted percentage dissatisfied draught rating on Y-axis plane and 1.1m X-axis plane. The two simulations are the curved window and straight window with the same opening size- 12cm. The goal of this simulation is to find how window opening method influences indoor comfort. The inlet air velocity is 2m/s. (**Figure 25**)

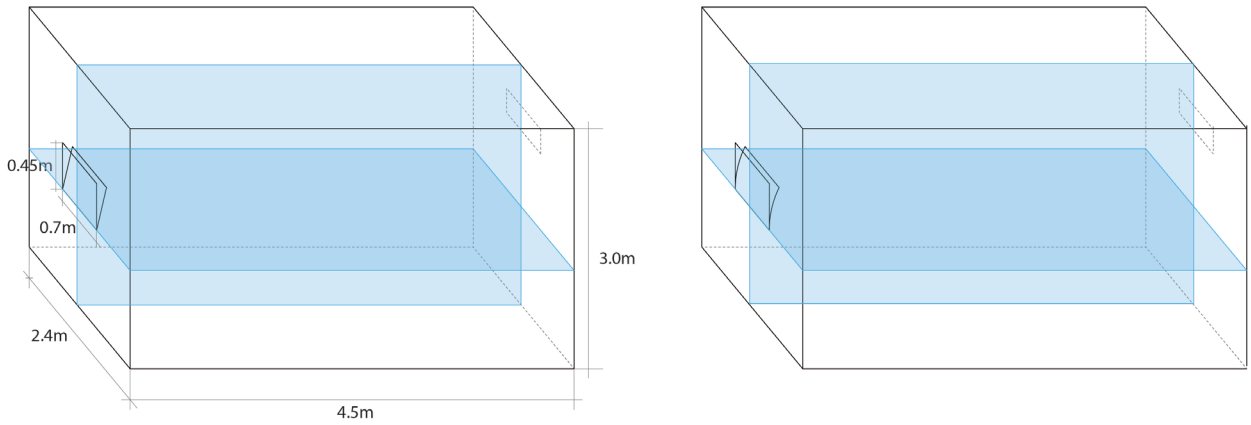

Figure 25:
Standard room with straight window and curved window
Source: Own image

From the results below, it is obvious that air velocity in room A center is higher than air velocity in room B center. This area is highly human activated zone. And the air velocity is about 0.6m/s which will cause the uncomfortable feeling in the working area. (**Figure 26-27**)

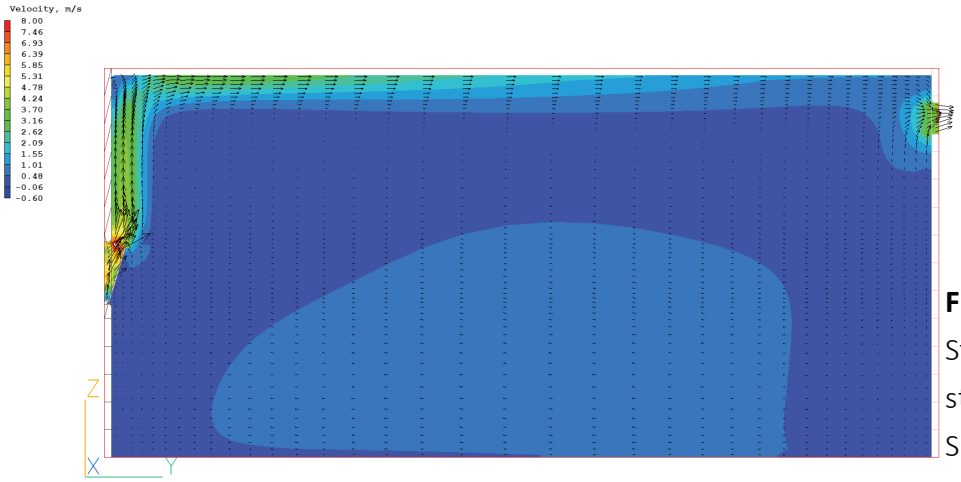

Figure 26:
Standard room with straight window simulation
Source: Own image

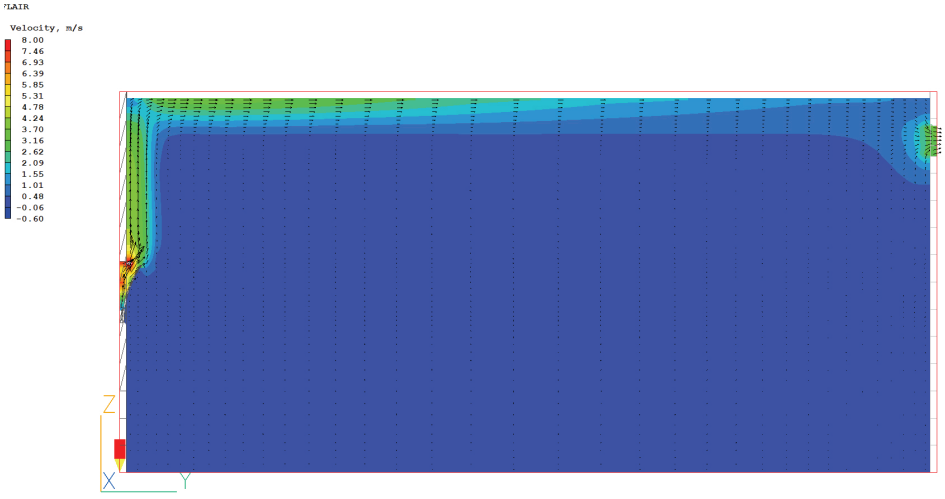

Figure 27:
Standard room with straight window simulation
Source: Own image

PPDR in this simulation shows the results in the 1.1M high plane. Because human's neck is very sensitive and the hight when they are working is abound 1.1m. From the result below, it is clear that people will complain about the draught much more in room A than in room B. The pattern in the middle and the edge is almost red in room A simulation. Compare with room A, room B has a pleasant indoor environment. The working area in room B has low PPDR numbers. This means curved window improves indoor environment. (**Figure 28-29**)

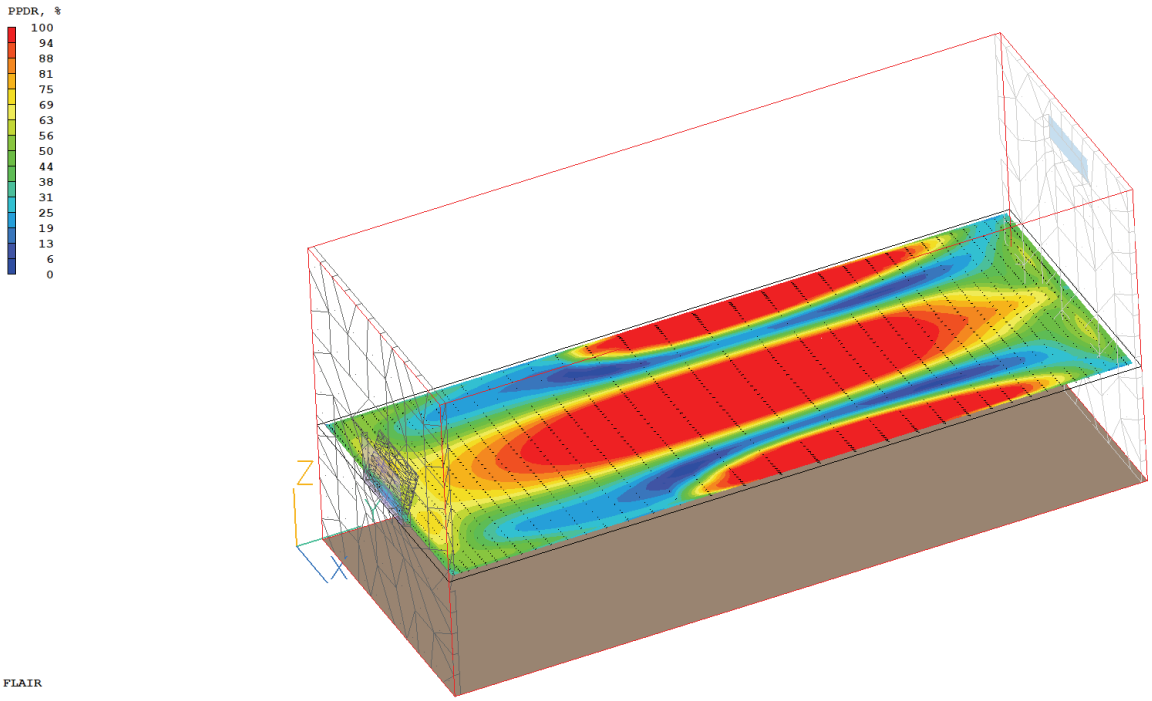

Figure 28:

Standard room with straight window simulation

Source: Own image

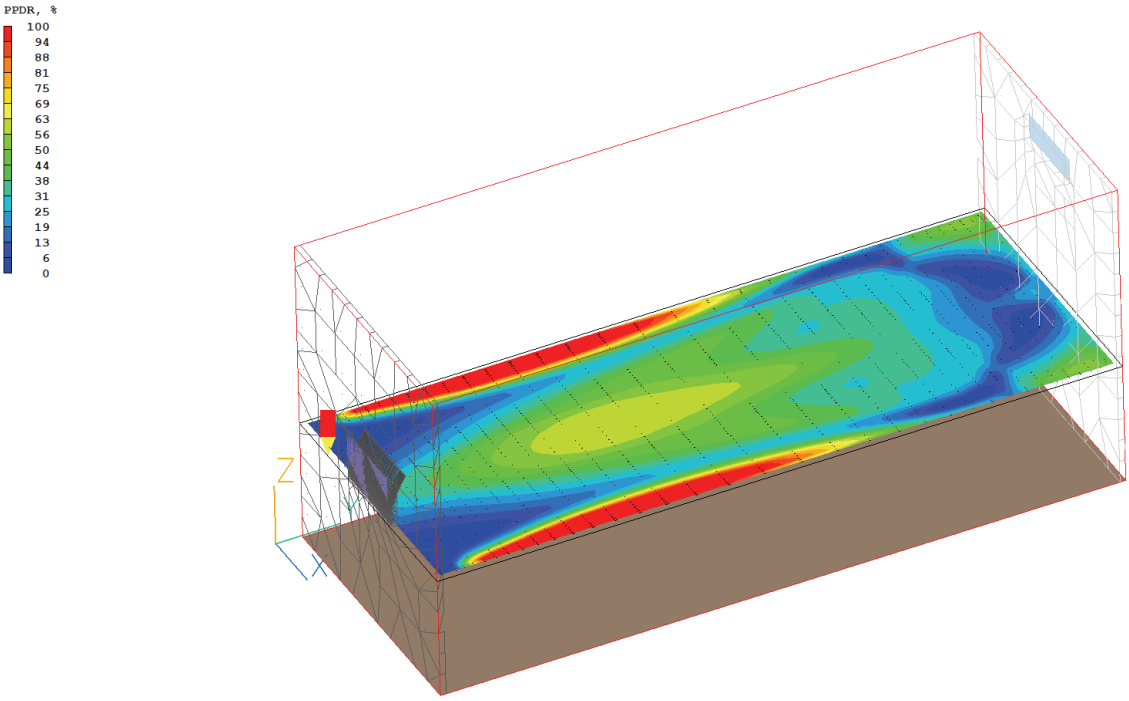

Figure 29:

Standard room with curved window simulation

Source: Own image

In the vertical section, as the same results showed before working environment in room A is worse than room B. PPDR is related to air velocity, air temperature, and turbulence intensity. From the previous research, straight window panel may generate turbulence airflow instead of laminar air flow. Also because of the room temperature is the same, air velocity and turbulence intensity are the main reasons causing comfort in the room. (**Figure 30-31**)

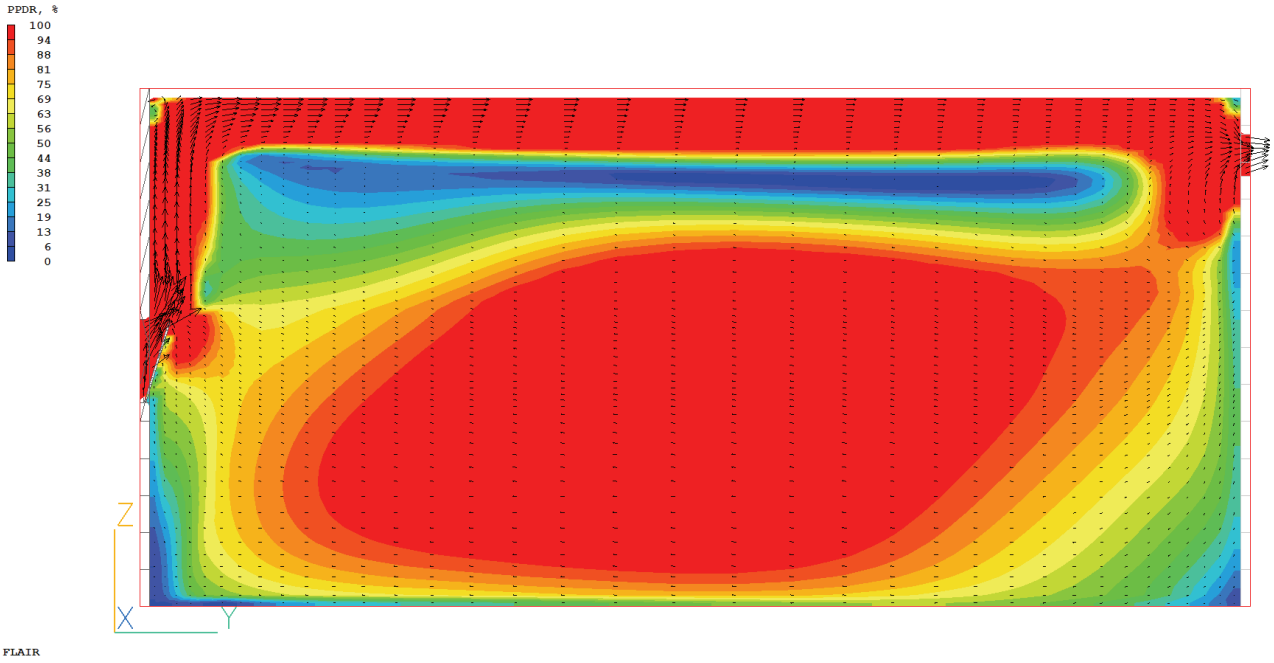

Figure 30:
Standard room with straight window simulation
Source: Own image

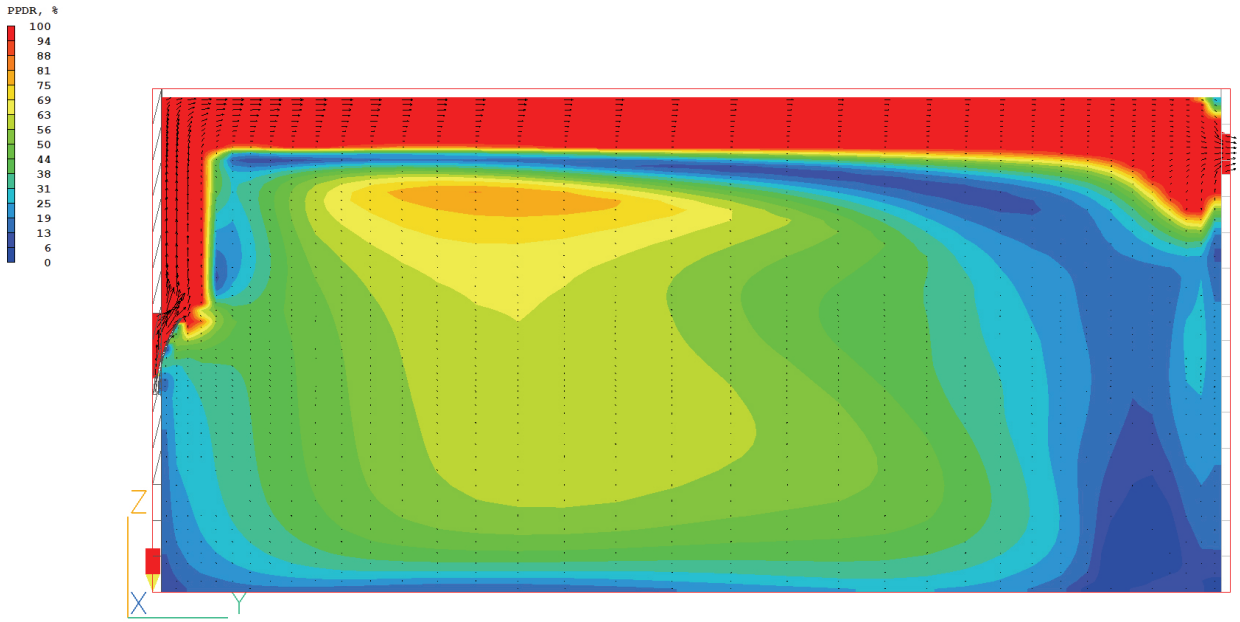

Figure 31:
Standard room with curved window simulation
Source: Own image

In the previous simulations, outlets are placed on the top. The fresh air cannot ventilate the whole room. So, in the simulation below, I place the outlets on the bottom to ventilate the whole room and to analyze indoor comfort. Before running the simulation, I assumed that fresh air will flow the ceiling and drop on the floor to generate circular ventilation path. To prove my guessing, I still use Phoenix CFD to run the simulation. (**Figure 32-33**) From the result of simulation, I find that in the same situation, even the outlets are moved to the bottom, cureved window still provide better indoor environment.

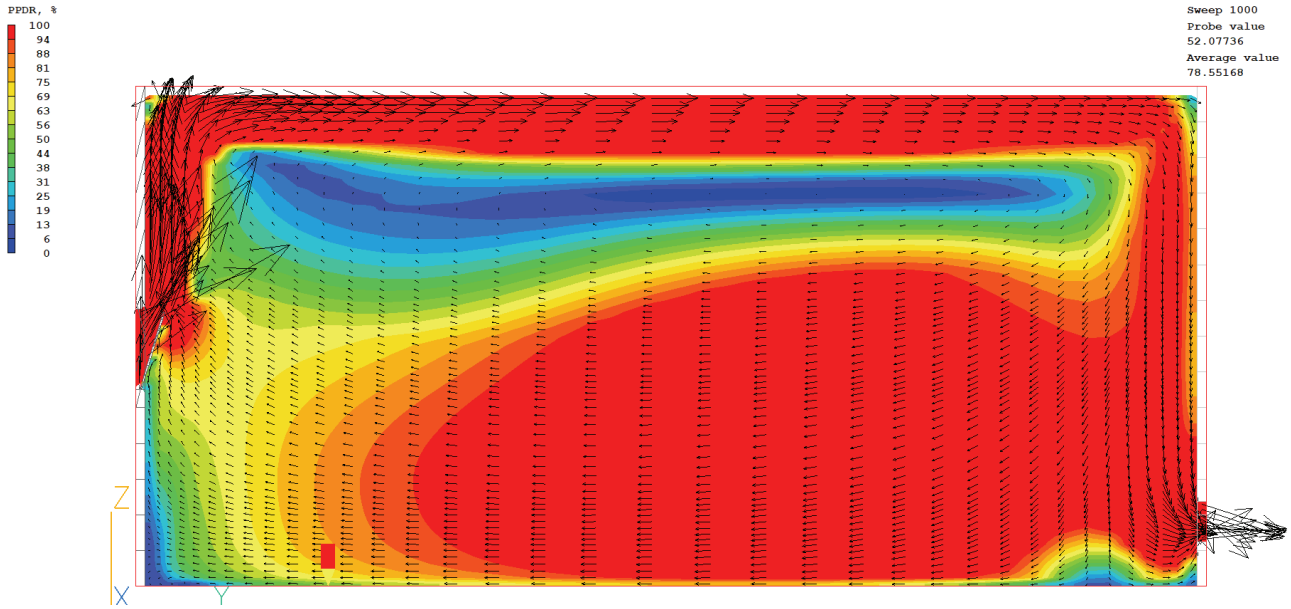

Figure 32:
Standard room with straight window simulation
Source: Own image

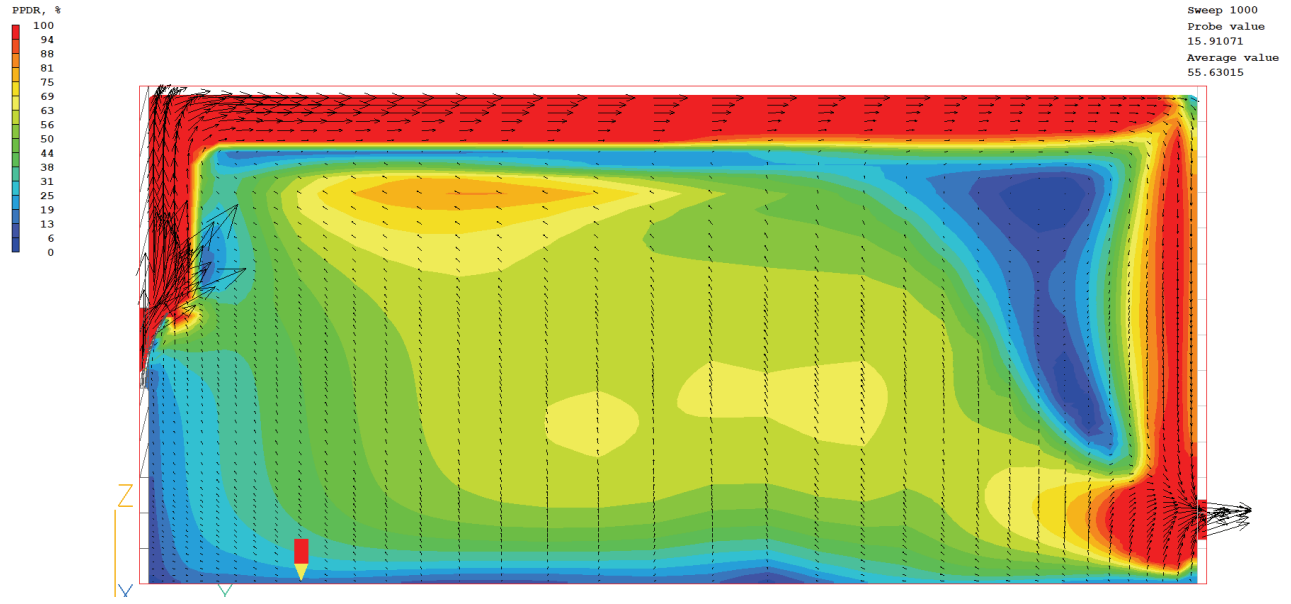

Figure 33:
Standard room with curved window simulation
Source: Own image

In the 1.1m high simulation, it is clear that PPDR is higher in the working area when window is straight. In curved window situation, except for areas closed to the wall, the other place has lower PPDR result. (**Figure 34-35**)

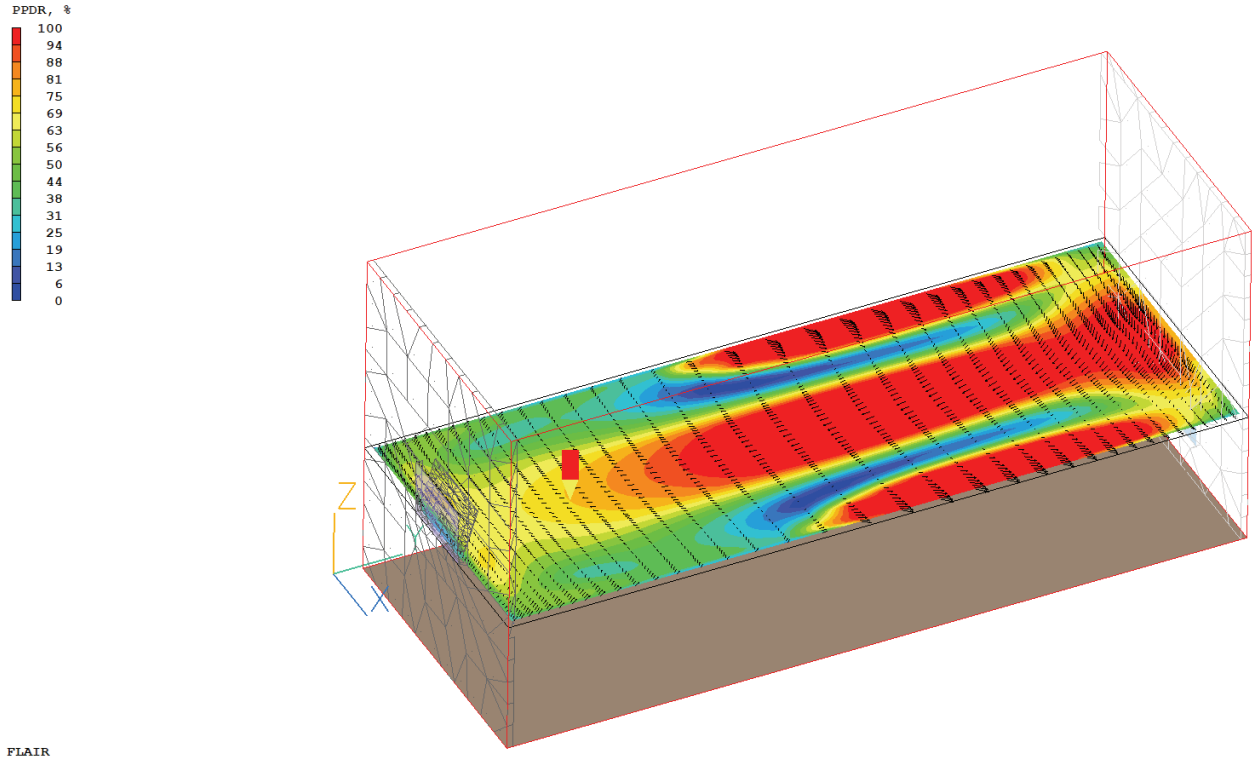

Figure 34:

Standard room with straight window simulation

Source: Own image

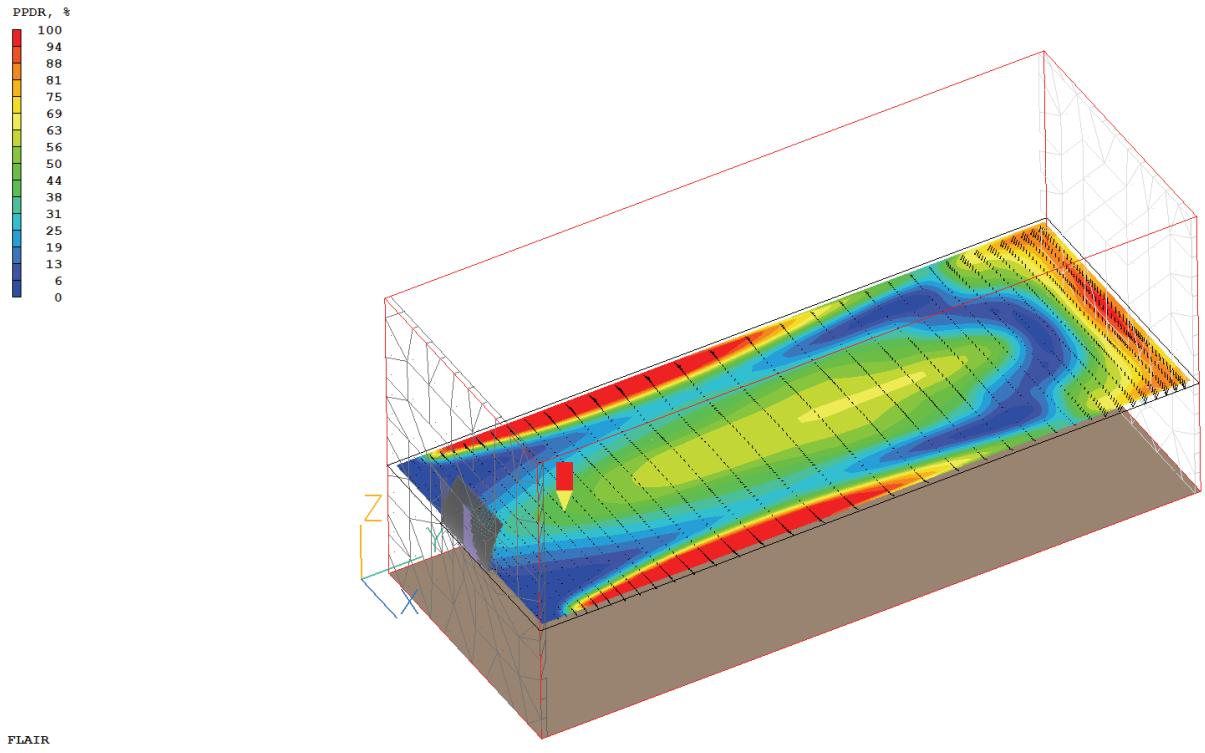

Figure 35:

Standard room with curved window simulation

Source: Own image

From the previous research, I know the PPDR result is determined by three aspects, which are air speed, air temperature, and turbulence intensity. Because of air temperature is kept the same in the simulation process, I simulate the airspeed and turbulence intensity respectively. At first, I run turbulence intensity simulation. Curved window room can create less turbulence intensity in working area. However, in the straight window room, the comfort zone is near floor. (**Figure 36-37**)

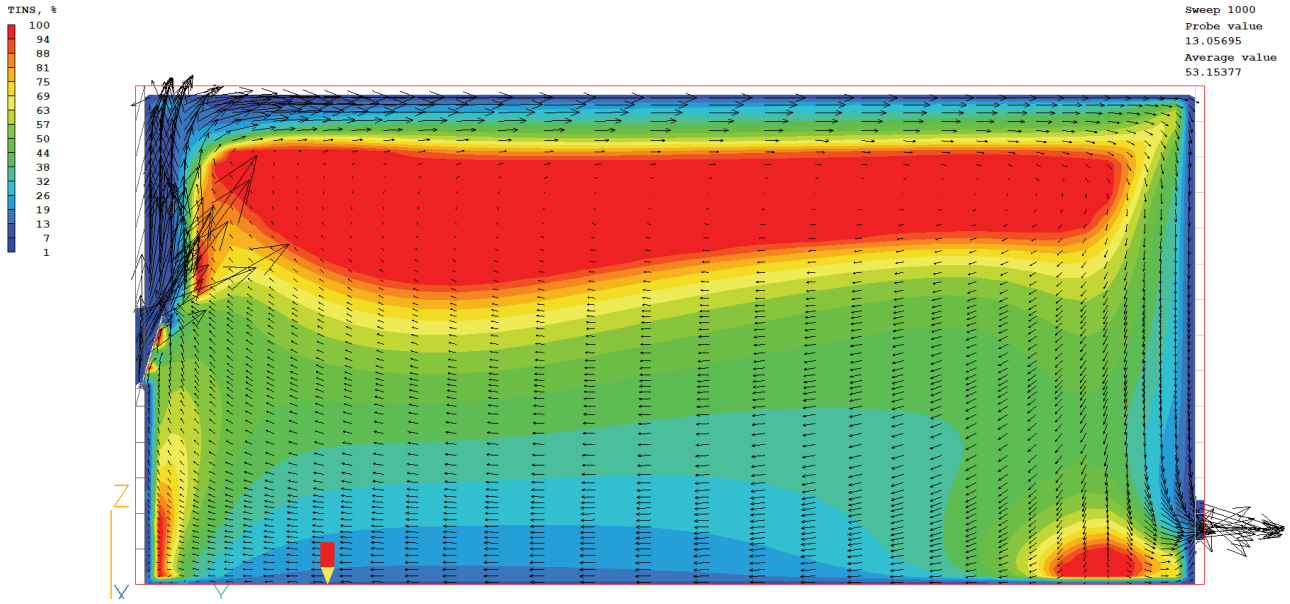

Figure 36:
Standard room with straight window simulation
Source: Own image

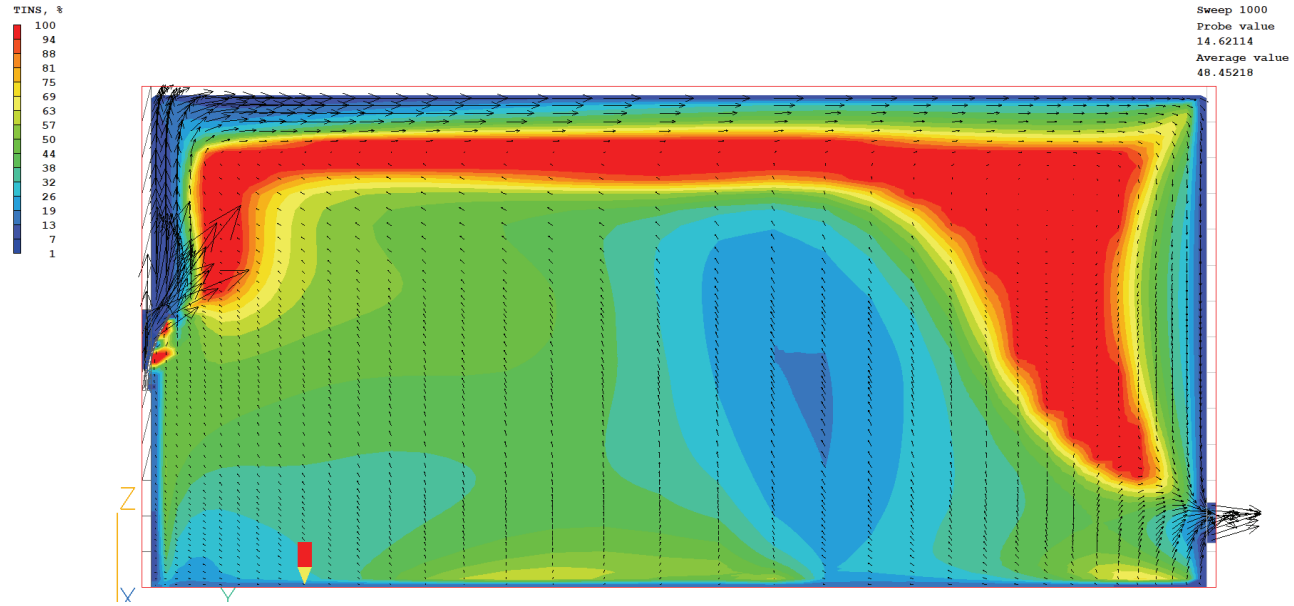

Figure 37:
Standard room with straight window simulation
Source: Own image

In the air speed simulation, I kept the inlet air velocity the same. From the result, it is clear that in the straight window room, working area air speed is higher than that in curved window room. This can also be the reason PPDR is higher in straight window room. (**Figure 38-39**)

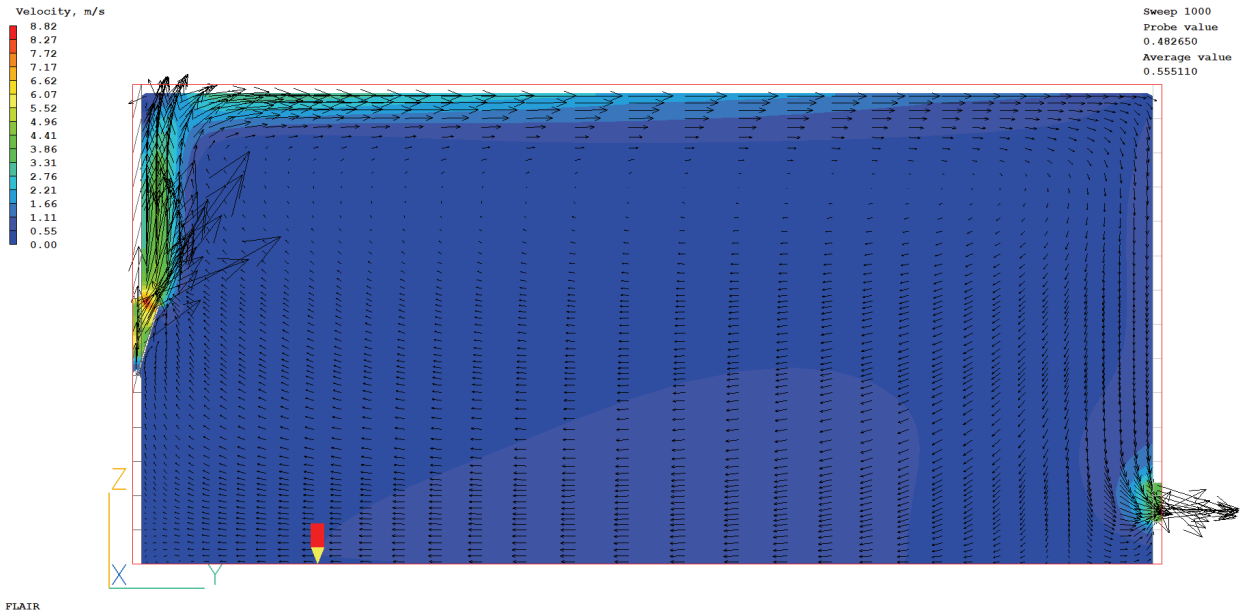

Figure 38:

Standard room with straight window simulation

Source: Own image

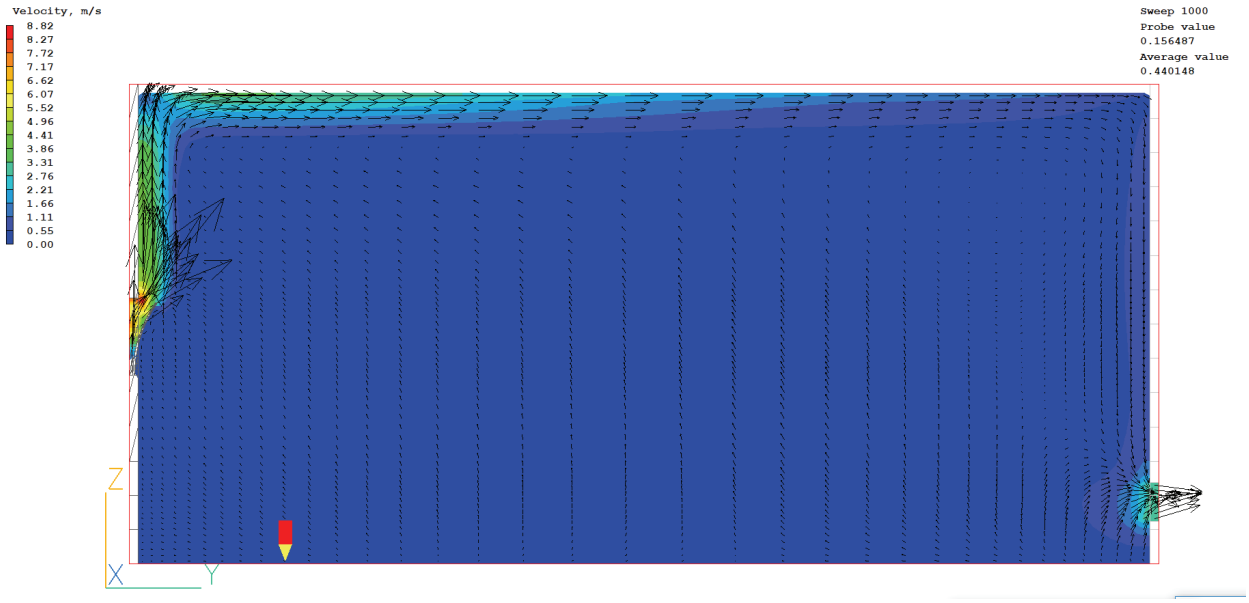

Figure 39:

Standard room with curved window simulation

Source: Own image

10. PHYSICAL MODEL

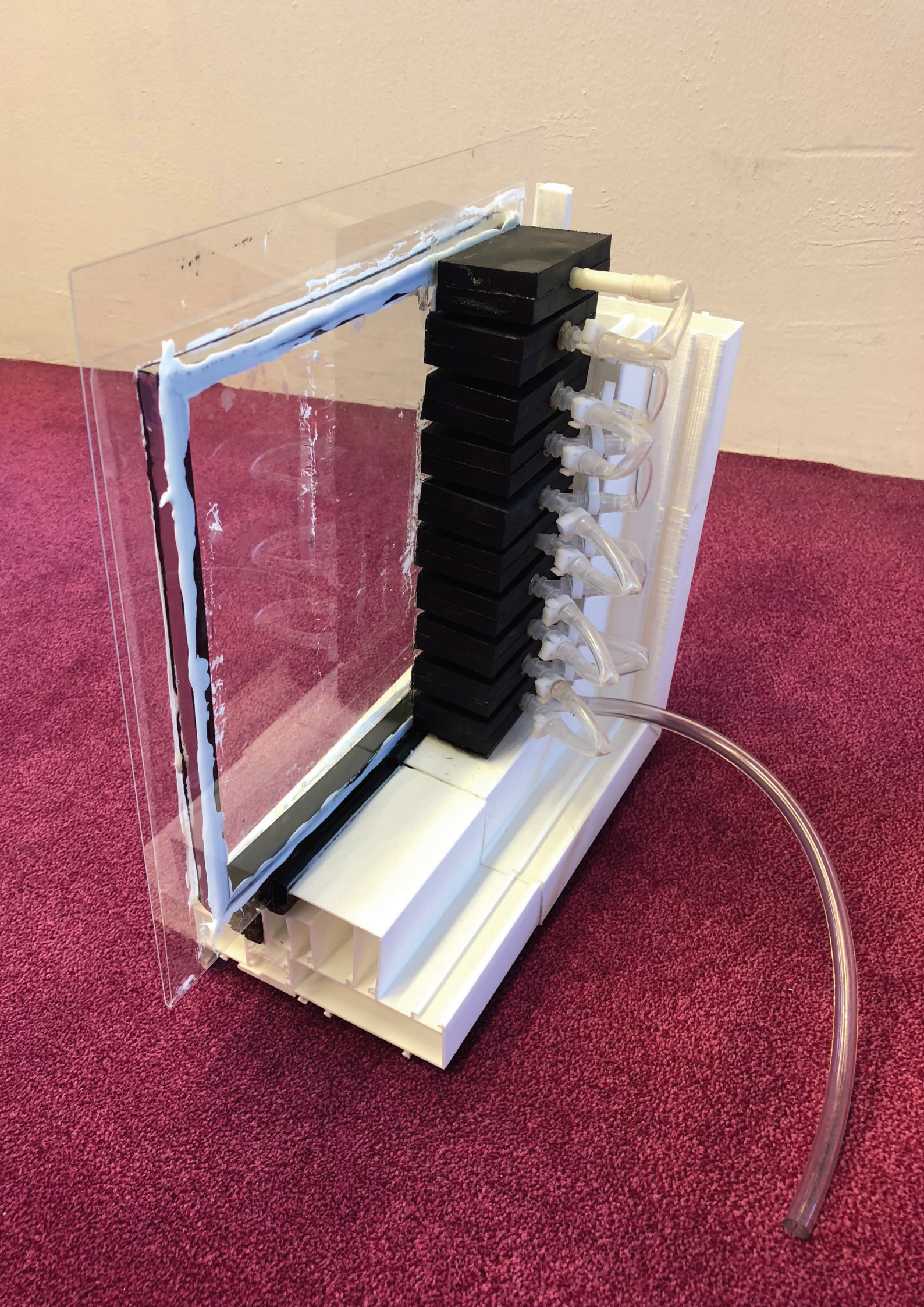

In this chapter, I will discuss the final model I made to test bending behavior. At first, I 3D printed the window frame to clamp two thin glass and attached the pneumatic actuators on the thin glass. In the first mock-up, I use silicon adhesive to glue thin glass and super spacer. From the pictures(**Figure 1-4**), we can see liquid adhesive looks not good. And it is difficult to clean off the silicone adhesive. After inflating, the insulating window starts to bend.

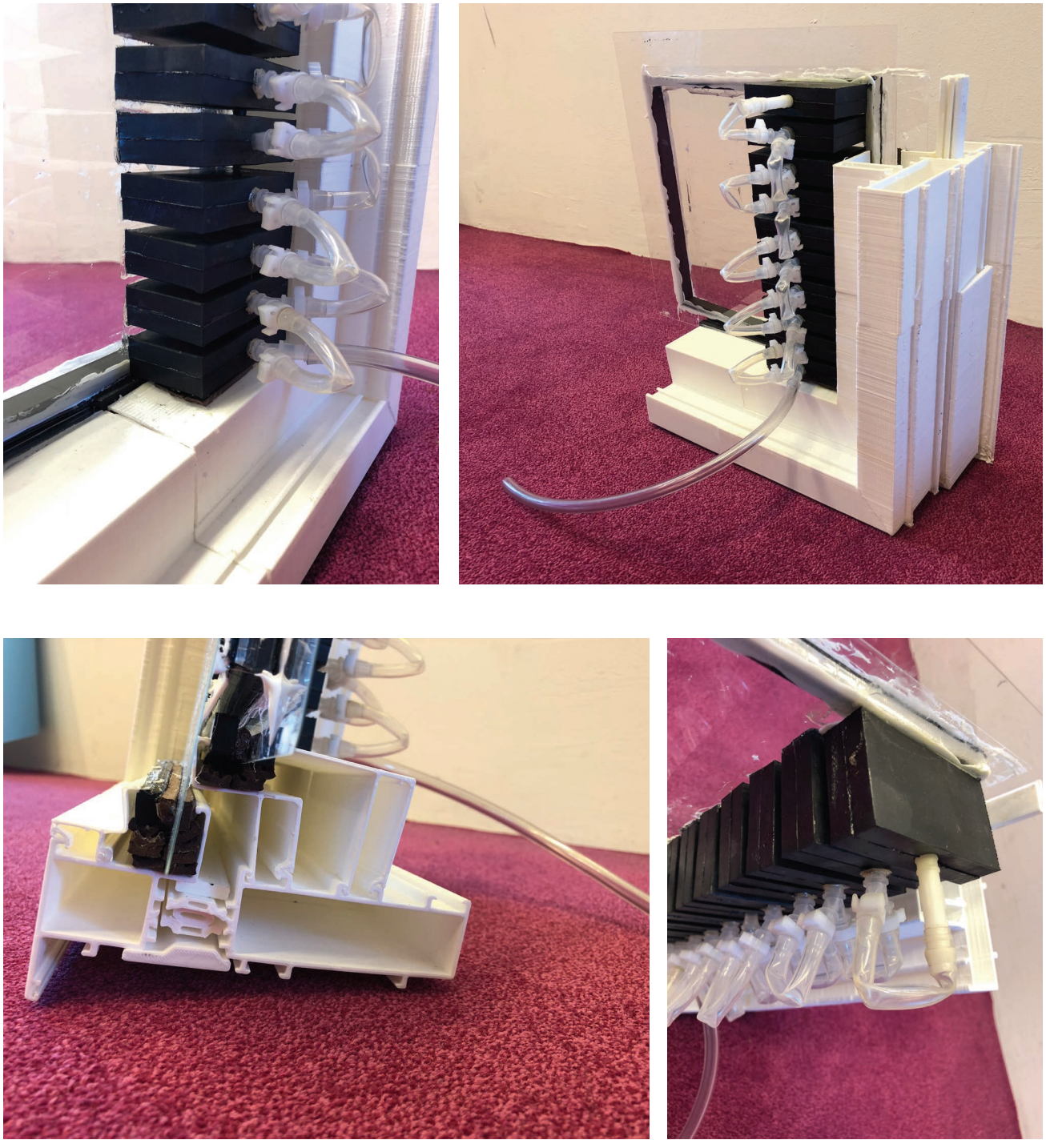

Figure 1-4:
Pictures of first mock-up
Source: Own image

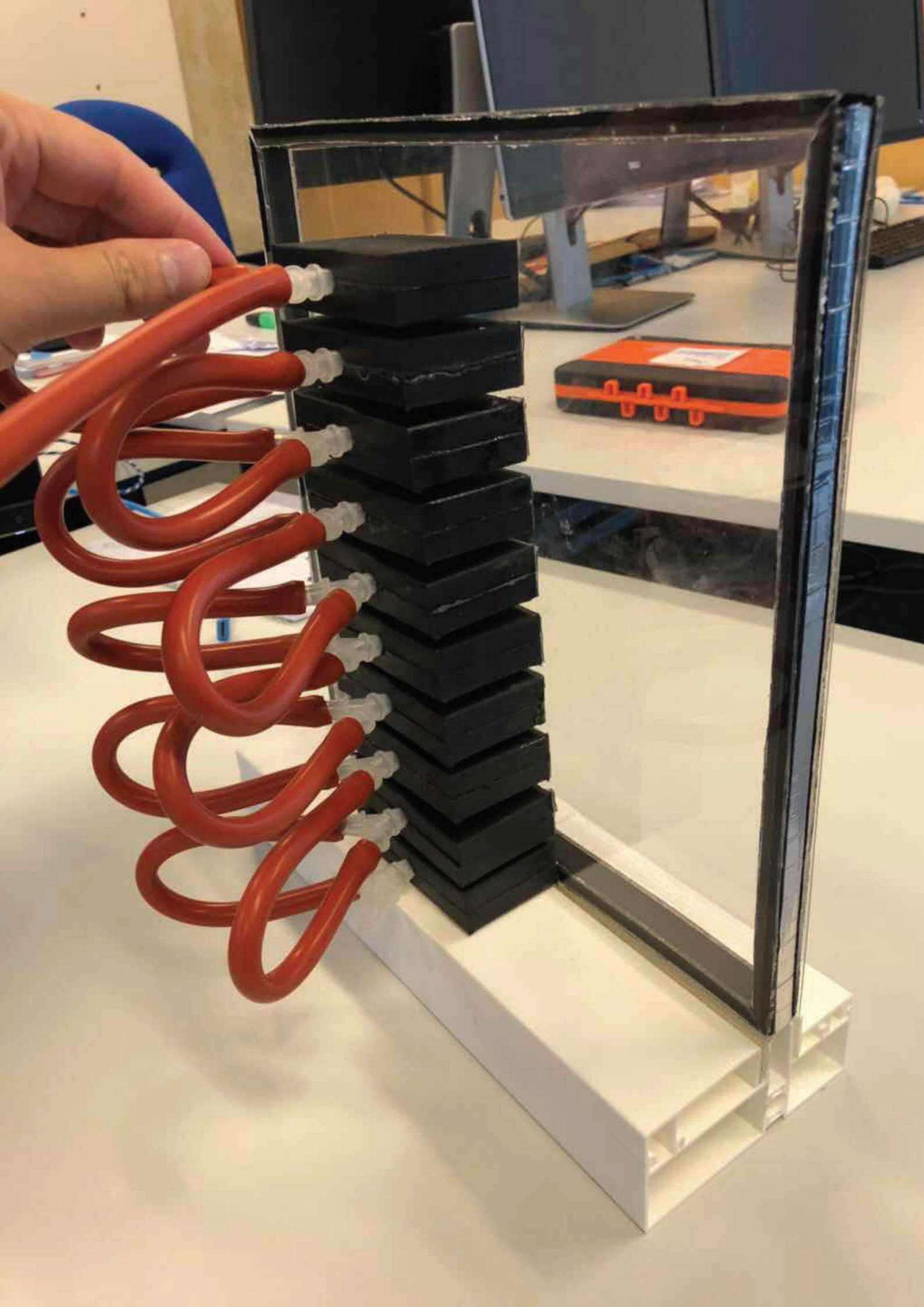

To improve the mock-up, I changed the soft pipe to let the air going smoother, also, I use silicone double sided tape instead of silicone liquid to make sure the product will look clean. (**Figure 5-7**)

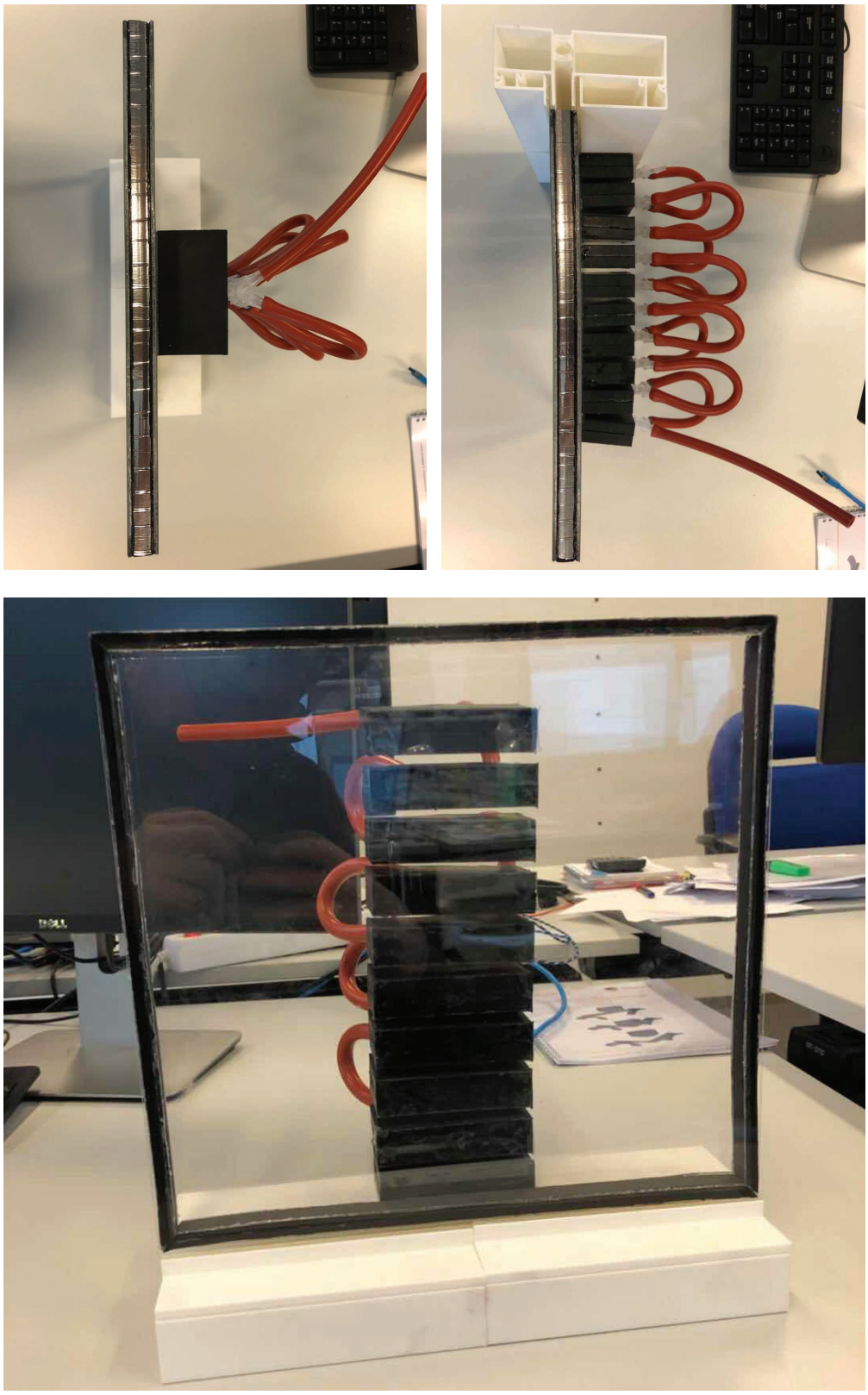

Figure 5-7:
Pictures of second mock-up
Source: Own image

11. CONCLUSION

11.1. Conclusion

In this chapter, I will start answering my research questions and sub-questions. And then the result of previous research need to be concluded. The last paragraph will be the explanation of how I come to this conclusion.

11.1.1. Answer to main research question

The main question is “How can soft pneumatic actuator(SPA) bend thin-glass windows structurally for natural ventilation?” To answer this question, research on structure mechanism of different soft robotics, thin glass prestress process and flexible IG unit is found that can be used as references to guide building up the mathematical model and designing further.

Soft pneumatic actuators are applicants, thin glass window are recipients. Applicants use stretching bending moment and contacting bending moment from air pressure to activate thin glass windows. Stretching bending moment is much smaller than contacting bending moment, so the bending moment due to stretching can be neglected in the calculation. Contacting bending moment comes from air chamber deforming and contacting, which depends on air pressure, material tensile strength, the distance between segments, wall thickness, segments geometry and air chamber geometry.

Thin glass window bending behavior comes from bending moment on the surface. Thanks to high tensile strength from medically prestress process, the thin glass surface can resist relatively tensile stress which helps provide certain curvature.

Windows need to be insulated, flexible IG unit is used to decrease window stiffness. In this project, I use silicone adhesive and super spacer from Edgetech to generate inner shear movements when the window is bent.

11.1.2. Answer to sub-research questions

Sub-questions are:

- How to prove curved window can decrease predict dissatisfied percentage due to draft
- Considering natural ventilation function, which window configuration can be developed
- What is the relationship between SPA geometry, air pressure and bending radius
- How to design window frame

How to prove curved window can decrease predict dissatisfied percentage due to draft

This question can be answered by using aerodynamic theory and Fanger's draught model. When wind hit on the curved surface, wind becomes laminar; however, when the wind hit on straight panel, wind becomes turbulent. In Fanger's draught model, laminar air flow makes people more comfortable than turbulent airflow does. In my expectation, this theory will also work in my project.

In CFD simulation chapter, I use Phoenics CFD to calculate mean air velocity indoor and predict dissatisfied percentage due to draft (PPDR), the result shows curved window room has lower air velocity and lower PPDR in the 1.1m high plan. The limitations of CFD analysis will be discussed in next chapter.

Considering natural ventilation function, which window configuration can be developed

To answer this question, two chapters are made in this report. First is draft design chapter, the other one is further designed chapter. In draft design chapter, designs are conceptual. To simplify the design process in the later chapter, I choose the basic window configuration, which is rectangular thin glass panel with two parallel soft pneumatic actuators. The other reason is that the main challenge on comfort is to compare effectiveness on the curved surface and straight surface, the complicated configuration will create unpredictable outcome influencing CFD result.

What is the relationship between SPA geometry, air pressure and bending radius

This question can be answered by equations and simulation. In the equations, I use contacting coefficient to assuming contacting area and get bending moment on the thin glass panel. Also, I use equivalent window stiffness calculation to replace real insulation window stiffness aiming to calculate window bending radius. Then, neglecting stretching bending moment from SPA, I calculate bending angle between every two segments. At last, by summing up each small opening size, I got the total window opening size.

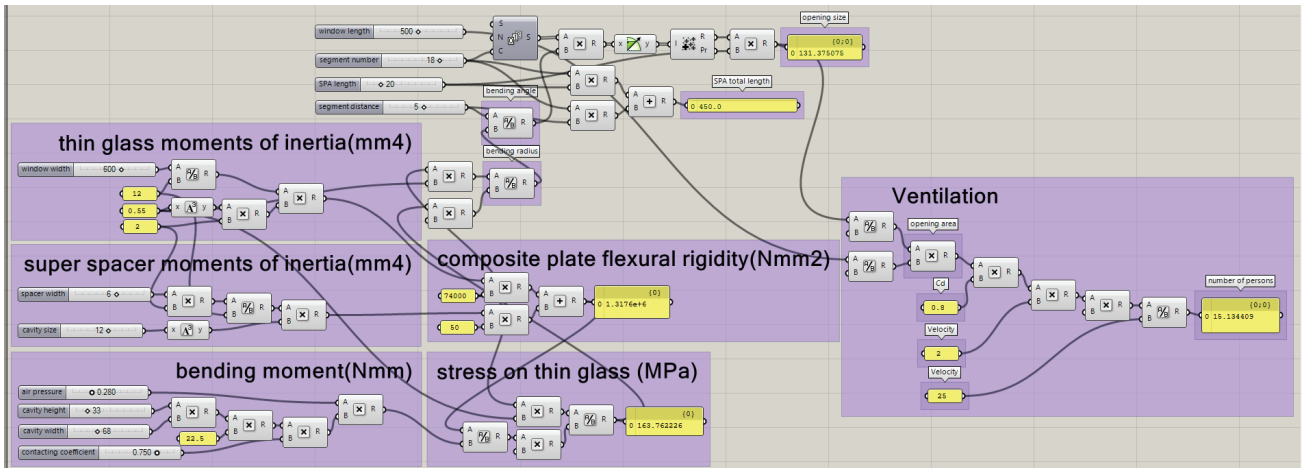

How to design window frame

The exoskeletwindow is clumped on the bottom and supported on the edge. I use aluminum window frame to clump thin glass plate separately on the bottom and movable locking system on the inner surface.

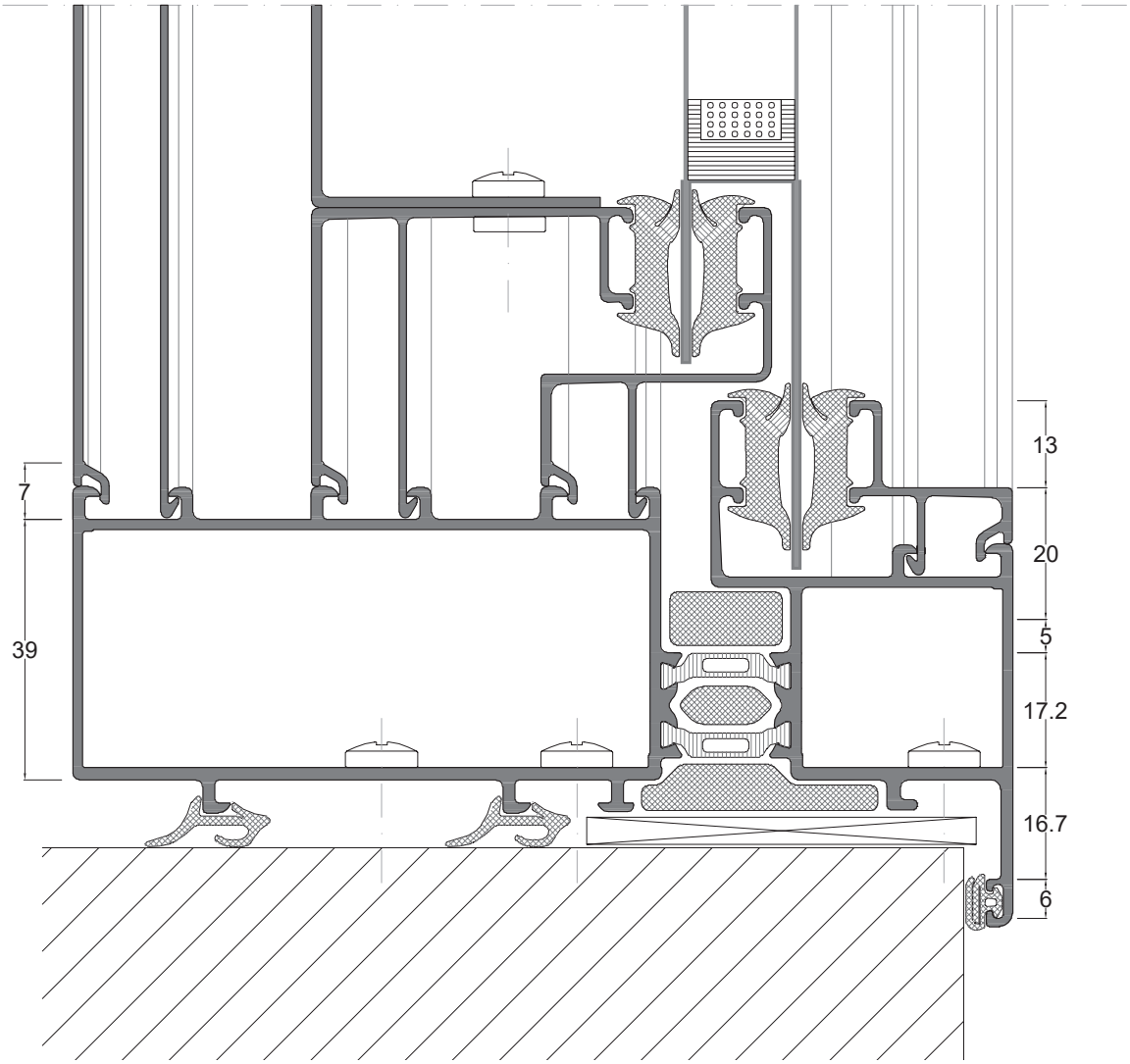

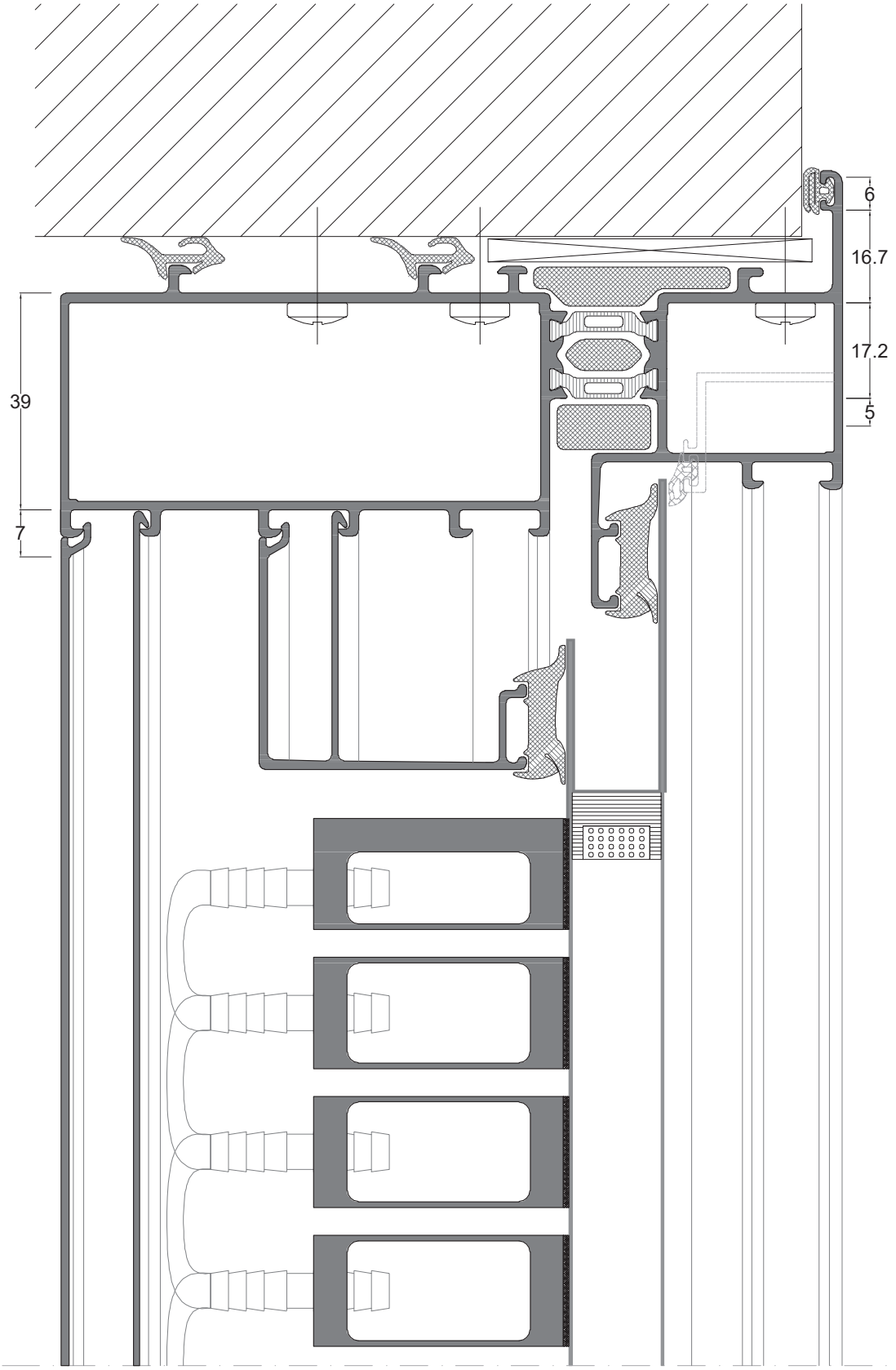
6
16.7
17.2
5
39
7

11.1.3. Market potential

Advantages

Exoskeletwindow belongs to center-controlled responsive facade system. It can not only provide comfortable indoor environment automatically but also it can be customized controlled. The target market is responsive window system. Without motors and mechanical equipment, exoskeletwindow owns big advantages on cost-efficient.

Different from another responsive facade, exoskeltwindow is the primary facade and can provide certain thermal insulation. The insulation capability can be improved by coating and using triple-glazing strategy. And the method to decrease window stiffness we discussed above will also fit in this proposal.

The other advantage of exoskeletwindow is the geometry potential. In this thesis, I use the simple facade geometry, but it owns more possibilities on generating complex geometry in the future. Also, this concept can be integrated with the sun shading system.

Disadvantages

The first disadvantage of exoskeletwinow is its low thermal insulation compared to the insulated window in the market like RT 82 HI+ aluminum-frame window from KAWNEER.

The other disadvantage is wide window frame which will block the view of users. The window frame is wide because of the size of actuators. To provide the large bending moment, the size of the actuators is limited, however, there are possibilities in choosing higher tensile strength material to decrease size.

The last disadvantage is the low durability of rubber actuator exposing outside. The UV, rain and organic liquid will corrode the actuator.

Conclusion

To sum up, exoskeletwindow is not ready for the market right now, but this product owns potential in the future. And it worth time doing further research on solving disadvantage problems.

12. DISCUSSTION

12.1. Discussion and limitation

In this chapter, I will start with the result of hand calculation and simulation. Then, expectations from the desktop research will be discussed. Followed by an explanation of meeting or not meeting the expectation. Limitations of my research will also be discussed and explained how to improve in future research. Last but not least, this chapter will end with the suggestions for possible follow up research.

12.1.1. Interpretation of results

Structure result

From the hand calculation and simulation, in 2.8 bars air pressure, the insulation window 600mm*450mm with 18 segments (80mm*45mm*20mm) as actuators each edge, 5mm distance between two segments can open 131mm on the top. The maximum tensile stress on the thin glass surface is 163.8MPa.

From the relevant literature research, my expectation is that it is possible to bend thin glass window for ventilation. In terms of structure mechanism, the hand calculation and simulation result both meet my expectation.

Window detailing result

In the window detail design process, I use silicone adhesive to decrease the window stiffness which makes it possible to be bent by the soft pneumatic actuator. The result from structure calculation shows the possibility of bending behavior. However, after multiple times of bending, delamination happens between the thin glass layer and super spacer because silicone adhesive is not strong enough. If I switch to use the stronger adhesive material, it is not easy to provide shear movement. This can be the next research topic in the future.

CFD analysis result

In the CFD simulation, I got the result of air velocity in curved window room and normal window room. This result shows in normal window room, air velocity is higher than that in curved window room. The other result is predicted dissatisfied percentage due to a draft. In 1.1m height, PPDR in normal window room is much higher than it in curved window room, which meets my expectation.

The possible reason could be turbulence intensity. However, if turbulence intensity in curved window room is very low, this means fresh air cannot come in working zone and CO2 concentration will increase.

12.1.2. limitation

Structure

The main question is related to structure mechanism. First of all, the limitation of the structure is calculating composite window flexural stiffness. By using super spacer and silicone adhesive, I suppose that silicone adhesive doesn´t have shear modulus and the equivalent stiffness equals to two thin glass combined with super spacer, which is not accurate, but this method gives approximation window stiffness.

Secondly, to simplify the design process, in calculating bending behavior, wind load is not under consideration. If the window load is positive outside, the wind will help to open the window. If the situation is another way around, the actuator has to resist wind load and open the window. It is possible to calculate it by connecting wind load and direction to senators and pick responsible air pressure in air chambers. However, this is not the main question in this thesis.

CFD analysis

The simulation to prove that curved window can improve indoor environment has limitations. First of all, the simulation is under the 2m/s stable wind speed which is not possible in reality. Local weather data should be imported in CFD model. Secondly, the opening size is 10cm both on the curved window and straight window, which is not comprehensive because more opening size configurations need to be simulated. Thirdly, from the simulation result, turbulence intensity is low in curved window room. This means that it is possible fresh air cannot go into the working area and CO2 concentration will increase.

12.1.3. Possible follow up research

This project is a start of bending thin glass window by soft robotic. The future research can be more advanced in geometry generation and double-curvature form finding system. Because of the environment is integrated by different factors, to respond environment, organic geometry is needed. Soft robotics can provide this potential.

13. REFLECTION

This chapter is the reflection of my master thesis. The idea comes from Christian Louter's topic "Thin glass composite with 3D printed spacer pattern". Based on the Christian's introduction about thin glass and 3D printing technology combination, I introduced my proposal about thin glass embedded with pneumatic soft robotic technology, which uses air pressure changing to manipulated curving geometry adapting to thin glass curvature.

The main goal of my graduation project is to design a thin glass window bending by the soft pneumatic actuator for natural ventilation. To achieve this design, a lot of research on different aspects should be done. Based on the design objective, there are three main research areas which are thin glass technology, soft pneumatic actuator technology, and indoor comfort. Each research area will support and improve my design process.

Basically, this project is a window design integrated with structure design, geometry generation, production process, material properties and climate design knowledge. The integration and computational design mindset come from my master track-Building Technology. The knowledge gains from Bucky Lab, I learned computational design, production, structural mechanics and building physics in the first semester. After that, I chose façade design, climate design, design informatics and structure design in semester 2 which helps me create the computational design and integration design mindset. It seems complicated to combine many aspects together and use them in one graduation project, but it is how the world in building environment will look like, also it is my interest.

Since my graduation topic includes three main research areas which I am not familiar with, additionally, this topic is new and never be researched before, these external factors and my own limited knowledge make me do research by design. In other words, I kept doing research when the design is stuck even after P2. With the help of Christian Louter and Tillmann Klein, research and design process went very well.

In the scientific framework, thin glass technology and soft robotics technology are newly coming. More and more pioneers are willing to spend time on both applications. However, both two technology did not meet in the building environment. In my graduation project, I created a platform and integrated both technologies and made a bridge between both technologies for the purpose of adapting indoor comfort and decreasing window weight and cost. This project results will belong to TU Delft, but I would love to continue this research after graduation if this project can be funded.

This design and research is just a start of this project, there will be a long way to go. Based on the main research question and sub-questions, the main challenge in the next two months will be window detail design and soft robotics production. Normally, soft robotics can be 3D printed or cast by silicon, however, because of the 3D printer size limitation, and vacuum machine size limitation, producing large size soft robotics will be a challenge.

Overall, this research and design help me strengthen my research skills and systematic thinking. Also, this research created a bridge between two new technologies. I hope this design can inspire other graduation students

14. APPENDIX

ADDITION-CURING GRADES

ELASTOSIL®													
Product	Properties		Consistency	Color	Mixing Viscosity	Density	Hardness	Tensile Strength	Elongation at Break	Tear Strength	Mixing Ratio A : B	Pot Life at 23 °C	Demolding Time
					[mPa•s]	[g/cm3]	[Shore A]	[N/mm2]	[%]	[N/mm]	[wt.-%]	[min]	[h]
M 4115 A/B	Very soft; high heat resistance, high thermal conductivity	A	Pourable	Translucent	2,500	1.05	17	3.0	400	5	1 : 1	12	1
M 4118 A/B	Soft; high heat resistance, high thermal conductivity	A	Pourable		2,500	1.10	20	3.5	400	4.5	1 : 1	6	0,5
M 4125 A/B	Soft	A	Pourable	Translucent	6,000	1.05	25	5.0	500	25	1 : 1	60	12
M 4370 A/B	Hard	LM	Pourable	Reddish brown	8,000	1.43	55	3.0	130	4	9 : 1	80	6
M 4600 A/B	Soft; ■ ⧫	A	Pourable	Translucent	15,000	1.10	20	7.0	800	20	10 : 1	90	12
M 4601 A/B	Soft; ■ ⧫	A	Pourable	Reddish brown	10,000	1.13	28	6.5	700	30	9 : 1	90	12
M 4615 A/B	Very soft; ■ ⧫	A	Pourable	Blue	5,000	1.03	13	3.0	700	10	100 : 15	90	12
M 4630 A/B	Soft; ■ ⧫	A/CM	Pourable	White	10,000	1.13	28	6,5	700	0	10 : 1	90	12
M 4635 A/B	Medium hard; ■ ⧫	A/CM	Pourable	White	15,000	1.14	37	7.0	480	30	10 : 1	90	12
M 4641 A/B	Medium hard	RPT	Pourable	Transparent	30,000	1.07	43	4.5	300	28	10 : 1	90	15
M 4642 A/B	Medium hard; ■	A	Pourable	Dark red	15,000	1.14	37	7.0	550	30	10 : 1	90	12
M 4643 A/B	Medium hard	A	Pourable	Gray	25,000	1.35	48	5.0	300	10	9 : 1	70	12
M 4644 A/B	Medium hard; slightly oil-bleeding	RPT	Pourable	Transparent	50,000	1.07	40	5.5	400	28	10 : 1	90	15
M 4645 A/B	Medium hard; strongly oil-bleeding	RPT	Pourable	Transparent	35,000	1.06	40	5.0	330	28	10 : 1	90	15
M 4670 A/B	Hard	RPT, A	Pourable	Beige	80,000	1.34	55	5.5	300	12	10 : 1	90	12
RT 620 A/B	Very soft; ■	PP	Pourable	Translucent, pigmentable	20,000	1.05	17	5.0	900	12	10 : 1	35	4
RT 623 A/B	Medium hard; ■	PP	Pourable	Reddish brown	10,000	1.12	31	7.5	700	30	9 : 1	30	5
RT 629 A/B	Medium hard; antistatic	PP	Pourable	Turquoise	8.000	1.13	31	6.0	500	25	10 : 1	40	3
C 1200 A/B	Soft	CO	Spreadable	Blue	20,000	1.05	25	5.0	500	25	1 : 1	20	1

A = all-round grade
LM = especially for low melting metal alloys
CM = especially for concrete molding
RPT = especially for rapid prototyping
PP = especially for pad printing
CO = especially for composite applications

■ very high mechanical strength
⧫ very high elasticity

Wacker Chemie AG is certified to ISO 9001 and ISO 14001.

The figures and information contained in this table are intended as a guide only.
You can obtain detailed information from your technical advisor.

ELASTOSIL®														
Product	Properties		Consistency	Color	Mixing Viscosity	Density	Hardness	Tensile Strength	Elongation at Break	Tear Strength	Linear Shrinkage after 7 Days	Catalyst	Dosage	Pot Life*	Demolding Time*
					[mPa•s]	[g/cm3]	[Shore A]	[N/mm2]	[%]	[N/mm]	[%]		[wt.-%]	[min]	[h]
M 1470	Hard	A	Kneadable	Pink	> 1,000,000	1.28	50	4.5	230	10	0.2	Paste T 40	2	70	5
M 3502	Soft; ■ ⧫	A[1]	Spreadable, Non-sag	White	> 1,000,000	1.24	26	4.5	450	23	0.4	T 21 / T 51	5	65	9
M 4400	Soft	A	Pourable	Pale yellow	25,000	1.30	23	2.0	250	3	0.7	T 37	3	90	12
M 4440	Medium hard	A	Pourable	Beige	20,000	1.22	37	2.5	200	3	0.4	T 37	3	80	10
M 4470	Hard; high heat resistance, high thermal conductivity	LM	Pourable	Reddish brown	10,000	1.44	60	4.5	120	4	0.8	T 37	3	90	24
M 4500	Very soft; ⧫	A	Pourable	White	20,000	1.20	14	3.0	450	15	0.6	T 12	3	60	7
M 4503	Soft	A	Pourable	White	40,000	1.16	25	5,0	350	20	0.5	T 35	5	90	20
M 4511	Very soft; ■ ⧫	A[1]	Pourable	White	20,000	1.22	12	3.5	600	18	0.4	T 21 / T 51	5	75	10
M 4512	Soft; ■ ⧫	A[1]	Pourable	White	25,000	1.19	20	3.5	500	24	0.4	T 21 / T 51	5	75	10
M 4514	Soft; ■ ⧫	A[1]	Pourable	White	25,000	1.25	25	4.5	450	25	0.4	T 21 / T 51	5	75	10
M 4541	Soft; ■	A[1]	Pourable	White	30,000	1.16	32	5.0	400	30	0.4	T 21 / T 51	5	75	10
RT 402	Very soft; antistatic	PP	Pourable	Gray	13,000	1.28	11	2.0	350	3	0.3	T 12	3	75	5

A = all-round grade
[1] = outstanding resistance to polyester and polyurethane resins
PP = especially for pad printing
LM = especially for low melting metal alloys

■ very high mechanical strength
⧫ very high elasticity

Wacker Chemie AG is certified to ISO 9001 and ISO 14001.

The figures and information contained in this table are intended as a guide only.
You can obtain detailed information from your technical advisor.

* at 23 °C / 50% rel. humidity

Technical data sheet TPU 95A

Ultimaker

Chemical name	Thermoplastic polyurethane
Description	Highly versatile for industrial applications, TPU 95A filament is the go-to choice for a wide array of manufacturing projects that demand the qualities of both rubber and plastic. Designed for 3D printing consistency, TPU 95A is a semi-flexible and chemical resistant filament with strong layer bonding. In addition, it is easier and faster to print than other TPU filaments.
Key features	Exceptional wear and tear resistance, high impact strength, Shore-A hardness of 95, up to 580% elongation at break, and good corrosion resistance to many common industrial oils and chemicals.
Applications	Functional prototyping, grips, guides, hinges, sleeves, snap-fit parts and protective cases.
Non-suitable for	Food contact applications and in-vivo applications. Long term UV and/or moisture immersion and applications where the printed part is exposed to temperatures higher than 100 ˚C.

Filament specifications	Value	Method
Diameter	2.90±0.13 mm	2-axis laser gauge
Max roundness deviation	0.07 mm	2-axis laser gauge
Net filament weight	750 g	-
Filament length	~96 m	-

Color information	Color	Color code
	TPU 95A White	RAL 9010
	TPU 95A Black	RAL 9005
	TPU 95A Red	RAL 3031
	TPU 95A Blue	RAL 5002

Mechanical properties (*)	Injection molding		3D printing	
	Typical value	**Test method**	**Typical value**	**Test method**
Tensile modulus	-	-	26.0 MPa	ASTM D638
Tensile stress at yield	-	-	8.6 MPa	ASTM D638
Tensile stress at break	-	-	39.0 MPa	ASTM D638
Elongation at yield	-	-	55.0 %	ASTM D638
Elongation at break	-	-	580.0 %	ASTM D638
Flexural strength	-	-	4.3 MPa	ISO 178
Flexural modulus	-	-	78.7 MPa	ISO 178
Izod impact strength, notched (at 23˚C)	-	-	34.4 kJ/m^2	ISO 180
Charpy impact strength (at 23˚C)	-	-	-	-
Hardness	-	-	95 (Shore A) 46 (Shore D)	ASTM D2240 Durometer
Abrasion resistance	-	-	0.06 g	ASTM D4060 (mass loss, 10000 cycles)

Thermal properties	Typical value	Test method
Melt mass-flow rate (MFR)	15.9 g/10min	ISO 1133 (225 ˚C, 1.2 kg)
Heat deflection (HDT) at 0.455 MPa	74 ˚C	ASTM D648
Heat deflection (HDT) at 1.82 MPa	49 ˚C	ASTM D648
Glass transition	-24 ˚C	DSC
Coefficient of thermal expansion	100·10^{-6} ˚C^{-1}	ASTM E693
Melting temperature	220 ˚C	DSC
Thermal shrinkage	-	-

Electrical properties	Typical value	Test method
Volume resistivity	10^{11} Ω·m	IEC 60093
Surface resistance	2·10^{14} Ω	IEC 60093

Other properties	Typical value	Test method
Specific gravity	1.22	ASTM D782
Flame classification	HB Class	ICE 60695-11-10
Moisture absorption	0.18 %	ASTM D570 (24h)

Quanex
building products

Insulating Glass Systems

Super Spacer® TriSeal™ Premium Plus

Super Spacer® TriSeal™ Premium Plus is a flexible, silicone spacer designed to satisfy the toughest commercial glazing demands including silicone structural glazing (SSG). Its unique triple-seal design incorporates an inner acrylic adhesive seal for immediate unit handling.

Basic Use

Super Spacer is a dual seal insulating glass spacer system that uses a high-performance acrylic adhesive for its structural seal and is backed with a proprietary multi-layer moisture vapor seal.

Super Spacer TriSeal comes complete with a polyisobutylene primary seal for enhanced gas retention and low moisture vapor transmission. A customer-applied silicone seal provides proven structural performance. Polyurethane, polysulfide and hot melt butyl / DSE's are acceptable sealants for captured glazing applications.

Colors

Black, Grey, and Aluminum.

Composition

Silicone base with desiccant pre-fill and minimum 6.56 grams / lineal metre (2 grams / lineal foot) pre-applied PIB.

Desiccant Fill

3A molecular-sieve; 47% minimum by weight.

Protective Packaging

To provide desiccant protection, the reels are sealed in moisture-proof foil bags. The reels are then shipped in recyclable cardboard boxes.

Performance	Norm
Thermal conductivity 0.117 W/m°K when used with PIB primary sealant	ASTM C 518
Gas / Moisture vapor barrier WVTR: Below detectable limits Oxygen: Below detectable limits	ASTM F 1249 ASTM D 3985
Primary structural seal Acrylic adhesive	
Intermittent temperature range -40°C to 121°C / -40°F to 250°F	—
Verified secondary sealants Reference IG sealants Technical Bulletin RDQ0018	—
Fogging No fog in visual area.	ASTM E 2190 EN 1279 - 6 CAN/CGSB 12.8
Gas Retention	EN 1279 - 3
I.G. Durability	ASTM E 2190 EN 1279 - 2

Quanex
building products

Insulating Glass Systems

Super Spacer® TriSeal™ Premium Plus

Warm-Edge Silicone Features & Benefits

- Superior silicone insulation
- Low thermal conductivity
- Substantially reduced perimeter condensation
- Typical overall 0.2 W/m²K (0.04 BTU/h-ft²-°F) U-value window improvement (vs. aluminum)
- Excellent UV resistance
- Excellent temperature performance
- Fast dew-point drop
- Superior compression-set resistance
- Excellent color stability
- Enhanced sound dampening

Edge-Seal Durability

- High performance multi-layer vapor barrier film
- Continuous vapor barrier at corners
- No chemical fogging
- Very high desiccant content
- Proven edge-seal technology
- Thermoset silicone durability

Unique Triple-Seal Design

- Inner acrylic adhesive seal for immediate unit handling
- Customer applied polyisobutylene primary seal for enhanced gas retention and low moisture vapor transmission
- Outer secondary seal for proven performance

Improved Productivity

- Fast spacer application
- Elimination of desiccant filling
- No corner key assembly
- No butyl extruding of frames
- Simplified production of shaped units
- High-volume production with reduced labor force

Pleasing Aesthetic Appearance

- Smooth matte surface finish
- No surface blistering or bubbling
- Straight-line application with sharp 90° corners

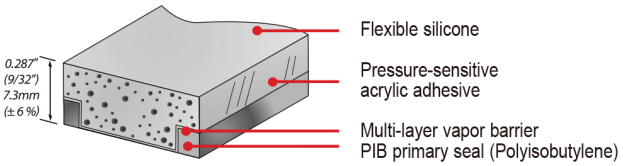

Reel Sizes

Width mm	Width inches	Meter/ Reel	Feet/ Reel	Final Corner Sealing Strip* Nominal Wdith	Final Corner Sealing Strip* Part Number	Final Corner Sealing Strip* pieces per bag
8.2 mm	.323"	244	800	8 mm	002064	150
9.5 mm	.375"	213	700	9 mm	003235	150
10.2 mm	.402"	198	650	10 mm	002455	150
11.1 mm	.438"	183	600	11 mm	003262	150
12.2 mm	.480"	168	550	12 mm	002456	150
12.7 mm	.500"	152	500	12 mm	002456	150
14.2 mm	.559"	145	475	14 mm	002457	150
14.3 mm	.563"	130	425	14 mm	002457	150
15.9 mm	.625"	137	450	15 mm	003236	150
16.2 mm	.638"	137	450	16 mm	002063	150
17.5 mm	.688"	137	450	17 mm	003263	150
18.2 mm	.717"	107	350	18 mm	002458	150
19.05 mm	.750"	107	350	19 mm	003264	150
20.2 mm	.795"	99	325	20 mm	002065	150
22.2 mm	.874"	91	300	22 mm	002459	150

Note: Nominal sizes larger than 0.375" (3/8") have a tolerance of +/- 3% for the width (airspace) and +/- 6% for the height (thickness). For nominal sizes 0.375" (3/8") and lower the tolerance is +/- 0.010" on the width (airspace) and +/- 6% for the height (thickness).
Note: All metric dimension equivalent sizes are for reference only.

*Based upon testing, for systems using secondary sealants other than hot melt butyl or curative butyl, sealing of final corner with PIB backed strips are mandatory for inert gas retention and resistance to moisture ingression.

Additional Requirements Contact Quanex for:

- Shuttle - Part # E-10300000
- Reel Stand - Part # 001078

Quanex warm-edge IG spacer systems are used by our customers to assemble ENERGY STAR® qualified windows and doors.

ISO 9001:2008 with design Certificate Registration 08.185.1

Quanex IG Systems
800 Cochran Avenue
Cambridge, OH 43725
T 800-233-4383
F 740-439-0121
www.quanex.com

15. REFERENCE

activPilot Select The fully concealed tilt and turn gearing activPilot Select The fully concealed tilt and turn gearing for precise requirements. (n.d.).

Aflaki, A., Mahyuddin, N., Al-Cheikh Mahmoud, Z., & Baharum, M. R. (2015). A review on natural ventilation applications through building façade components and ventilation openings in tropical climates. Energy and Buildings. https://doi.org/10.1016/j.enbuild.2015.04.033

Alici, G. (2009). An effective modelling approach to estimate nonlinear bending behaviour of cantilever type conducting polymer actuators. Sensors and Actuators, B: Chemical, 141(1), 284–292. https://doi.org/10.1016/j.snb.2009.06.017

Alici, G., Canty, T., Mutlu, R., Hu, W., & Sencadas, V. (2017). Modeling and Experimental Evaluation of Bending Behavior of Soft Pneumatic Actuators Made of Discrete Actuation Chambers. Soft Robotics, soro.2016.0052. https://doi.org/10.1089/soro.2016.0052

ASHRAE. (2004). ASHRAE Standard 55-2004, Thermal environmental conditions for human occupancy. American Society of Heating, Refrigerating and AirConditioning Engineers, Inc, 26. Retrieved from http://arbis.arb.ca.gov/fuels/gasoline/ethanol/ethfate/Report.doc

Bluyssen, P. M. (2013). The healthy indoor environment: How to assess occupants' wellbeing in buildings. The Healthy Indoor Environment: How to Assess Occupants' Wellbeing in Buildings (Vol. 9781315887). https://doi.org/10.4324/9781315887296

Cambridge University Engineering Department. (2003). Materials data book. Materials Courses, 1–41. https://doi.org/10.1016/0261-3069(88)90026-X

Centre, N., & Pavilion, T. (2015). T o n a , 9(2), 59–74.

Chung, J., Lee, S. H., Yi, B. J., & Kim, W. K. (2010). Implementation of a foldable 3-DOF master device to a glass window panel fitting task. Automation in Construction, 19(7), 855–866. https://doi.org/10.1016/j.autcon.2010.05.004

Cianchetti, M., Ranzani, T., Gerboni, G., De Falco, I., Laschi, C., & Menciassi, A. (2013). STIFF-FLOP surgical manipulator: Mechanical design and experimental characterization of the single module. In IEEE International Conference on Intelligent Robots and Systems (pp. 3576–3581). https://doi.org/10.1109/IROS.2013.6696866

Controls, P. B. (1925). Pneumatic Building Controls Overview and Conversion to Direct Digital Controls (DDC) Pneumatic Building Controls Difference Between Electrical Based DDC and Pneumatic Systems, (Ddc), 1–2. Retrieved from www.millennialnet.com

Cui, W., Cao, G., Ouyang, Q., & Zhu, Y. (2013). Influence of dynamic environment with different airflows on human performance. Building and Environment, 62, 124–132. https://doi.org/10.1016/j.buildenv.2013.01.008

de Payrebrune, K. M., & O'Reilly, O. M. (2017). On the development of rod-based models for pneumatically actuated soft robot arms: A five-parameter constitutive relation. International Journal of Solids and Structures, 120, 1339–1351. https://doi.org/10.1016/j.ijsolstr.2017.05.003

Deimel, R., & Brock, O. (2016). A novel type of compliant and underactuated robotic hand for dexterous grasping. International Journal of Robotics Research, 35(1–3), 161–185. https://doi.org/10.1177/0278364915592961

Fanger, P. O., Melikov, A. K., Hanzawa, H., & Ring, J. (1988). Air turbulence and sensation of draught. Energy and Buildings, 12(1), 21–39. https://doi.org/10.1016/0378-7788(88)90053-9

Galloway, K. C., Polygerinos, P., Walsh, C. J., & Wood, R. J. (2013). Mechanically programmable bend radius for fiber-reinforced soft actuators. In 2013 16th International Conference on Advanced Robotics, ICAR 2013. https://doi.org/10.1109/ICAR.2013.6766586

Galuppi, L., & Royer-Carfagni, G. (2012). The Effective Thickness of Laminated Glass Plates. Journal of Mechanics of Materials and Structures, 7(4), 375–400. https://doi.org/Doi 10.2140/Jomms.2012.7.375

Galuppi, L., & Royer-Carfagni, G. (2015). Cold-lamination-bending of glass: Sinusoidal is better than circular. Composites Part B: Engineering, 79, 285–300. https://doi.org/10.1016/j.compositesb.2015.04.024

Gere, J., & Goodno, B. (n.d.). Mechanics of materials.

Griefahn, B., Künemund, C., & Gehring, U. (2000). The significance of air velocity and turbulence intensity for responses to horizontal drafts in a constant air temperature of 23°C. International Journal of Industrial Ergonomics, 26(6), 639–649. https://doi.org/10.1016/S0169-8141(00)00033-0

Guilherme C.C. Carrilho da Graça. (2003). Simplified models for heat transfer in rooms.

Hofer, J., Groenewolt, A., Jayathissa, P., Nagy, Z., & Schlueter, A. (2016). Parametric analysis and systems design of dynamic photovoltaic shading modules. Energy Science & Engineering, 4(2), 134–152. https://doi.org/10.1002/ese3.115

Karava, P., Stathopoulos, T., & Athienitis, A. K. (2004). Wind Driven Flow through Openings – A Review of Discharge Coefficients. International Journal of Ventilation, 3(3), 255–266. https://doi.org/10.1080/14733315.2004.11683920

Kim, S., Laschi, C., & Trimmer, B. (2013). Soft robotics: A bioinspired evolution in robotics. Trends in Biotechnology. https://doi.org/10.1016/j.tibtech.2013.03.002

Laschi, C., Mazzolai, B., & Cianchetti, M. (2016). Soft robotics: Technologies and systems pushing the boundaries of robot abilities. Science Robotics, 1(1), eaah3690. https://doi.org/10.1126/scirobotics.aah3690

Li, Y., Chen, Y., Yang, Y., & Wei, Y. (2017). Passive Particle Jamming and Its Stiffening of Soft Robotic Grippers. IEEE Transactions on Robotics, 33(2), 446–455. https://doi.org/10.1109/TRO.2016.2636899

Limited, R. B. E. (2002). WATER PENETRATION RESISTANCE OF WINDOWS – STUDY OF MANUFACTURING , BUILDING DESIGN , INSTALLATION.

Liu, S., Schiavon, S., Kabanshi, A., & Nazaroff, W. W. (2017). Predicted percentage dissatisfied with ankle draft. Indoor Air, 27(4), 852–862. https://doi.org/10.1111/ina.12364

Mertens, K. P. (2015). LOAD SHARING AND SPACER FLEXIBILITY IN DOUBLE PANE AND TRIPLE PANE, (May).

Molnár, G., Vigh, L. G., Stocker, G., & Dunai, L. (2012). Finite element analysis of laminated structural glass plates with polyvinyl butyral (PVB) interlayer. Periodica Polytechnica Civil Engineering, 56(1), 35–42. https://doi.org/10.3311/pp.ci.2012-1.04

Mosadegh, B., Polygerinos, P., Keplinger, C., Wennstedt, S., Shepherd, R. F., Gupta, U., … Whitesides, G. M. (2014). Pneumatic networks for soft robotics that actuate rapidly. Advanced Functional Materials, 24(15), 2163–2170. https://doi.org/10.1002/adfm.201303288

Nippon Electric Glass Co., L. (2007). Experimental study of flexibility ofthin sheet glass based on fatigue fracture.

Occupancy, H., Eddy, J., Alspach, P. F., Arens, E. A., Bean, R., Farese, P., … Humble, J. (2017). Thermal Environmental Conditions for Human Occupancy, 8400.

Ouyang, Q., Dai, W., Li, H., & Zhu, Y. (2006). Study on dynamic characteristics of natural and mechanical wind in built environment using spectral analysis. Building and Environment, 41(4), 418–426. https://doi.org/10.1016/j.buildenv.2005.02.008

Özhan, T. (2017). Kinetic Thin Glass Façade.

Polygerinos, P., Lyne, S., Wang, Z., Nicolini, L. F., Mosadegh, B., Whitesides, G. M., & Walsh, C. J. (2013). Towards a soft pneumatic glove for hand rehabilitation. In IEEE International Conference on Intelligent Robots and Systems (pp. 1512–1517). https://doi.org/10.1109/IROS.2013.6696549

Polygerinos, P., Wang, Z., Overvelde, J. T. B., Galloway, K. C., Wood, R. J., Bertoldi, K., & Walsh, C. J. (2015). Modeling of Soft Fiber-Reinforced Bending Actuators. IEEE Transactions on Robotics, 31(3), 778–789. https://doi.org/10.1109/TRO.2015.2428504

Schulze, T., & Eicker, U. (2013). Controlled natural ventilation for energy efficient buildings. Energy and Buildings, 56, 221–232. https://doi.org/10.1016/j.enbuild.2012.07.044

Short, C. A., Dipl, C., Riba, A., & Cook, M. J. (2015). Technical note Design guidance for naturally ventilated theatres, 3(2005), 259–270.

Tapper, A. (n.d.). International Façade Master Delft University of Technology . Subject : Construction.

Topçu, Ö. (2017). Kinetic Thin Glass Façade, (June).

Vander Heiden, M. G. (2011). Targeting cancer metabolism: A therapeutic window opens. Nature Reviews Drug Discovery. https://doi.org/10.1038/nrd3504

Wang, Z., Polygerinos, P., Overvelde, J. T. B., Galloway, K. C., Bertoldi, K., & Walsh, C. J. (2017). Interaction Forces of Soft Fiber Reinforced Bending Actuators. IEEE/ASME Transactions on Mechatronics, 22(2), 717–727. https://doi.org/10.1109/TMECH.2016.2638468

Wurm, J. (2007). Glass structures: design and construction of self-supporting skins.

Yang, D., Verma, M. S., Lossner, E., Stothers, D., & Whitesides, G. M. (2017). Negative-Pressure Soft Linear Actuator with a Mechanical Advantage. Advanced Materials Technologies, 2(1). https://doi.org/10.1002/admt.201600164

Yap, H. K., Lim, J. H., Nasrallah, F., Goh, J. C. H., & Yeow, R. C. H. (2015). A soft exoskeleton for hand assistive and rehabilitation application using pneumatic actuators with variable stiffness. In Proceedings - IEEE International Conference on Robotics and Automation (Vol. 2015–June, pp. 4967–4972). https://doi.org/10.1109/ICRA.2015.7139889

Yap, H. K., Ng, H. Y., & Yeow, C.-H. (2016). High-Force Soft Printable Pneumatics for Soft Robotic Applications. Soft Robotics, 3(3), 144–158. https://doi.org/10.1089/soro.2016.0030

Zhou, J., Chen, S., & Wang, Z. (2017). A Soft-Robotic Gripper With Enhanced Object Adaptation and Grasping Reliability. IEEE Robotics and Automation Letters, 2(4), 2287–2293. https://doi.org/10.1109/LRA.2017.2716445